

Scraper Springs Project

Elko County, Nevada

2023 NI 43-101 Technical Report

Ethos Geological Inc.
902 North Wallace, St A
Bozeman, MT 59715
www.ethosgeological.com

Scott Close, M.Sc, P.Geo

-for-

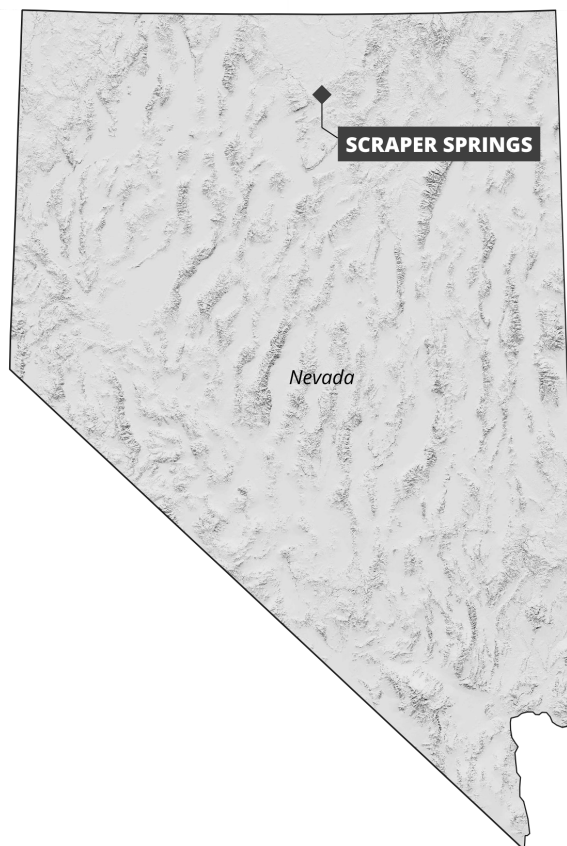
Red Canyon Resources Ltd.
1210 - 1130 West Pender Street
Vancouver, British Columbia
V6E 4A4
www.redcanyonresources.com

-report date-

September 26, 2023

-effective date-

September 26, 2023



CERTIFICATE OF AUTHOR & CONSENT OF QUALIFIED PERSON

Scott Close, M.Sc., P.Geol
Ethos Geological
902 North Wallace
Bozeman, MT U.S.A. 59715
scott@ethosgeo.com

I, Scott Close, do hereby certify:

1. I am the Chief Geologist and President of Ethos Geological, Inc., with an office at 902 North Wallace, Bozeman, Montana, USA;
2. I am a graduate of Montana State University (2004) with a Bachelor of Science degree in Earth Science, and a graduate of Simon Fraser University in Burnaby, British Columbia (2006) with a Master of Science degree in Earth Science;
3. I have practiced my profession continuously since 2004;
4. I am presently the President and Chief Geologist of Ethos Geological Inc., a geological and mineral exploration consulting firm based in Montana, USA, and have been so since May 2008;
5. I am a registered Professional Geologist and member #158157 in good standing with the Engineers and Geoscientists of British Columbia since July 2012;
6. This report is based on publicly available reports, maps, and on original interpretation;
7. My relevant experience for the purpose of this Technical Report is over 17 years of work and research in the field of geology and mineral exploration, of which ten years were spent as an independent consultant for mineral targeting, mineral resource estimation, ore body modeling, and mineral resource auditing;
8. I have read the definition of "qualified person" set out in National Instrument 43-101 (NI 43-101) and certify that by reason of my education, affiliation with a professional association (as defined by NI 43-101) and past relevant work experience, I fulfill the requirements to be a "qualified person" for the purposes of NI 43-101;
9. I have not been affiliated with the Project prior to involvement in the authorship of this Report, and I am independent of the Issuer, vendor, and property applying all of the tests in section 1.5 of NI 43-101.;
10. I have overseen authorship of this report entitled "Scraper Springs Project, 2023 Technical Report" and I am responsible for this report in its entirety;

11. I visited the Scraper Springs Project for approximately eight (8) hours on September 11, 2023, and verified the general geology and geography of the Project as described in this Report.
12. I state that, as the date of the certificate, to the best of my qualified knowledge, information and belief, the Report contains all scientific and technical information that is required to be disclosed to make the Report not misleading;
13. I have no personal knowledge, as of the date of this certificate, of any material fact or material change that is not reflected in this Report;
14. I have read the National Instrument NI 43-101 and the June 30th, 2011 Form 43-101 F1, and this Report has been prepared in compliance with that instrument and form.
15. I consent to the public filing of the Technical Report titled "Scraper Springs Project, Elko County, Nevada 2023 NI 43-101 Technical Report" effective as of the date signed below.
16. I consent to extracts from the Technical Report being disclosed in Red Canyon Resources', or as assigned, News Releases.
17. The Effective Date of this Report is September 26, 2023.

Signed this 26th day of September, 2023

(signed) "Scott J. Close"

Scott J. Close, M.Sc., P.Geo
EGBC #158157

Table of Contents

1 Summary	8
2 Introduction	9
2.1 Terms of Reference	9
2.2 Sources of Information	10
3 Reliance on Other Experts	10
4 Project Description and Location	10
4.1 Location	10
4.2 Property Ownership, Mineral Tenure, Agreements and Encumbrances	11
4.3 Permitting	14
4.3.1 Reclamation	14
4.3.2 Enforcement	15
5 Accessibility, Climate, Local Resources & Physiography	15
5.1 Accessibility	15
5.2 Climate	15
5.3 Local Resources	15
6 History	17
6.1 US Steel (1983), Freeport (1984) and Hecla (1985)	20
6.2 Cordex (1989-1991)	20
6.3 Western States Minerals (1994)	20
6.4 Metallic Ventures & Cordex (2003)	20
6.5 Newmont & Cordex (2008)	21
6.6 Genesis Gold (2018)	22
6.7 NQ Holdings (2020)	22
6.8 Red Canyon Resources (2021-Present)	22
6.9 Historical Sample Preparation & Analysis	24
7 Geological Setting & Mineralization	25
7.1 Regional Geology	25
7.2 Regional Mineralization	27
7.3 Regional Structure	28
7.4 Project Geology	29
7.4.1 Ordovician Vinini Quartzites	29
7.4.2 Pennsylvanian-Permian Carbonaceous Sandstones	29
7.4.3 Tertiary Volcanics	31
7.4.4 Breccias	32
7.4.5 Eocene Intrusives	33
7.5 Project Structure	34
7.6 Project Mineralization	36
7.7 Alteration	37
7.7.1 Silicification	38

7.7.2 Argillic	38
7.7.3 Advanced Argillic	38
7.7.4 Quartz-Sericite-Pyrite (QSP)	38
7.7.5 K-feldspar Alteration	39
7.7.6 Endoskarn	39
8 Deposit Types	41
8.1 Carlin-Type Gold Deposit	41
8.2 Epithermal Au-Ag	41
8.3 Epithermal Quartz-Alunite Au	42
8.4 Polymetallic Au-bearing Skarn	43
8.5 Porphyry	43
9 Exploration	45
9.1 Geophysics	45
9.1.1 Regional Isostatic Gravity	45
9.1.2 Ground Magnetic Survey (2004)	47
9.1.3 Hyperspectral Imaging (2008)	49
9.1.4 Induced Polarization (IP) & Resistivity Survey (2008)	51
9.1.5 Induced Polarization (IP) & Resistivity Survey (2021)	55
9.2 Sampling	58
9.3 Petrography	61
9.4 Multivariate Exploratory Factor Analysis	61
9.4.1 Soil Geochemistry Factors	62
9.4.2 Rock Chip Geochemistry Factors	64
9.4.3 Historic Drill Hole Geochemistry Factors	67
9.5 3D Modeling	68
9.6 Age Dating	69
10 Drilling	71
11 Sample Preparation, Analyses, and Security	71
12 Data Verification	71
13 Mineral Processing and Metallurgical testing	71
14 Mineral Resources Estimate	72
15 Mineral Reserve Estimate	72
16 Mining Methods	72
17 Recovery Method	72
18 Project Infrastructure	72
19 Market Studies and Contracts	72
20 Environmental Studies, Permitting & Social Impact	72
21 Capital and Operating Costs	73
22 Economic Analysis	73
23 Adjacent Properties	75
23.1 Midas Mine (Miocene)	75
23.2 Hollister Mine (Miocene)	77
23.3 Tuscarora Deposit (Eocene)	77

23.4 Goldstrike Mine (Eocene)	78
24 Other Relevant Data and Information	80
25 Interpretations and Conclusions	80
25.1 Alteration	81
25.2 Genesis	81
25.3 Conclusions	82
26 Recommendations	84
26.1 Structural Analysis	84
26.2 Gravity Survey	84
26.3 Descriptive Field Mapping	85
26.4 CSAMT	85
26.5 Drilling	86
26.6 Budget	89
27 References	91

List of Figures

Figure 1. State of Nevada, regional gold trends, major cities, and active gold mines.	12
Figure 2. Property outline, lode claims and private lands.	13
Figure 3. Physiography of the Scraper Springs Project, viewing southwest.	16
Figure 4. Historic drill hole collar locations.	19
Figure 5. Regional geology in North and central Nevada showing generalized lithology, regional gold trends, active gold mines and trend of the Northern Nevada Rift (NNR).	26
Figure 6. Tertiary magmatism in the North American cordillera (Castor et al., 2003).	27
Figure 7. Scraper Springs geologic map displaying lithology, structural features, and select zones of interest (adopted from J.M Wise, 2008).	30
Figure 8. North and South Breccia Zones outcrop maps (Cantor and Thompson, 2012).	32
Figure 9. Structure, interpretations and potential stress field.	35
Figure 10. Alteration assemblage diagram (Corbett and Leach, 1997).	37
Figure 11. Project alteration map adapted from Wise (2008).	40
Figure 12. Schematic of a Carlin-type gold deposit (Miranda et al, 2019).	41
Figure 13. Schematic cross section of alteration through a generalized Goldfield, NV, and Summitville, CO quartz-alunite hydrothermal system with a moderate pH intrusion system at depth (Plumlee et al 1996).	43
Figure 14. Telescoped porphyry system model (Sillitoe, 2010).	44
Figure 15. Regional isostatic gravity map of the greater Scraper Springs region (USGS, 1998).	46
Figure 16. Ground magnetics survey from Zonge Geoscience for Cordex (2004) showing total magnetic field intensity in nT, upward continued to 10 ft and reduced to pole.	48
Figure 17. Hyperspectral composite map of alteration minerals (Newmont, 2008).	50
Figure 18. IP line locations from Newmont, Cordex and Red Canyon.	52
Figure 19. IP survey line 6065 showing interpreted chargeability (upper) and resistivity (lower) across at least one major basement fault (Flt), two diorite stocks (Td) and the South Breccia Zone (Bx).	53

Figure 20. Plan view of IP resistivity and chargeability horizontal interpolation at 1750m elevation above sea level.	54
Figure 21. IP survey Line 1 2021 location.	56
Figure 22. Line 1 2021, chargeability, viewing NE.	57
Figure 23. Line 1 2021, resistivity, viewing NE.	57
Figure 24. Gold in soils geochemistry map showing both Newmont and Red Canyon soil assay results.	59
Figure 25. Rock chip sampling geochemistry map showing Au assay results.	60
Figure 26. Multi-element factor analysis on soil samples from Newmont's and Red Canyon's soil campaigns.	64
Figure 27. Multi-element factor analysis on rock samples from Newmont and Cordex (2004, 2008).	66
Figure 28. Multi-element factor analysis on drill data from Cordex/Metallic Ventures (2004).	68
Figure 29. 3D model preview showing alteration zones and proposed drill holes.	69
Figure 30. Age dating of the northern diorite stock.	70
Figure 31. Map showing adjacent properties and generalized active mining claims.	74
Figure 32. Cross section and mineralization of the Midas Mine.	76
Figure 33. Schematic cross section showing geology, structure and mineralization at the Hollister Mine (John et al., 2010).	77
Figure 34. Goldstrike mine maps.	79
Figure 35. Schematic cross section through Yerington porphyry system (Blakely et al 2010).	82
Figure 36. Proposed drill plan map showing proposed drill pads, drill holes, drill hole traces, and CSAMT lines.	87
Figure 37. Proposed drill plan in 3D showing drill traces, major structures, IP chargeability, and the diorite stock.	88

List of Tables

Table 1. Exploration activities outlined in the Notice of Intent (NOI) data May 9, 2023.	14
Table 2. Summary of work at the Scraper Springs Project.	18
Table 3. Summary of historic drilling data and targets of previous drill operations at Scraper Springs.	18
Table 4. Historic drill highlights observed from the unverified historic drill data.	23
Table 5. Historic drill sample assay methods and laboratories.	24
Table 6. Soil factors showing positive and inverse correlations and interpretation.	63
Table 7. Rock factors.	65
Table 8. Drill hole factors.	67
Table 9. Proposed drill holes.	86
Table 10. Proposed Phase 1 exploration budget summary and itemized estimates.	89
Table 11. Proposed Phase 2 exploration budget summary and itemized estimates.	90

Appendices

Appendix A: Lode Claims	94
--------------------------------	----

1 SUMMARY

This Report was prepared in compliance with National Instrument 43-101 regulations for Red Canyon Resources Ltd. (“Red Canyon Resources” or the “Company”) accumulating the available information pertaining to the Scrapper Springs Project (“Scrapper Springs” or the “Project”) located in northwestern Elko County, Nevada.

Scrapper Springs is an exploration stage project held by Red Canyon Resources. The Technical Report provides geological interpretation, exploration results and analysis, and recommended exploration.

The Project sits on BLM and private land at the north-westernmost extent of the Carlin-trend, approximately 74 miles north of Battle Mountain and 89 miles north of Elko, where suites of volcanic rocks and paleozoic sediments host the Midas, Hollister, and Goldstrike mines.

Carlin-type mesothermal gold deposits in the region sit with Paleozoic limestones, calcareous rocks and quartzites during transtensional plate convergence conditions in the Eocene-Early Miocene (Bahadori and Holt, 2019). Later epithermal Au-As systems align with faults created during the mid Miocene Northern Nevada Rift.

At Scrapper Springs, rifted Tertiary volcanic rocks expose a window to the Ordovician Vinini Formation (Ovi), of the Upper Plate of the Roberts Mountain allochthon, and the unit hosting mineralization at the nearby Hollister mine.

Scrapper Springs is a high-sulphidation, acidic epithermal system cored by diorite and breccia, and is unlike the low sulphidation epithermal veins of the Miocene or the Eocene Carlin-type disseminated gold mines elsewhere in the region. The alteration minerals zunyite and pyrophyllite concentrate along two east-northeast trends hosting internal faulting, a diorite intrusion, breccia, and advanced argillic alteration. These two trends implicate important conduits to a magma source at depth.

Highly anomalous silver (2379 g/t Ag) and gold (> 1g/t Au) sit within vuggy quartz and along intense fracturing along one of the trends in the southwest of the Project area. Howell (2007) reports 0.52 g/t Au over 140ft in drill core from the central Project area. The distribution of gold mineralization is sporadic, however, and the Project lacks consistent exploration methodology.

The Author recommends the collection of soils to extend surface geochemical knowledge into new areas, structural and descriptive field mapping to further define relationships of hydrothermal fluids and mineralizing conduits, CSAMT and ground gravity surveys to identify the geometry of a potential mineralizing intrusive center at depth, and drill test the plunge of altered conduits from 500m - 1000m deep to target porphyry base metal +/- gold mineralization.

2 INTRODUCTION

This Report on the Scraper Springs Project was prepared as a NI 43-101 compliant technical report (the “Report”) for Red Canyon Resources (‘Issuer’, ‘Company’) by Ethos Geological, Inc., of Bozeman, MT. The information and conclusions contained herein are based on: i) information available at the time of preparation made available by the Issuer, ii) data supplied by historic operators, iii) data provided by outside sources, iv) and original analysis, subject to the assumptions, conditions, and qualifications outlined in this Report.

Scott Close, Author of this Report and agent for Ethos Geological, Inc. performed an approximate eight hour field investigation during a site visit at Scraper Springs on September 11, 2023, examining and confirming the general location and accuracy of the geographic and surface geologic information supporting this Report.

2.1 Terms of Reference

Abbreviations utilized in this report reference standards within the scientific, geology and mining industries- such as the periodic table of elements- and other commonly-used resources; additionally, imperial and metric units are used interchangeably, reflecting the origin and history of a given dataset or source, the setting of the Project in the USA, and assessment by both USA and Canada-based workers.

Several abbreviations used within the report include, but are not limited to:

%	Percent	K	Thousand
oz/t	Ounces per tonne	M	Million
Au	Gold	Ma	Million years ago
Ag	Silver	Ga	Billion years ago
Ar	Argon	RC	Reverse Circulation
CTGD	Carlin-type Gold Deposits	CE	Categorical Exclusion
Cu	Copper	NOI	Notice of Intent
K	Potassium	BLM	Bureau of Land Management
F	Fahrenheit	DMEA	Department of Mineral Exploration Administration
ft	foot	NEPA	National Environmental Protection Act
Km	Kilometer	NNR	Northern Nevada Rift
m	meter	USFS	United States Forest Service
ppb	Parts per billion	USGS	United States Geological Survey
ppm	Parts per million		
g/t	Grams per tonne		

2.2 Sources of Information

A portion of the background and technical information presented in this report was obtained from the following document:

Bradford M. Cantor and Dr. Tommy B. Thompson's 2012 report "Petrography and Field Mapping of Eocene Intrusions and Adjacent Breccia Zones at the Scrapper Springs Prospect, Elko County, Nevada".

The information contained in current report Sections 7 and 8 was largely presented in, and in some cases is excerpted directly from, the paper listed above. Ethos has reviewed this material in detail, and finds the information contained herein to be factual and appropriate with respect to guidance provided by NI 43-101 and associated Form NI 43-101F1.

Additional information was requested from and provided by the Company. In preparing Sections 9 through 12 of this report, the authors have sourced information from historical documents including exploration reports, technical papers, sample descriptions, assay results, computer data, maps and drill logs generated by previous operators and third party contractors. Documents and data sources used during the preparation of this report are cited in the text as appropriate and summarized in Section 27.

3 RELIANCE ON OTHER EXPERTS

Not applicable.

4 PROJECT DESCRIPTION AND LOCATION

4.1 Location

Scraper Springs sits within the Snowstorm Mountain range, Elko County, Nevada, USA, approximately 80 miles each from the towns of Winnemucca, Battle Mountain and Elko. The property may be further described as sitting in township 40 north, range 47 east, within sections 2-5, 7-11, 14-18, 20, and 21, centered at latitude 41.36, longitude -116.67, only eight miles northeast of the Midas mine (Figure 1).

4.2 Property Ownership, Mineral Tenure, Agreements and Encumbrances

Under the administration of the BLM, ownership of unpatented mining claims in the U.S. is in the name of the claimant. The Mining Law of 1872- which governs the location of unpatented mining claims on federal lands- grants the claimant the right to explore, develop and mine minerals on unpatented mining claims without payments or royalties to the federal government.

The Project currently comprises 190 count unpatented lode claims (Figure 2) declaring 'RC METALS Inc', the wholly owned subsidiary of Red Canyon Resources, as the claimant. Excluding the overlap with private lands and private mineral rights and other senior lode claimants in the area (Genesis), the total coverage of the Red Canyon holdings are approximately 3444.71 acres.

A list of the lode claims, claimant, name and ID can be found in Appendix A. The Author performed an independent search of BLM records on August 2, 2023 and can verify the claims' status as active in the BLM MLSR system. The Author did not validate the claims in the local Elko county recorders' office nor check claims posts on the ground.

To the extent known by the Author, there are no significant factors or risks that may affect access, title, or the right or ability to perform work on the property. However, the Company has not disclosed to the Author any existing royalties, payments or other encumbrances that may be held by the Company in obtaining the rights to the Project from previous claimants.

To maintain the lode claims in good standing, an annual lode claims fee of \$165 per claim is to be paid to the Bureau of Land Management (BLM) prior to September 1st of each year to hold and maintain these claims. Additionally, an affidavit stating the Company's intent to hold these claims (a 'Notice of Intent to Hold') is to be filed before November 1 of each year with the Elko County Recorders' Office at \$2/claim plus a fee for the Nevada Department of Minerals at \$10/claim, and a \$12 document filing fee. In total, the estimated annual filing fees to maintain the current Scrapper Springs lode claims group of 190 claims in good standing is \$33,642.

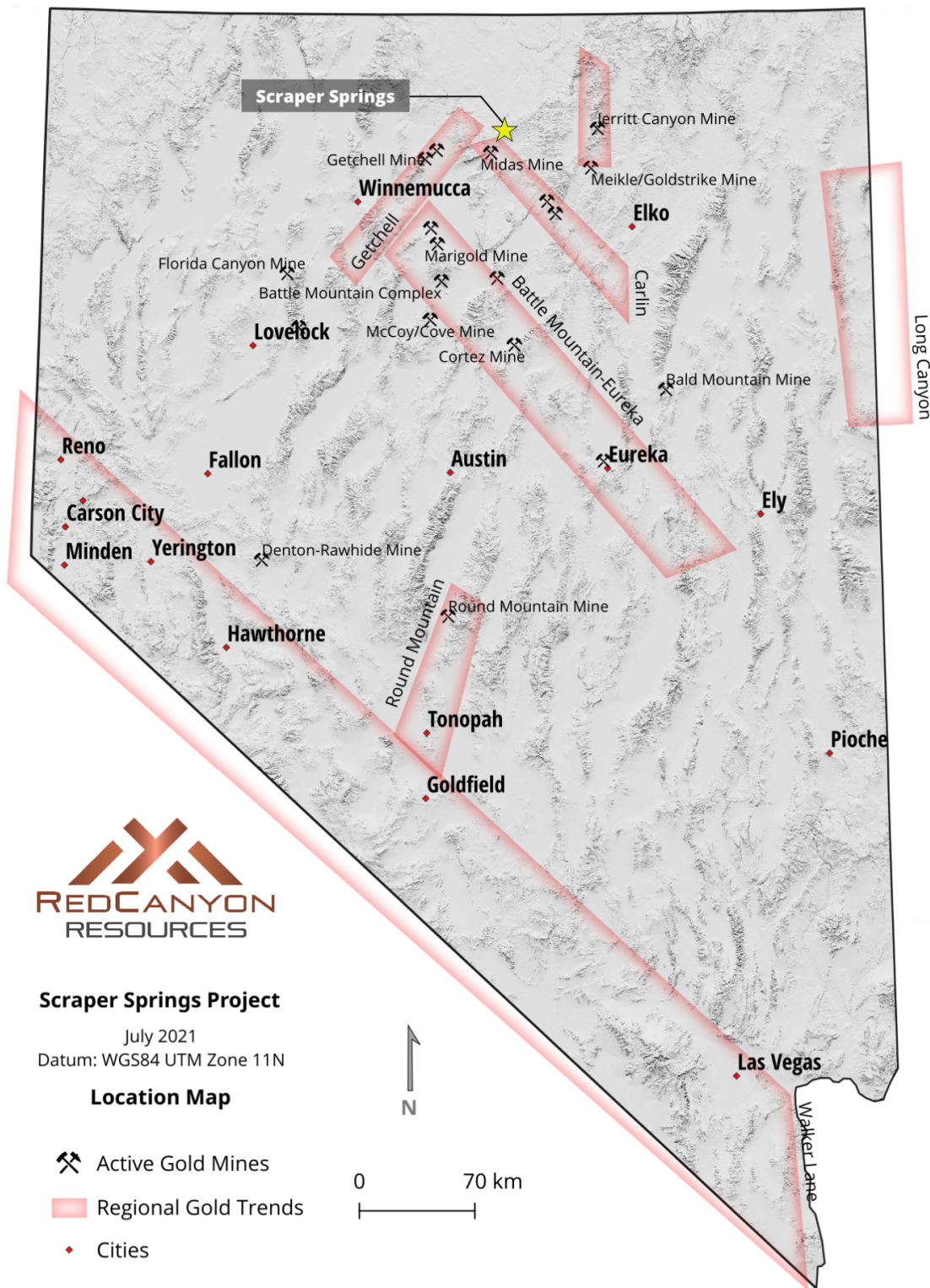


Figure 1. State of Nevada, regional gold trends, major towns, and active gold mines.

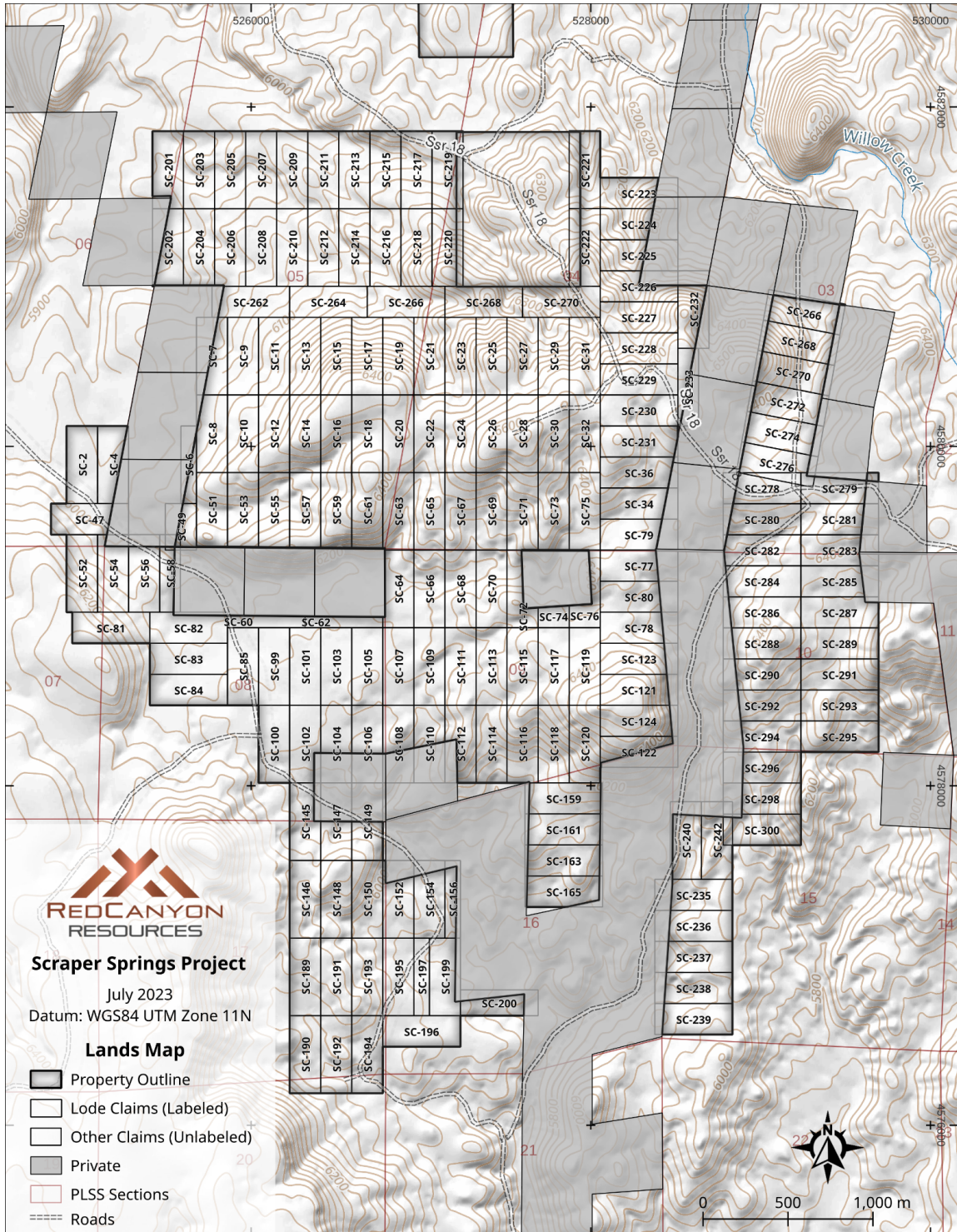


Figure 2. Property outline, lode claims and private lands.

4.3 Permitting

Notices of Intent (NOI) cover and administer all exploration activities with a less-than-5-acre disturbance on BLM land, which the Company submitted on May 9, 2023 covering nine proposed drill sites, sumps and approximately 2,870 ft of new road construction, totaling approximately 1.95 acres of disturbance.

Table 1. Exploration activities outlined in the Notice of Intent (NOI) dated May 9, 2023.

Exploration Component	Slope %	Count	Length (ft)	Width (ft)	Total Area (acres)
Exploration Drill Sites	<30	9	70	30	0.55
Sumps	<30	9	20	10	0.15
New Road Construction	<30		2,870	14	1.16
Overland Travel	<10		630	6	0.09
Total					1.95

4.3.1 Reclamation

Financial security bonds are assessed to cover the cost of reclaiming the proposed disturbance and associated administration fees.

The following reclamation actions are often used to calculate reclamation bonds;

Access Roads and Drill Pads

1. Mobilization and demobilization
2. Recontouring the land to approximate the original topography
3. Removal of culverts
4. Ripping or scarifying the surface
5. Water diversion construction
6. Restoration or stabilization of drainage areas or stream beds
7. Revegetation

Drill Hole and Well Abandonment

1. Mobilization and demobilization
2. Drill hole abandonment (excepting those plugged as per Nevada statute NAC 534)

4.3.2 Enforcement

In addition to annual inspections, other site visits and communication between reclamation staff and company personnel occur as needed. BLM staff work with the Company or Operator to resolve any non-compliance or reclamation issues should these develop.

5 ACCESSIBILITY, CLIMATE, LOCAL RESOURCES & PHYSIOGRAPHY

5.1 Accessibility

The Scraper Springs Project can be reached by 4WD or high clearance vehicle from Winnemucca, near the Golconda Exit traveling northeast on US Highway 18 (Midas Mine Road); north from Battle Mountain on highway 35 for 39 miles to its junction with the Midas Mine Road; or, north from Elko on highway 225, then west on highway 226 past Tuscarora on Midas-Tuscarora road. These routes range from paved to well-maintained dirt roads.

The junction for the Scraper Springs Road, officially named, sits about 1.5 miles east of the Midas mine site and access road where a weakly-maintained two-track dirt road that turns north toward Scraper Springs proper; the southern boundary sits approximately 9.5 miles north from this junction. Travel times from Winnemucca, Battle Mountain, or Elko to the site range from two to three hours.

5.2 Climate

The climate in Northern Nevada holds hot summers and mild winters. Average daily summer temperatures range from 50 degrees Fahrenheit (°F) to 95°F, and average winter temperatures range from 15°F to 40°F. Temperature extremes may reach above 100°F and below 0°F for short periods. Winter snowfall ranges from 30-50 inches and melts out by mid March. Total annual precipitation averages 10 inches.

Vegetation in the area is sparse and comprises sagebrush, rabbitbrush, cheatgrass, and grama. Juniper trees, pinyon pine, and mountain mahogany grow in pockets and along drainages (Figure 3).

5.3 Local Resources

The closest cities to the Project area are Winnemucca, Battle Mountain, and Elko. Elko has a population of 20,476 as of the 2020 U.S. census report; supplies, groceries, and other necessities

are readily available. Elko is a long-established mining hub and holds heavy equipment dealers, repairs and maintenance, mining workforce, and serves as a basecamp to mining companies.

Passenger bus service to Elko is available on Greyhound Lines; Amtrak's daily California Zephyr provides train passenger service via Elko Station. SkyWest Airlines (operating as Delta Connection) serves Elko Regional Airport with regional jet service nonstop to Salt Lake City.

The Midas Mine, 8 miles to the southwest of the Project, is an established mine site with extensive underground mine workings and a processing facility with capacity of 1,200 tonnes per day. Power is supplied via NV Energy Corp transmission lines from the Osgood substation (*"Preliminary Feasibility Study for the Midas Mine, Elko County, Nevada" 2015*).

Surface water occurs on the Project as a series of small springs and ephemeral streams, mostly in the southern Project area. A sizable body of water, the Willow Springs Reservoir, sits 21 miles to the southeast and drains westward.



Figure 3. Physiography of the Scrapper Springs Project, from the central Project area viewing southwest.

6 HISTORY

Exploration at the Project began in the mid 1980's and continued for nearly 20 years; drilling on the property began in 1984 and continued to 2008 (Tables 2 and 3, Figure 4). The Project was released and sat dormant until being acquired and renewed by the Company in 2021. Work prior to the 1980's is either unreported or unknown to the Author.

US Steel explored the vein system at the Hill anomaly (Rebel Fault Zone Area) in the southwestern portion of the Project in 1983. Freeport and Hecla Mining further tested this area in 1984 and 1987, respectively. Cordex Exploration performed a wide array of drill testing from 1989-1991, targeting areas to the north and northwest of the present claim block.

Western States Minerals held the Project from 1994-1997 and focused on skarn / Carlin-type mineralization, focusing on Vinini sediments along the margins of Tertiary granodiorite intrusives. In late 2001, the claims were leased to Cordex's subsidiary Cordilleran, and in 2004 (funded by Metallic Ventures) drilled 12 widely spaced holes. Newmont optioned the project from Cordex/Cordilleran and in 2008 tested the South Breccia Zone with three holes before dropping the Project..

NQ Holdings Inc. re-staked the Project in 2020 and transferred ownership to Red Canyon Resources in 2021, recognizing a potential for a porphyry-style mineral system at depth (this Report).

Assays and intercepted widths listed here are reported in the following Sections are for reference only, have not been verified, and do not indicate or guarantee mineral intercepts that may be intersected in future drill campaigns.

Table 2. Summary of work at the Scrapper Springs Project.

Year	Company	Soils	Rocks	Drill Holes	Geophysics	Other
1983	US Steel					
1984	Freeport			10 (4,100 ft)		
1987	Hecla			7 (2,415 ft)		
1989	Cordex	*	*	40 (21,475 ft)	CSAMT*	
1994	Western States	*	*	13 (8,535 ft)		
2003	Cordex / Metallic Ventures	1787	170	12 (8,380 ft)	Ground Magnetics	Diorite age dating
2008	Cordex / Newmont	767	145	3 (2,605 ft)	11 lines km IP/RES (28.62 km)	Hyperspectral, Petrography, Volcanic age dating
2021	Red Canyon Resources	240			3.3 line km IP/RES	
2022	Red Canyon Resources					3d modeling
		~ 2794	~ 315	85 (47,510)		

Table 3. Summary of historic drilling data and targets of previous drill operations at Scrapper Springs.

Dates	Operator	Holes	Target Type	Amount (ft)	Assays	Logs	Alteration
1983	US Steel						
1984	Freeport	10	Epithermal	4,100			
1987	Hecla	7	Epithermal	2,415			
1989-1991	Cordex	40	Carlin	21,475			
1994-1997	Western States Minerals	13	Carlin, Skarn	8,535	✓		
2003	Metallic Ventures/Cordex	12	Carlin, Skarn	8,380	✓	✓	✓
2008	Newmont, Cordex	3	Breccia	2,605	✓	✓	✓
	Total	85		47,510			

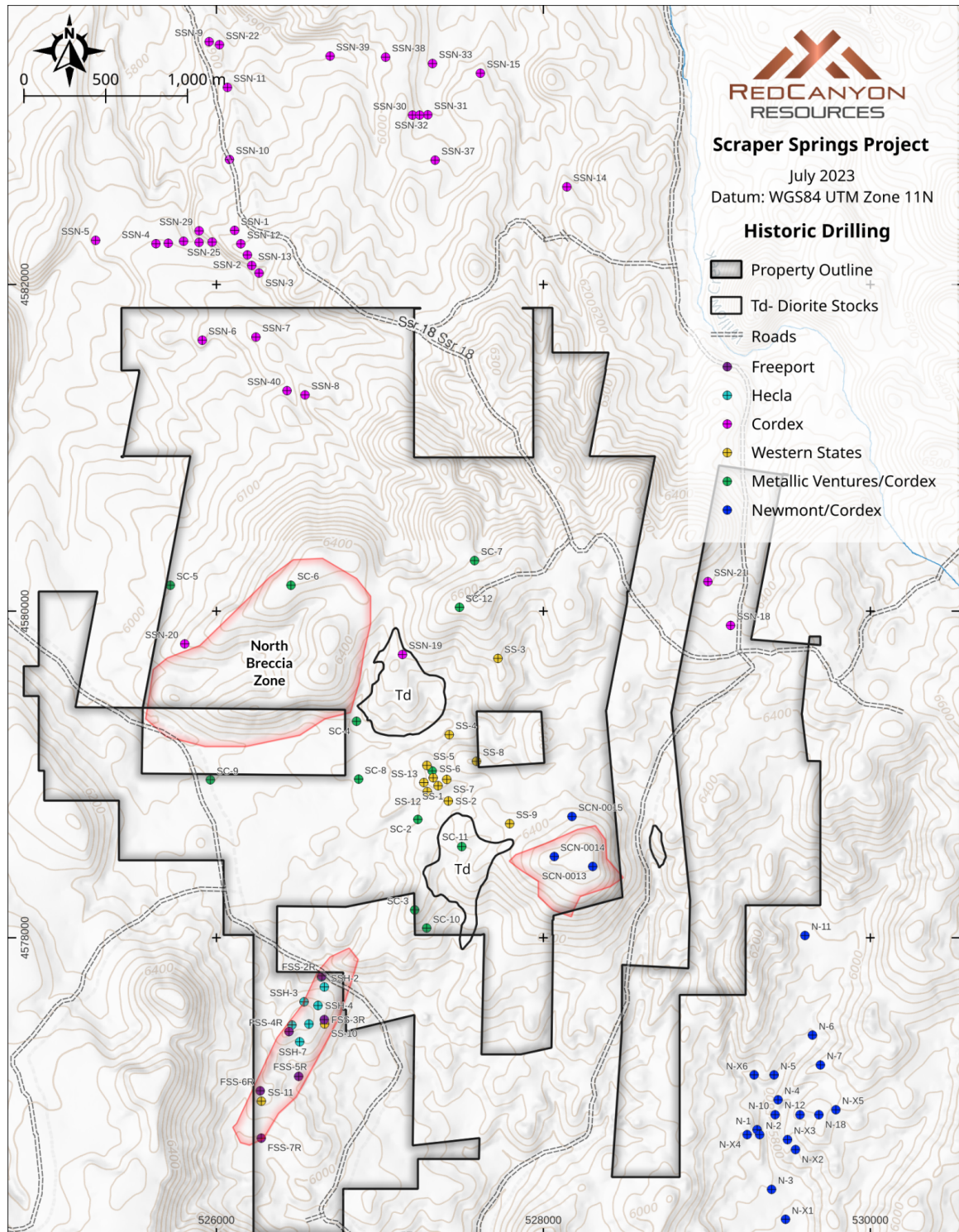


Figure 4. Historic drill hole collar locations.

6.1 US Steel (1983), Freeport (1984) and Hecla (1985)

US Steel first explored a vein system in 1983 at the Rebel Fault Zone (formerly the 'Hill' anomaly) located in the southwestern part of the Project. Freeport drilled 10 RC holes in this area totaling 4100 ft in 1984, and Hecla followed this effort by drilling seven holes totaling 2145 ft in 1987. Both drill programs intercepted weakly-anomalous gold and anomalous to significant silver hosted in quartz veins, breccias, and altered volcanic rocks (Howell, 2007).

6.2 Cordex (1989-1991)

Between 1989-1991 Cordex Exploration performed extensive exploration which included mapping, rock and soil sampling, gridded auger drilling, CSAMT, and completed 40 shallow RC holes totaling 21,475 ft. Most of Cordex's early work targeted areas to the north and northwest of the current claim block (Howell, 2007). No drill logs or assay results are currently available.

6.3 Western States Minerals (1994)

Western States Minerals operated the Project from 1994-1997. Mapping, rock and soil sampling, and drilling focused on the central Paleozoic exposure between two intrusive stocks, and to a lesser extent, the Rebel Fault Zone. Of the 13 RC holes drilled, totaling 8535 ft, (SS 1-13, 8535'), two holes intercepted significant mineralization in altered Vinini sediments along the margins of a Tertiary granodiorite intrusive.

Drill hole SS-1 intercepted 140 feet (320-460') assaying 0.017 ounces per ton (oz/t) gold including a 20 and 10 ft intercept containing 0.031 and 0.050 oz/t Au respectively; drill Hole SS-6 intercepted 25 feet (25-50') of 0.020 oz/t Au (Howell, 2007). Of the 13 holes drilled, complete drill logs are available from SS-1, SS-5, and SS-9.

The drill logs provide insight into the alteration assemblages through Oviq quartzite, where the past operator was targeting Carlin type mineralization. SS-1 drill log indicates that higher gold values are associated with elevated concentrations of disseminated pyrite. Over the interval from 265-280 ft., pyrite constitutes greater than 20% of the groundmass and locally accounts for 30% of the minerals within the RC chips. In these zones pyrite occurs as massive, sooty aggregates and is disseminated through the groundmass (Cantor and Thompson, 2012).

6.4 Metallic Ventures & Cordex (2003)

In 2003, Cordilleran (a Cordex Company) was funded by Metallic Ventures to perform extensive soil sampling and a ground magnetic survey. This venture dated the diorite intrusive and drilled 12 widely-spaced RC holes totaling 8380 ft (SC-1-SC-12). Unfortunately, of the 1787 soils

collected from the central Project area, only Au, As and Hg were assayed. Metallic dissolved their interest in the venture in 2006 and the Project reverted to Cordex/Cordilleran.

Encouraging drill results included SC-1, which was drilled to a depth of 1900 feet. This drill hole encountered variably altered Lower Plate rocks thought to be Devonian Rodeo Creek Formation at a depth of 1650 feet (Cantor and Thompson, 2012). This hole contained anomalous gold both in the Upper and Lower Plates with strongly anomalous to significant copper and zinc in Lower Plate sedimentary rocks. Many of the other shallow holes intercepted weakly anomalous gold, anomalous zinc, lead and silver (SC-11) (Howell, 2007).

SC-1 is the deepest historic drill hole on the Scraper Springs Project. Near the bottom of the hole, between 1815 and 1850 ft, the rock is carbonate-rich. Although the final 100 ft of this hole were not assayed, it is notable that this carbonate-rich lithology occurs here, as geochemical anomalies in copper and zinc spike just above this unit (Cantor and Thompson, 2012). Between 1765 and 1800 ft, Cu values jump from low values under 100 ppm to over 2100 ppm. Over this same interval, Zn values are elevated from low-hundreds ppm to above 1000 ppm and between 1765 – 1770 ft is measured at 10,000 ppm (Unpub. Cordex report 2004, sample SP066323).

6.5 Newmont & Cordex (2008)

In 2008, Newmont Mining formed a strategic alliance with Cordex/Cordilleran to further explore the breccias, adding additional expertise for re-mapping and re-interpreting the geology and alteration. They laid soil sample grids covering both the northeastern portion of the Project and the area identified as the “Diatreme Vent Target” (referred to in this report as the “South Breccia Zone”) into which they drilled 3 RC holes totalling 3,504 ft (Wise, 2008b). Newmont also contracted hyperspectral alteration mapping, 11 lines of IP geophysics, and assayed 767 soils for a wider suite of elements. Newmont and Cordex dropped the claims in 2012.

The three RC holes targeting an interpretive “diatreme vent” structure, a feature in which mineralization occurs in breccia bodies when magma rises up through the Earth's crust and makes contact with a shallow body of groundwater, rapid expansion of heated water, vapor, and volcanic gases and causes a series of explosive events (Sillitoe, 1985). New mapping by Brad Cantor in 2012 revealed that the breccia textures and mineral assemblages on the Project suggest that the breccias are magmatic hydrothermal (Sillitoe, 2010, Cantor 2012), and not diatreme breccias.

The three drills holes, SCN-00013, SCN-00014, and SCN-00015, all collared in tertiary volcanics (Tvt) quickly encountered the diorite intrusive unit (Td) from 25 to 325 ft deep, which continued to each hole's terminal depth. Moderate to intense quartz-sericite-pyrite (QSP) alteration occurs in the diorite, with as much as 15% disseminated pyrite in veinlets and the groundmass locally. Additionally a chlorite-dominant propylitic assemblage from 1105 at 1300 ft (Cantor and Thompson, 2012).

Although drilling produced core mostly barren of ore minerals, this area is significant because widespread quartz-sericite-pyrite (QSP) alteration, with molybdenite, supports the notion that

there is widespread alteration at depth, which provides a vector toward higher temperature parts of the system.

6.6 Genesis Gold (2018)

Portions of the Project area were staked by Altan Rio and Genesis Gold in 2018. Altan Rio and Genesis Gold dropped the claims in 2019.

6.7 NQ Holdings (2020)

NQ Holdings staked 96 claims covering the core area of the Project in October 2020. Following acquisition, NQ Holdings began assimilating the area's historic data.

6.8 Red Canyon Resources (2021-Present)

Red Canyon acquired the property from NQ Holdings in February of 2021. Following the acquisition, Red Canyon located an additional 94 claims, for a total of 190 by the date of this report. In 2021, Red Canyon contracted Zonge Geoscience to perform an Induced Polarization (IP) and Resistivity survey comprising 3.3 line-kilometers of coverage, and in November and December collected 240 soil samples covering a broad area to obtain multi-element data where coverage was previously incomplete.

Since 2001, the Company worked to compile the new and available historic data to construct a 3D model in LeapFrog geological modeling software, generate a new interpretation, and prepare an exploration drilling permit. The model includes subsurface geology, alteration and structures to assist in planning accurate drill holes and investigating subsurface trends, for which the Company has outlined an approximate 7,500 metre drill program pending positive additional results (this Report).

Table 4. Historic drill highlights observed from the unverified historic drill data.

Year	Hole ID	From (ft)	To (ft)	Au ppm	Ag ppm	Cu pm	Mo ppm	Pb ppm	Zn ppm	
2004	SC-01	40	45	0.346	18.3	35.4	5.37	24.7	24.8	
		55	60	0.47	22	66.3	1.43	16.9	27.7	
		170	175	0.423	15.7	34.3	3.13	25	64.5	30ft Average: 0.28 g/t Au 19.7 g/t Ag
		175	180	0.382	18.3	40.3	3.53	25.6	65	
		180	185	0.272	18.4	39.7	3.9	34.9	74.4	
		185	190	0.13	21.7	53.9	3.48	18.1	58.7	
		190	195	0.106	15.4	41.1	2.95	11.3	40.2	
		195	200	0.338	28.9	56.9	3.58	18.1	75.9	
		1765	1770	0.008	7.3	2160	1.46	90.6	10000	
		1775	1780	0.006	5.2	2400	2.01	471	1670	
		1780	1785	0.008	1.81	2290	1.14	43.2	228	
		1785	1790	0.01	2.09	78.2	4.82	493	106	
		1790	1795	0.012	2.09	1860	1.08	51.8	191	
		1795	1800	0.008	1.9	2970	1.01	34.4	277	
2004	SC-02	375	380	0.018	5.51	149	2.61	319	2130	
2004	SC-03	135	140	0.018	35	17.7	8.4	37.8	44.6	
2004	SC-11	230	235	0.048	60	146	4.97	6950	10000	20ft Average: 35 g/t Ag 0.42 % Zn 0.32 % Pb
		235	240	0.031	29.7	50.1	4.08	3120	3130	
		240	245	0.015	36.6	25.9	3.83	1270	810	
		245	250	0.019	15.5	37.3	3.41	1450	2740	
		265	270	0.022	28.7	35.3	5.16	1510	2020	
		365	370	0.027	8.13	104	3.21	1380	2910	
		380	385	0.012	6.61	18.6	2.51	2080	149	
2008	SCN-0013	320	340		0.03	15.1	168.5	12.8	16	

6.9 Historical Sample Preparation & Analysis

A compilation of the sample preparation and analyses from previous workers is tabulated in Table 5. 2004 RC chip samples (Cordex) were prepared by American Assay Laboratories (AAL). The 2008-era RC chip samples (Newmont), soil samples, and the 2021 era soil samples by the Company were prepared by ALS Laboratories (ALS). ALS uses a preparation method that involves a crush to 70% less than 2mm, riffle split off 250g, then pulverised to better than 85% passing 75 microns.

Cordex reported using American Assay laboratories ('AAL') in Reno, NV for all assayed samples, selecting the labs' ICP-2A assay method for drill hole SC-1, and the ICP-1D assay method for drill holes SC-2 through SC-11, all with AAL's FA30 process for gold (FA30 is a method not presently offered by AAL).

Newmont's samples were analyzed by ALS Minerals, a division of ALS Global, with labs located in British Columbia, Canada and Reno, Nevada. RC chips and soils from the 2008 program were assayed using the ME-MS41 assay method with an Au-AA23 or ICP21-Au for gold, respectively. ICP and MS methods use acid to digest the sample, aerosolized with Argon, and quantified through count via mass spectrometry for gold and multi-element determination. The FA30 and Au-AA23 processing describe a fire assay method, the latter is a flux recipe on a sample of 30g in size to determine the presence of gold in trace limits greater than 0.005 ppm. The digestion quantitatively dissolves nearly all minerals in the majority of geological materials, however, barite, rare earth oxides, columbite-tantalite, and titanium, tin and tungsten minerals may not be fully digested.

Table 5. Historic drill sample assay methods and laboratories.

Year	Company	Sample type	Commodity	Method	Lab
2004	Cordex	RC chips	Au	FA30	American Assay Lab
2004	Cordex	RC chips	Au	FA30	American Assay Lab
2004	Cordex	RC chips	Multi-element	ICP-1D, ICP-2A	American Assay Lab
2008	Newmont	RC chips	Au	Au-AA23	ALS
2008	Newmont	RC chips	Multi-element	ME-MS41	ALS

7 GEOLOGICAL SETTING & MINERALIZATION

7.1 Regional Geology

The Scrapper Springs Project lies within the eastern-central portion of the Basin and Range physiographic province; a broad extensional landscape of N-S trending mountains and valleys that spans most of Nevada, Utah and Idaho.

Two distinct assemblages of marine sediments were deposited during the Paleozoic epoch within the former western margin of North America. Low angle decollement thrusting emplaced sediments of the Western siliciclastic provenance over the Eastern carbonate provenance, termed the Upper and Lower plates of the Roberts Mountain Allochthon and Roberts Mountain Thrust.

The Western assemblage, or the Upper plate, is a marine package of siliciclastic rocks comprising argillite, chert, siltstone, sandstone, and minor limestone. The Eastern carbonaceous sedimentary assemblage- the Lower plate- consists of limestone, dolomite, and lesser quartzite units. The Eastern assemblage underlies all other stratigraphic units in eastern and central Nevada (Gulluly et al., 1965); it is within this Lower Plate that Carlin-type gold mineralization (~42-35 Ma) was discovered at the Carlin Gold Mine.

The Paleozoic rocks are cut by Eocene-aged magmas and overlain by a range of Tertiary volcanic rocks. A diorite from Scrapper Springs produced a K-Ar age of 38.9 ± 1 Ma, and the volcanics range within a few million years from the intrusive bodies (Wallace, 2005; Howell, 2007, Figure 5). Granodiorite exposed in the Tuscarora volcanic caldera complex- the Mount Neva granodiorite, near Scrapper Springs- produced an Ar/Ar age of 39.37 ± 0.28 Ma (Henry and Boden, 1999). For comparison, The ages of alkaline porphyry intrusions from Bingham Canyon, UT- one of the largest open pit mines in the world- range from 38.6 to 37.8 Ma (Parry et al., 2001).

Eocene activity in this portion of Nevada are part of an overall north to south trend of magmatism extending from the older 54-47 Ma Colville province in eastern Washington, the 51-40 Ma Challis volcanic field in central Idaho, and the 43 Ma and younger magmatism in northern Nevada and the Great Basin (Figure 6, Christensen and Yeats, 1992, Castor et al., 2003).

Multiple caldera complexes within the region are likely the sources of these volcanic units; rocks in the Scrapper Springs region include ignimbrite ash flow, air-fall and lithic tuffs, volcanoclastics, and diorite stocks.

Rift faulting in the mid-Miocene the Northern Nevada Rift (NNR) occurred with localized volcanism, and hypabyssal basalt and gabbro; hydrothermal fluids along the structures produced several deposits of extensive gold-silver mineralization.

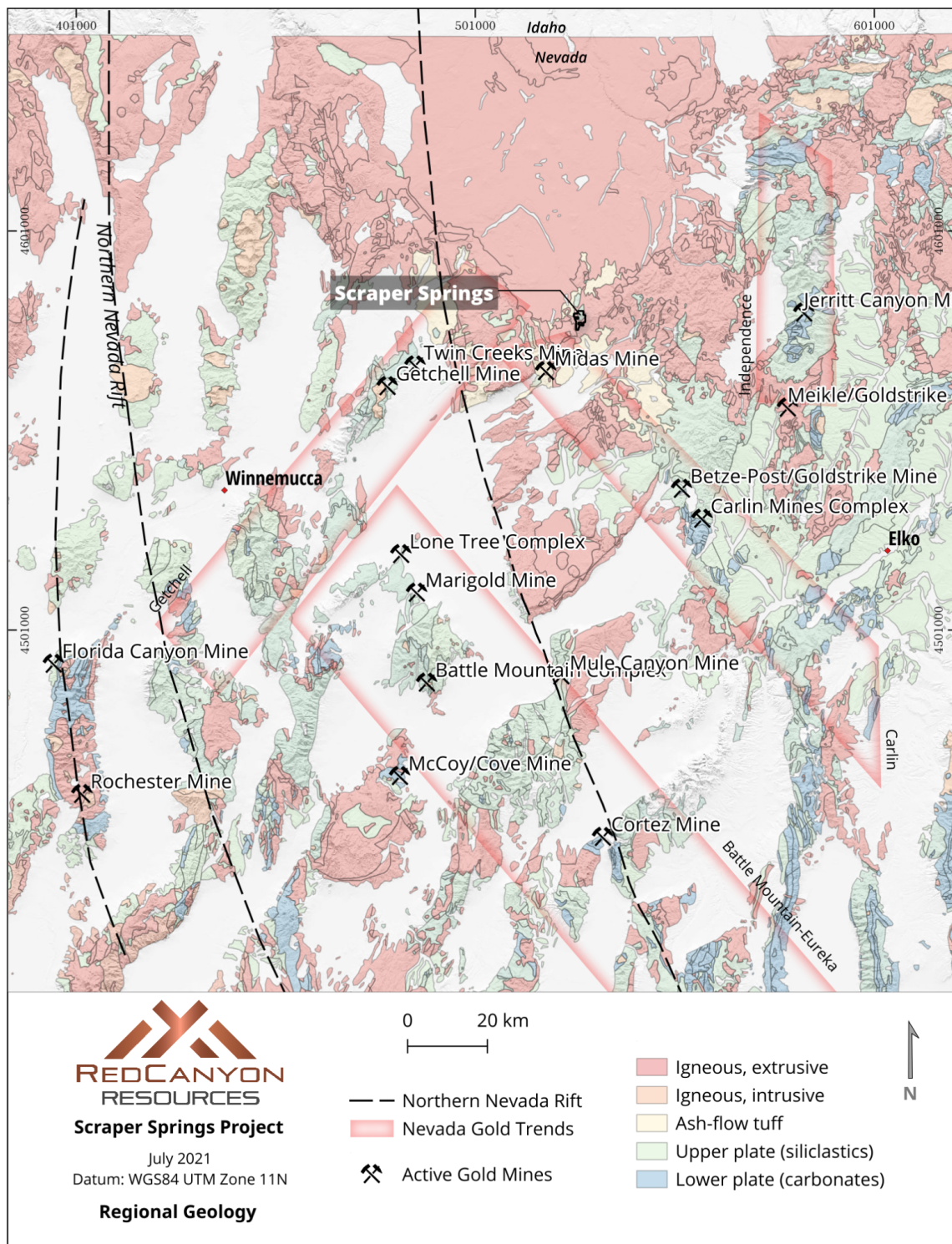


Figure 5. Regional geology in North and central Nevada showing generalized lithology, regional gold trends, active gold mines and trend of the Northern Nevada Rift (NNR).

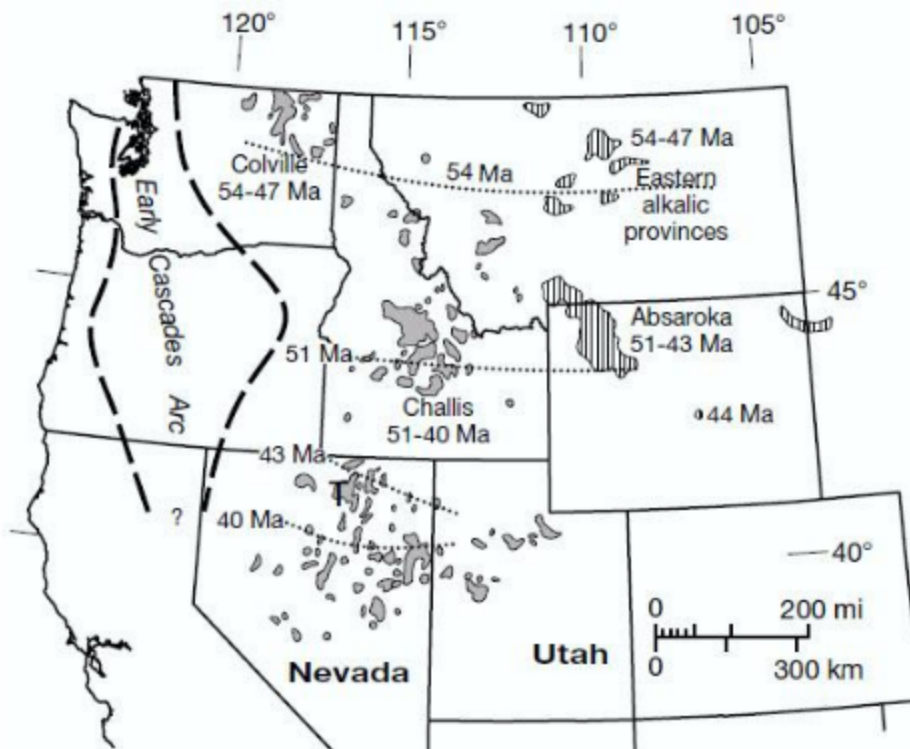


Figure 6. Tertiary magmatism in the North American cordillera (Castor et al., 2003).

7.2 Regional Mineralization

Mineralization in the region includes both Eocene-aged Carlin-type gold deposits along the Carlin trend to the south-southeast, and Miocene-aged epithermal vein deposits related to the Northern Nevada Rift (NNR).

The Midas mine is the largest known Au-Ag epithermal deposit along the NNR and belongs to a suite of middle Miocene low-sulfidation epithermal gold and silver mineralized systems associated with magmatism and secondary faulting. Mineralization at Midas occurs within a shallow low-sulfidation system containing steeply-dipping quartz-calcite-adularia precious metal veins; is associated with electrum, selenide and sulfide minerals; and hosts grades greater than 10 oz/t gold locally.

Southwest of the Project, the Hollister Mine hosts Miocene-aged gold mineralization within volcanic tuffaceous units, andesites, and the Ordovician Vinini Formation. High-grade gold and silver mineralization sit within banded quartz veins in a group of near-vertical faults and fissures that trend west-northwest to east-west between one hundred to several thousand feet. The host

rocks have been strongly altered by hydrothermal fluids with large areas of chalcedonic replacement bodies at the paleo water table and sinter deposits (Allen et al, 2020).

Further afield and approximately 200 miles to the east sits the Bingham Canyon, UT, copper-molybdenum-gold porphyry deposit. Production estimates from the mine are more than 16 Mt of copper, 24 Moz of gold, 190 Moz of silver, and 400 Kt of molybdenum (adapted from Bon and Krahulec, 2007, with annual production estimates from Rio Tinto website access 2023). Total production grades vary, with averages ranging near 0.6% Cu, 0.2 g/t Au, 0.04% Mo and 2 g/t Ag.

7.3 Regional Structure

The Northern Nevada Rift ('NNR', Figure 5) is strongly coincident with mineralization at Newmont's Mule Canyon Mine, Hecla Mining's Hollister and Midas Mines, and Klondex's Fire Creek Project. These mines share similar mineralization characteristics, epithermal textures, trace-elements, discrete high grades of Au and Ag, mid-Miocene ages of mineralization (15.1-15.6 Ma) and close temporal association with the Miocene host rocks (John et al., 2003; John, 2001; Leavitt et al., 2004; Wallace, 2003).

The NNR originated at the McDermitt caldera, in northwest Nevada, site of the initial eruption of the Yellowstone hotspot, and propagated 500 km to southeast Nevada (Zoback et al., 1994). The rift is readily visible on regional aeromagnetic maps as a narrow positive anomaly striking approximately 250 km and is further defined by an accumulation of basaltic to dacitic lava flows and dikes of mid-Miocene age (John et al., 2000). The NNR has been mapped within the central portion of the rift, between the Malpais Rim and Midas, where John et al. (2000) defined a 5- to 30-km wide, north-northwest-trending zone that corresponds to a magnetic high with anomaly-parallel mafic dikes and high-angle normal faults, overlain by middle Miocene volcanic flows

The primary extension direction during rift development and magmatism at 16.5 – 15 Ma was ENE to WSW, perpendicular to the axis of the rift. These syn-rift faults sharply bound the present-day NNR on the west and decrease towards the east. From 10 Ma to about 6 Ma, the regional stress field rotated clockwise, resulting in an extension direction that was NNW-SSE (Zoback et al., 1994). This resulted in the formation of horst and graben faults that cut the NNR to form ENE-trending grabens such as the Midas Trough, the Argenta Rim, and the Malpais Rim (Figure 5). Gold mineralization at the Midas Mine is structurally controlled by normal faults within the NNR, typical of rift-hosted epithermal style mineralization associated with an intrusive center (Zoback et al., 1994).

7.4 Project Geology

7.4.1 Ordovician Vinini Quartzites

Tertiary volcanic rocks and shallow igneous intrusions on the Project have been eroded to expose the Paleozoic Ordovician Vinini Formation (Ov), the primary local unit of the Upper Plate assemblage overlying the Roberts Mountain Thrust. Individual lithologies within Ov include siltstone, fine heterolithic sandstone, black chert, and argillites (Howell, 2004). Quartzite (Ovq) forms distinctive ridges in the north central Project area and hosts medium to coarse-grained sand that is clean, at nearly 100% quartz (Howell, 2004; Cantor and Thompson, 2012).

Ovq is commonly brecciated with a clast-supported matrix; locally, the breccias are matrix-supported and host sub-angular to sub-rounded quartzite clasts. It is unclear whether this brecciation is a result of hydrothermal events or tectonic events, though faults are mapped east of this Ovq exposure suggesting probable tectonic association (Cantor and Thompson, 2012, Figure 7).

7.4.2 Pennsylvanian-Permian Carbonaceous Sandstones

The Pennsylvanian-Permian Edna Mountain Formation (PPem) and younger Permian Havallah Sequence (Ph) are projected to occur underneath the Tertiary volcanic cover, unconformably-overlying the lower Paleozoic sequences, throughout north and eastern Nevada. These rocks were deposited as detritus from the denudation of the ancestral Rocky Mountains during the Antler Orogeny (Roberts, 1964).

The Edna Mountain Formation comprises limey silts, sandstones, and cherty conglomerates with a heterolithic assemblage of lithics and black chert clasts, and minor phosphorus-rich shale beds in a package up to several hundred feet thick (Howell, 2004).

The Havallah Sequence (Ph) overlies the Edna Mountain Formation along the Golconda thrust fault; members of the Havallah comprise various beds of black chert, sandstone, siltstone, and limestone each ranging as much as 2,000 or more feet in thickness.

These rocks are not exposed within the Project area. The sole major unconformity mapped in the center of the Project places Tertiary volcanics over the Vinini quartzites, but the Permian carbonates may exist elsewhere below Tertiary cover.

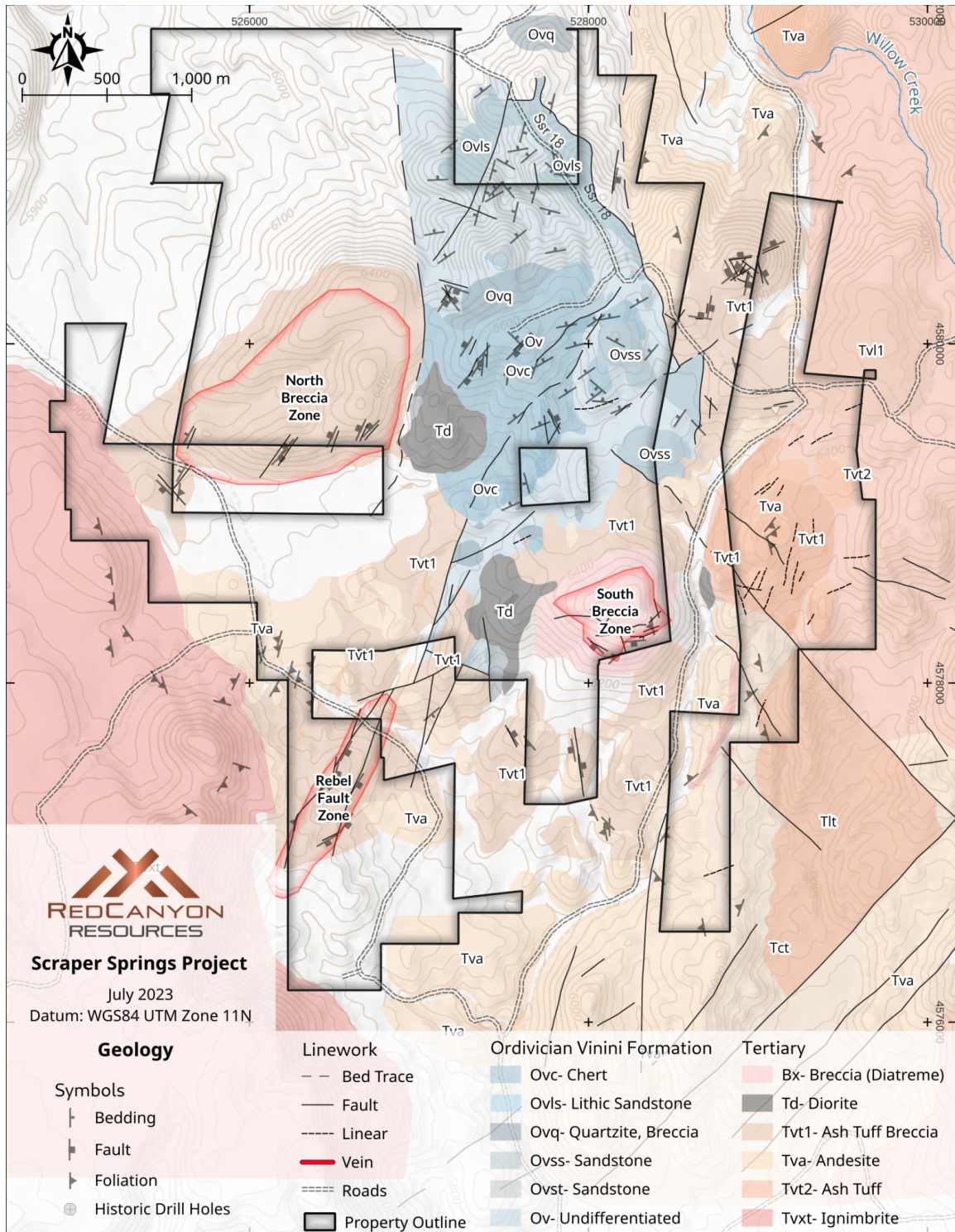


Figure 7. Scrapper Springs geologic map (adapted from J.M Wise, 2008).

7.4.3 Tertiary Volcanics

Tertiary-aged felsic rocks are abundant throughout the Basin and Range Province, largely related to a system of magmatism that youngs to the south across western USA. The volcanism ranges from felsic to intermediate, from rhyolite tufts, domes and caldera complexes to andesitic ash flows and minor mafic constituents.

Within the Project area, Tertiary volcanics are dated as late Eocene age (ranging from 39-37 Ma, Wise 2008), and likely contemporaneous and coeval with the diorites. Furthermore, these volcanics are altered with high sulphidation advanced argillic and argillic assemblages, indicating that one or more hydrothermal events is not older than 37 Ma.

The oldest and most voluminous rock type in the greater area is an ignimbrite (Tvxt, ~39.3 Ma) that occupies the east and western flanks of the Project area. Tvxt comprises crystalline and glassy pumice-rich ash-flow tufts, thin layers of vitrophyre, and tuffaceous volcanoclastics (Howell, 2004, age dates by Wise, 2008).

Internal to the Project sit felsic, ash-rich tufts (Tvt, ~39.3 Ma), and are commonly bleached, silicified and cut with quartz-stockwork and/or quartz breccia. Tvt contains fine quartz and sanidine phenocrysts (5- 10%) with less common hornblende and plagioclase, and cherty lithic fragments derived from the underlying Paleozoic sedimentary rocks. The density of phenocrysts and moderately-welded lithic fragments within the Tvt reportedly increase in proximity to the center of the Project area.

Intruding and/or interlayered with Tvt are andesite flows (Tva, ~37.3 Ma). Tva is a porphyritic volcanic rock containing plagioclase, hornblende, quartz, and local pyroxene phenocrysts, are olive-green to olive-tan and form both subcrop and prominent outcrops throughout the Project. These andesites host illite and minor dickite, kaolinite alteration (see Hyperspectral, below), but further fieldwork should seek to resolve the timing of the andesite volcanics and their relationships to the timing of faulting, mineralization and alteration.

External to the Project, Miocene-age volcanism and related volcanoclastic rocks indicate a younger, and the most recent expression of volcanic activity in the greater area.

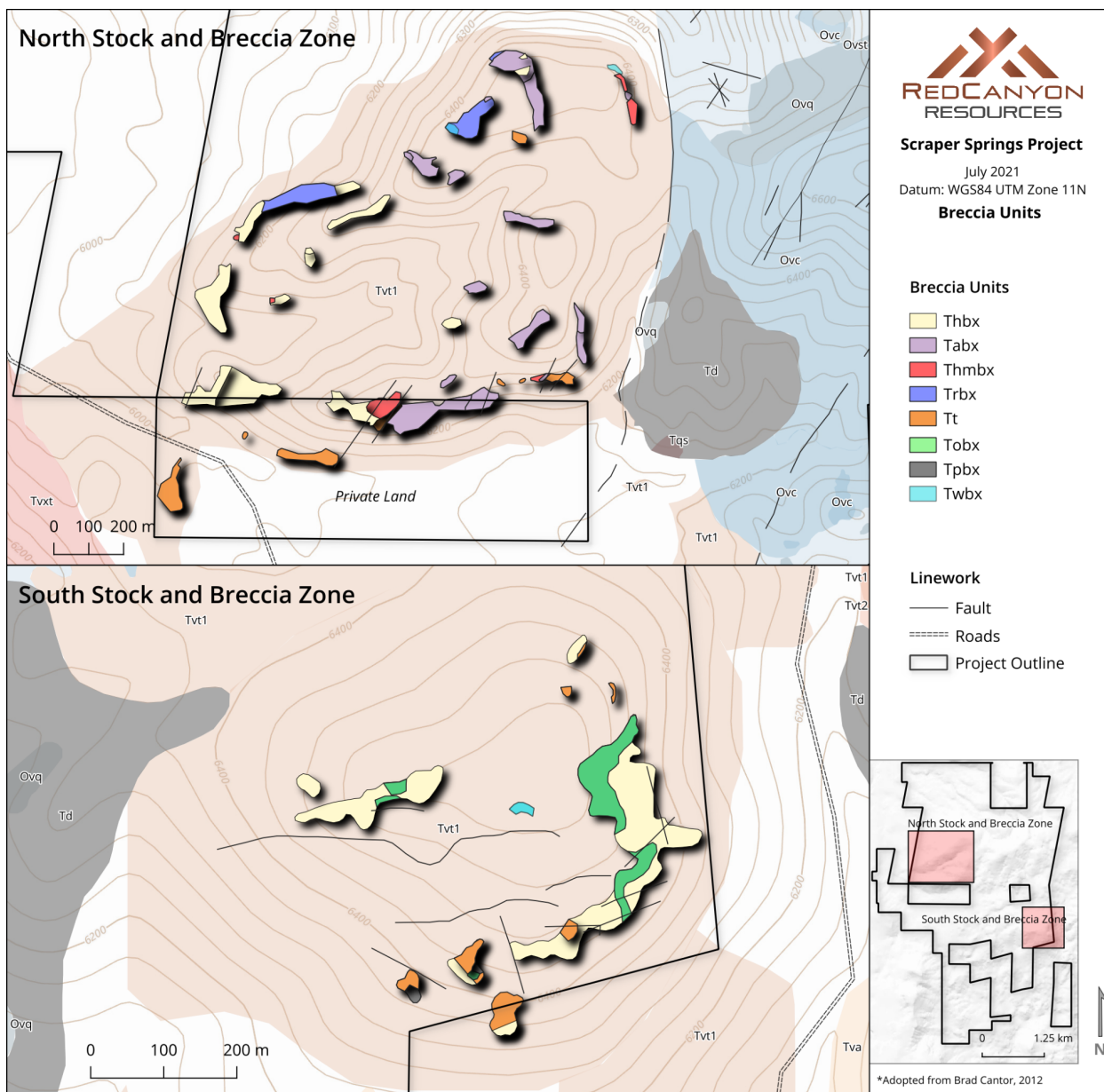


Figure 8. North and South Breccia Zones outcrop maps (Cantor and Thompson, 2012).

7.4.4 Breccias

Two breccia complexes sit adjacent to each of the diorite intrusive units (Td), labeled the North and South Breccia Zones after the North and South Stocks, respectively (Figure 8). These breccia units are associated with silification and advanced argillic alteration.

Six breccia types occur in the North Breccia Zone (from Cantor and Thompson, 2012):

Thmbx - “Contains rounded breccia clasts, with the hematite-matrix as the supporting material, including advanced argillic clasts of various advanced argillic assemblages, secondary breccia clasts, and vuggy silica clasts”.

Twbx - “Matrix-supported and rounded to sub-rounded clasts of 2 mm to 1 cm in diameter with massive or vuggy silica alteration”.

Trbx - “Heterolithic variably-sized sub-rounded to sub-angular clasts. Mostly silicified or altered to vuggy silica and does not exhibit obvious advanced argillic clasts”.

Thbx - “A heterolithic breccia with sub-rounded to sub-angular clasts, usually derived from other breccias. Acid sulfate breccia and vuggy silica clasts are common in this lithology, as well as pervasive red Fe-Ox”.

Tabx - “A distinctive advanced-argillic breccia easily recognized by its intense goethite-jarosite staining. It is both matrix- and clast- supported and contains clasts of vuggy silica and various advanced argillic assemblages”.

Tt - “Unit of tuffsite, a sub-volcanic lithology, occurs along structures in association with other breccias. Locally brecciated, includes fine-grained, leucocratic and ashy material that is locally silicified. Distinct sub-rounded cherty clasts, 2-4 mm, are included within this unit and likely represent material from the underlying Paleozoic stratigraphy”.

Five breccia types occur in the South Breccia Zone (from Cantor and Thompson, 2012):

Twbx - As described in above section, also occurs in north breccia and stock zone, spatially associated with and containing clasts of *Tobx* in the South zone.

Tobx - “This orange breccia is mostly matrix-supported and contains rounded to sub-rounded breccia clasts between 2 mm and 1 cm in diameter. Most of the alteration associated with *Tobx* is siliceous with a distinctive area on the east displaying an advanced argillic-jarosite stained signature”.

Thbx - As described in above section, also occurs in north breccia and stock zone.

Tpbx - “This purple breccia is matrix supported with rounded, cherty clasts on the centimeter-scale, and is commonly vesicular. *Tpbx* contains clasts of *Tt* within its matrix near these contacts and it can be determined that it was emplaced after the *Tt* unit. It is likely that *Tpbx* is also a type of tuffsite unit, as it shares similar characteristics as *Tt*”.

Tt - As described in above section, also occurs in north breccia and stock zone.

7.4.5 Eocene Intrusives

Two plugs of an Eocene intrusive rock are exposed within the Project (Figure 7). Cantor (2012) describes these intrusions as diorite with phaneritic to locally porphyritic textures and plagioclase-rich with minor (<10%) quartz and alkali-feldspar. Alkali feldspar and biotite occur within this intrusion as both primary and alteration products; plagioclase and quartz dominate the primary mineralogy. The diorite holds an Eocene, nearly Oligocene, K/Ar age date of 38.9 ± 1.0 Ma (Wallace, 2005). Networks of diorite stringers and dykes were also intercepted in drilling.

7.5 Project Structure

The predominant structures are visible as tight, north-northwest striking faults across the Project area that juxtapose Tertiary volcanics into western and eastern blocks separated by a window of Ordovician Vinini in the center.

The North Stock and Breccia Zones, and the South Stock and Breccia Zones both sit along two independent and possibly coeval, northeast-trending systems of faults (Figure 7).

The diorite intrusions and brecciated zones occur along the western-most of these basement faults, but the existing Project data does not discern if these bodies cut or are cut by this faulting.

The North Stock and Breccia Zones, and the South Stock and Breccia Zones both sit along two independent, and possibly coeval, east-northeast trending fault systems that are 200m-500m wide and cut both the Tertiary and Paleozoic rocks. At the Project scale, subordinate faults within each of these systems display an internal en-echelon or strike imbrication that imply top-left sinistral shearing.

Potentially symbiotic with this fault is a long and narrow north-northeast system of splays that strike from the southwest (Rebel Fault Zone) to the northeast connecting both the North and South fault systems.

The orientation of these east-northeast trending fault systems, and the Rebel Fault Zone are each consistent with lineations and trends in fabric of the background magnetic anomalies located further to the southeast (Figures 9 and 16).

An unconformity occurs in the central block, close to the Southern Stock and Breccia Zone. This unconformity isolates an erosional age gap between the Vinini and the overlying Tertiary volcanic rocks. Information in this area is sparse and should be inspected further.

The breccias are complex. It is unclear from field relationships whether the breccias are a result of hydrothermal or tectonic events, though their location along the east-northeastern fault systems suggest a tectonic affinity (Cantor and Thompson, 2012).

Structures within the Vinini sediments carry iron oxides, barite, minor thin quartz veining and/or silicification (Howell, 2007).

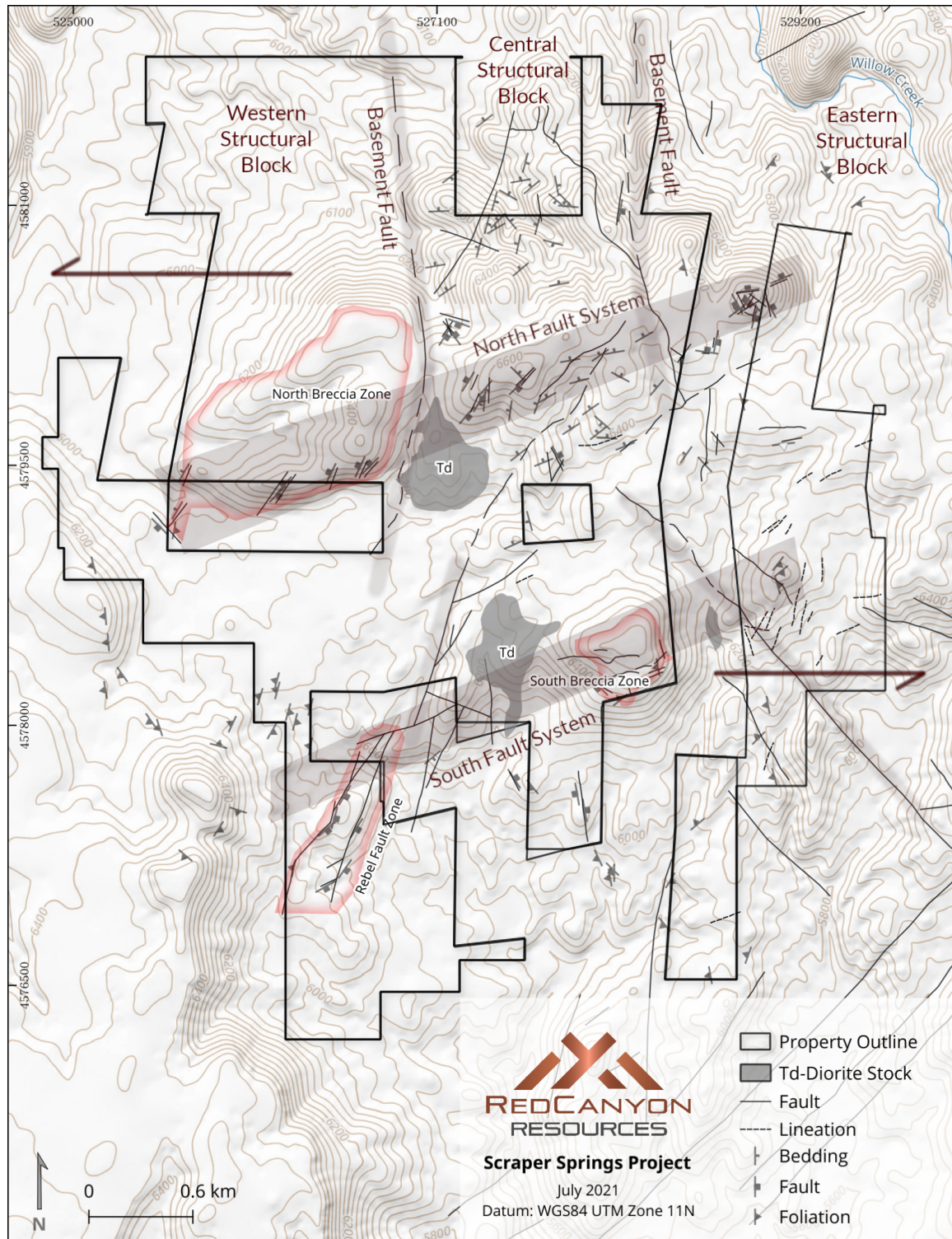


Figure 9. Structure, interpretations and potential stress field.

7.6 Project Mineralization

Gold, silver, and copper mineralization occur in a variety of styles and alteration assemblages at Scrapper Springs (Figures 10, 11). Typical to epithermal vein deposits, mineralization within the tuffaceous rocks comprise:

- (1) Massive silicification and bleaching over broad areas hosting local, weakly-anomalous gold generally coincident with advanced argillic alteration (quartz-zunyite-alunite).
- (2) Pronounced quartz veining along north-northeast trends with irregular but highly-anomalous gold and silver, specifically within the Rebel Fault Zone Area.
- (3) Disseminated gold mineralization in altered and hornfelsed Ordovician sediments adjacent to the diorite intrusives.
- (4) Porphyry-related base metal and copper mineralization in altered Ordovician sediments at depth.

A significant zunyite occurrence sits within the north and northeast parts of the Project (Figure 11). The largest occurrence at Scrapper Springs is hosted within what has been referred to as a “huge zunyite lode,” which is a vein striking approximately 1200 ft long and ranging between 10 and 60 ft wide. This vein crops out on the eastern margin of the Project and consists of intergrown quartz and zunyite, comprising up to 75% zunyite locally (Coats et al., 1979).

Highly fractured and In the southwest area of the Project, along the Rebel Fault Zone, sit epithermal quartz-gold-silver veins with several highly anomalous grab samples and associated soil anomalies.

The northern exposure of Vinni Formation is broadly altered to hornfels (Howell, 2007). Here, Au-bearing skarn mineralization is hosted along the contact with the diorite intrusion (Cantor and Thompson, 2012). This mineralization style was explored by Western States Minerals in 1994-1997 through several drill holes, intercepting anomalous gold mineralization in advanced argillic alteration assemblages. Within the diorite intrusion, pyrite occurs as disseminations and veinlets in the groundmass and with locally-anomalous chalcopyrite (Cantor and Thompson, 2012).

Mineralization within the Paleozoic sedimentary rocks is more representative of “Carlin Type” gold mineralization (CTGD); the Upper Plate Ordovician Vinni at Scrapper hosts disseminated gold mineralization in alterations zones along the margins of the Tertiary diorite intrusives, and Lower Plate rocks at depth- if present- may represents a reactive horizon yet explored. Drilling in 2003 intercepted rocks interpreted as the Lower Plate (Devonian Rodeo Creek Formation) that coincided with anomalous copper and zinc (Howell, 2007).

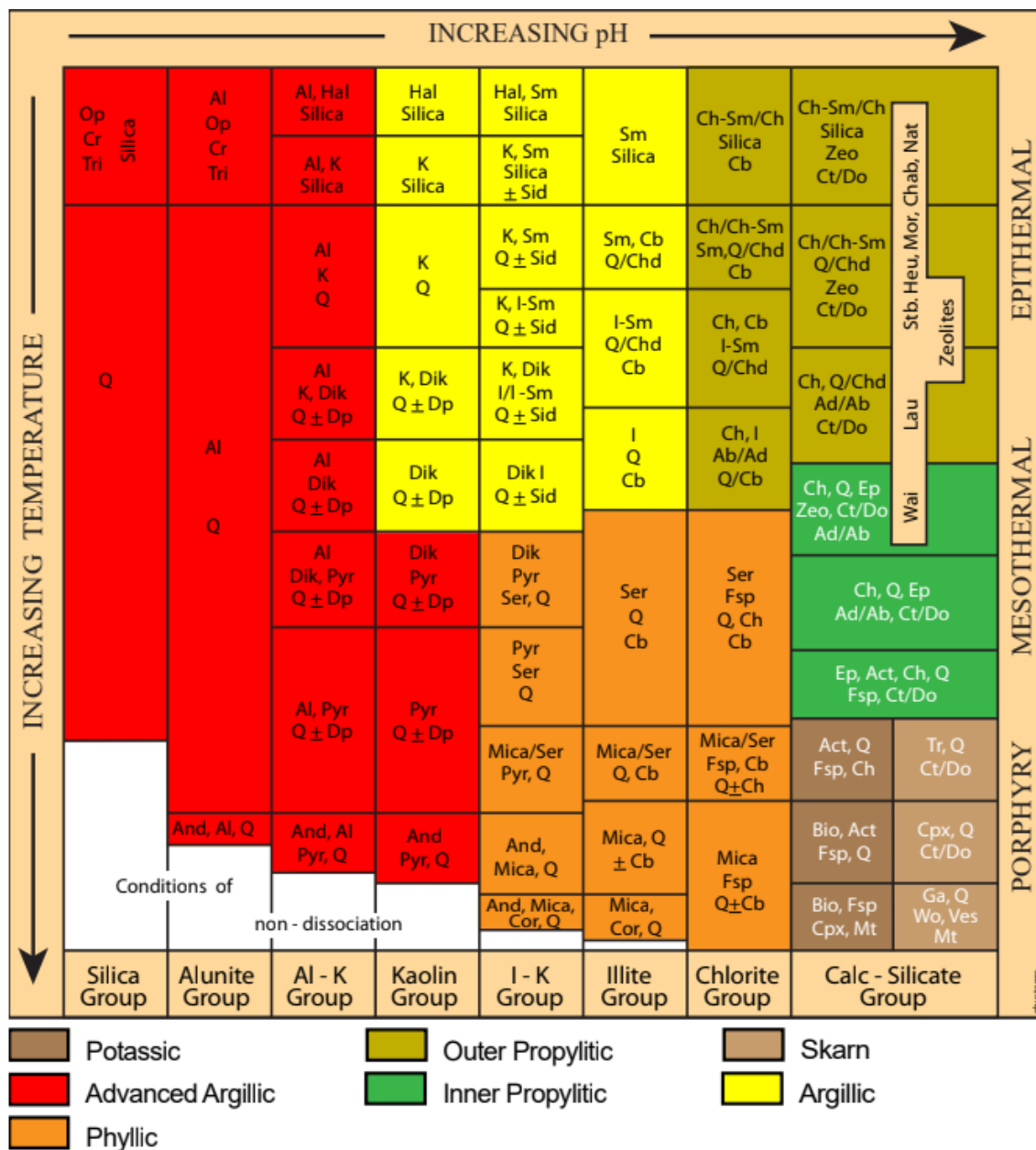


Figure 10. Alteration assemblage diagram (Corbett and Leach, 1997).

7.7 Alteration

Alteration analysis was performed by J.M. Wise (2008), and later by Brad Cantor (2012) who derived several assemblages from field mapping. Alteration zones include silicification, argillic, advanced argillic, endoskarn (North Stock only), zones of moderate K-feldspar alteration ranging

from moderate (15-29%) to strong (30-50%) and flooded (>50% K-feldspar, restricted to Tqs), silicification and advanced argillic zones.

7.7.1 Silicification

Silicification occurs in various forms throughout the Project area. Intense silica flooding has been mapped along the Rebel Fault Zone area and described along the boundaries of the diorite and breccia bodies. Reticulite quartz discretely occurs in the North diorite, where it is associated with hematite (Cantor and Thompson, 2012).

Opal sits adjacent to and within the South Breccia Zone; chalcedony also occurs within the South Breccia Zone as cross-cutting veinlets at the outcrop scale, in quartz vugs, and along veinlet margins in thin sections (Cantor and Thompson, 2012).

Vuggy silica is generally coincident with zunyite and other advanced argillic alteration assemblages throughout the Project. It also occurs in a band of outcrops forming a perimeter around the northern margins of the project.

7.7.2 Argillic

Field mapping describes clay alteration overlapping vuggy silicification, which is common, and likely indicates retrograde alteration. The hyperspectral work performed by Newmont (2008) displays broad distributions of illite and kaolinite throughout the area with a general concentration of dickite in the north, and very broadly-distributed montmorillonite (a common kaolinite alteration product).

7.7.3 Advanced Argillic

The most common advanced argillic assemblage mineral on the Project is the low-pH alunite, occurring often with zunyite and iron oxides. Pyrophyllite and diaspore, a high-temperature, low pH advanced argillic assemblage, sit north of and extend into the eastern portion of the North Breccia Zone, trending east-northeast.

Late kaolinite-quartz occurs in the North Breccia Zone and occupies quartz vugs, veinlets cross-cutting breccias, and the breccia matrix.

7.7.4 Quartz-Sericite-Pyrite (QSP)

Drilling the South Breccia Zone in 2008, Newmont intercepted quartz-sericite-pyrite underlying the advanced argillic alteration. Pyrite in this area reaches from 15 - 30% up to a metre-scale and occurs with elevated molybdenite. QSP alteration is also observed by Cantor (2012) in the SC-series drill holes from Cordex in 2004 within the central zone of the Project. The sericite is in name only, represented by illite, mixed illite/smectite, or muscovite.

7.7.5 K-feldspar Alteration

Cantor (2012) described potassic alteration within and surrounding the diorite intrusions. His field work documented k-feldspar encountered during staining of a leucocratic diorite, and k-feldspar flooding within the adjacent feldspar crystal tuff (Tvt, with flattened pumice fragments). Flooded groundmass and veinlets of k-feldspar are also described within thin sections. Biotite is described within the diorite stocks but the research is currently underdeveloped with respect to timing and primary/secondary alteration. Additionally, Cantor encountered a syenite intrusion body located within the North Stock.

The importance of k-feldspar as an alteration mineral lies within its formative temperature and pH window; higher than the conditions for adularia, implicating a potential shift away from the acidic advanced argillic alteration zones of an epithermal environment toward a more neutral and higher-temperature, intrusion-related core.

7.7.6 Endoskarn

Endoskarn mineralization, a carbonaceous assemblage of minerals derived from an intrusive host, is pervasive within the North Stock. Pyroxenes are aligned in coarse crystal bands with quartz gangue and are greenish-blue in color. Na-Cobaltinitrite staining of this assemblage also revealed the occurrence of K-feldspar (Cantor and Thompson, 2012).

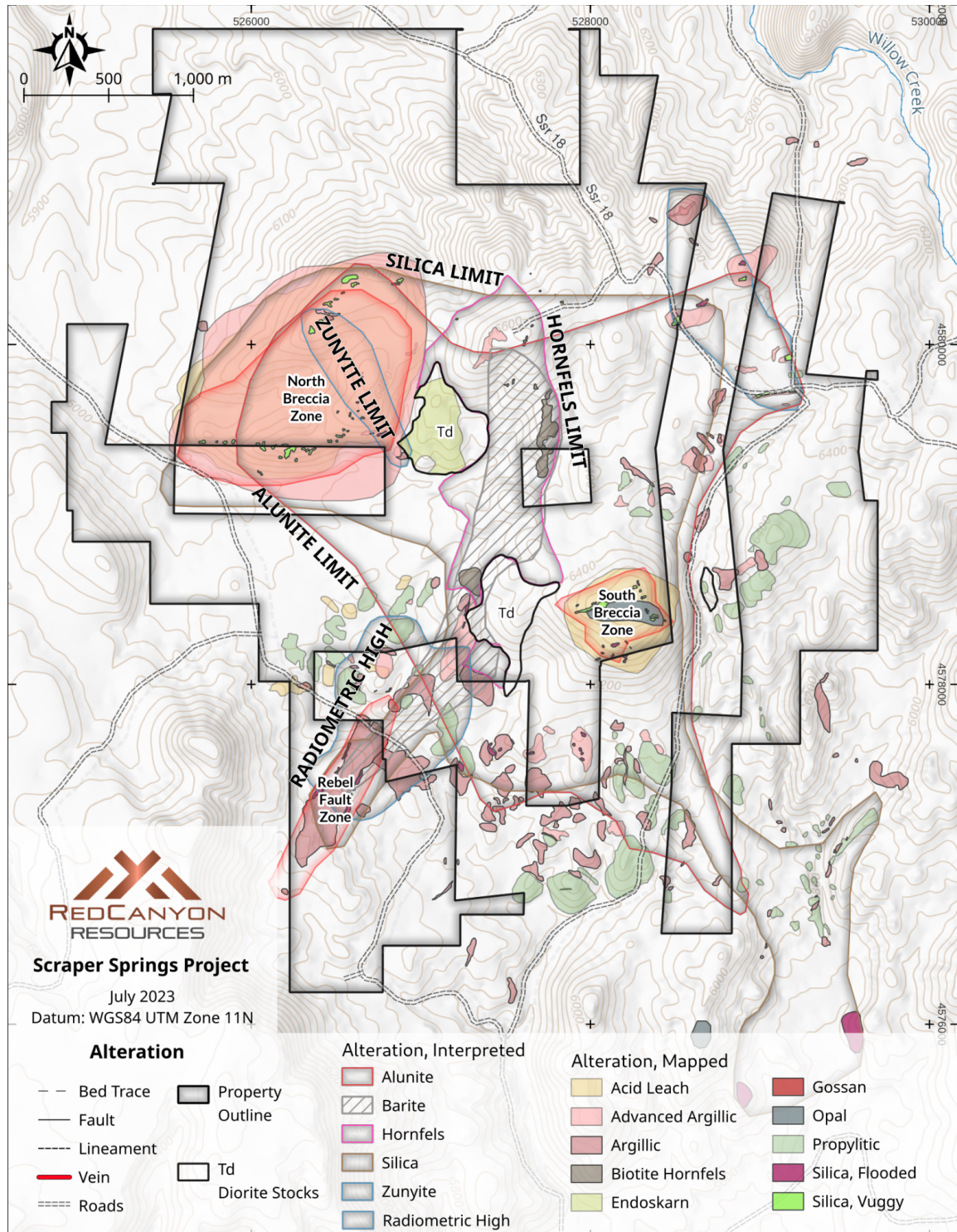
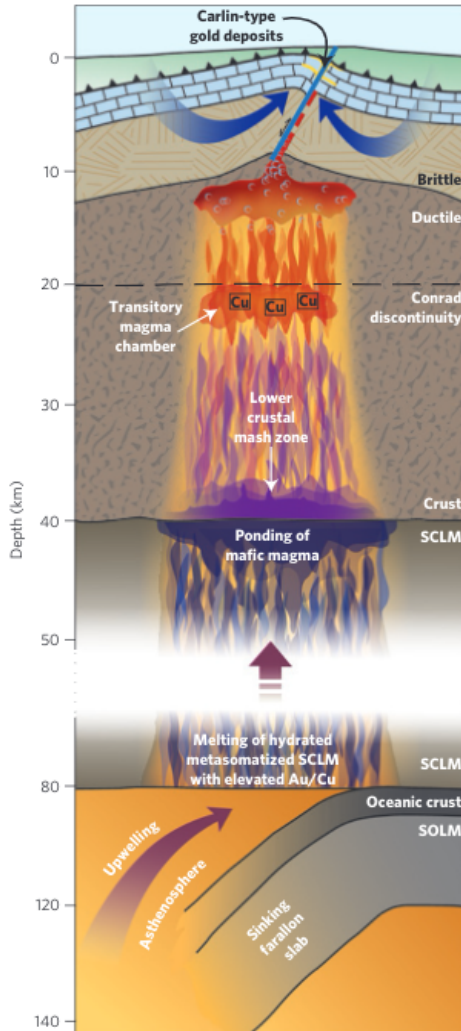


Figure 11. Project alteration map adapted from Wise (2008).

8 DEPOSIT TYPES

8.1 Carlin-Type Gold Deposit



“Carlin Type” (CTGD) gold mineralization occurs in both Paleozoic Upper Plate siliciclastic rocks, (Vinni Formation) outcropping as a tectonic window in the central portion of the Project and underlying Lower Plate carbonate rocks.

CTGD mineralization forms as structurally and/or stratigraphically controlled replacement bodies that host disseminated gold mineralization within stratabound and tabular horizons or discordant breccias in Silurian-Devonian, thinly bedded silty or argillaceous carbonaceous limestone or dolomite and carbonaceous shale or less frequently, within overlying siliciclastic rocks (Figure 12, Miranda et al, 2019).

Like epithermal deposits, CTGD mineralizing events are relatively short lived.

Figure 12. Schematic cross section showing the evolution of Carlin-type gold deposits from mantle to crust. SOLM= suboceanic lithospheric mantle. SCLM=subcontinental lithospheric mantle (Miranda et al, 2019).

8.2 Epithermal Au-Ag

Epithermal Au-Ag deposits form in the upper crust at temperatures that range from 100 to 300° C. Most systems are genetically related to subaerial volcanism and related intrusive activity, or

continental rifting. Diatremes, calderas, and lava domes are common lithologic features of epithermal systems (John et al, 2010).

Epithermal systems may be separated into subtypes by their acidity: high sulphidation epithermal environments are relatively highly acidic; low sulphidation, in contrast, contain neutral to slightly alkaline chemistry. North-central Nevada reportedly hosts numerous low-sulphidation veins in Eocene volcanics that contain anomalous gold, such as those associated with the Tuscarora Au-Ag district.

High sulphidation systems often present very low pH fluids below the paleowater table and display vuggy quartz coring outer adjacent quartz-alunite, kaolinite, dickite and advanced argillic assemblages. Low sulphidation systems, with a more intermediate pH, often contain adularia and or carbonate minerals within their core and electrum, silver sulfides and sulfosalts or tellurides as their ore mineralogy. Silica sinters are present within many low sulphidation environments but nearly absent from all high sulphidation environments (John et al, 2010).

Most epithermal systems are unique products reflecting the local inhomogeneities present in the host geology. However, steam-heated argillic and advanced argillic alteration assemblages commonly occur above the paleowater table at both types, and distal propylitic and argillic alteration are also common.

Epithermal systems range from low to moderate temperatures (100-300 C) through argillic to intermediate and/or advanced argillic alteration, often increasing in acidity as the system evolves. Though temperatures may reach mesothermal gradients, epithermal systems are often short-lived due to their occurrence near surface/ higher portions of the earth's crust (compared to porphyry systems).

8.3 Epithermal Quartz-Alunite Au

A specific subset of epithermal deposits are high-acid quartz-alunite related gold (+/- silver), of which numerous styles have long been recognized throughout the southwestern USA, and historically have significant development within the Goldfields district of the Walker Lane trend in southwestern Nevada. The host rocks are intensely-altered felsic volcanics- intrusions, plugs and domes- that often form portions of more regional volcanic complexes (eg Miocene mineralization at Goldfield, NV) and may be cored by porphyry intrusions at depth (e.g. Summitville, CO and suspected at Goldfield, NV, Figure 13).

These deposit styles are characterized by central vuggy silicic ledges and brecciated zones containing advanced argillic alteration, and Fe/Cu/As-rich sulfides. These areas are flanked by argillic and distal propylitic zones. The associated deposit types include porphyry copper, porphyry gold-copper, and porphyry copper-molybdenum (Cox and Singer, 1986).

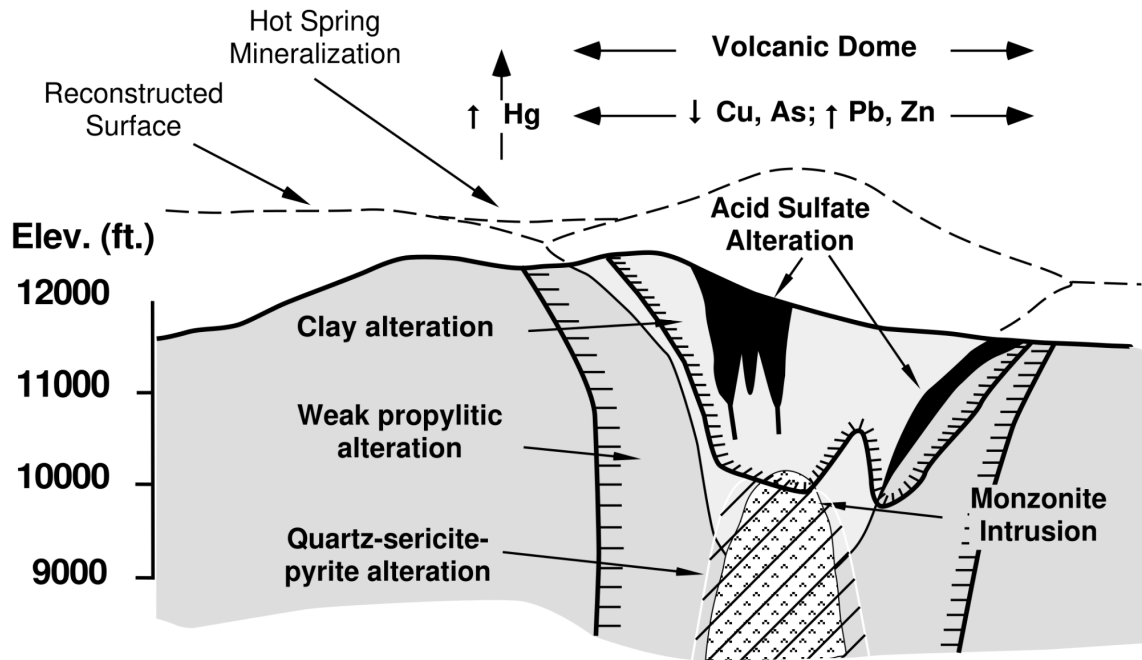


Figure 13. Schematic cross section of alteration through a generalized Goldfield, NV, and Summitville, CO quartz-alunite hydrothermal system with a moderate pH intrusion system at depth (Plumlee et al 1996).

8.4 Polymetallic Au-bearing Skarn

Polymetallic Au-bearing skarn mineralization may be hosted where Paleozoic sedimentary rocks contact with the diorite intrusion. This type is marked by skarn alteration of the host diorite-endoskarn- identified by greenish-bluish color and coarsely crystalline, aligned pyroxenes (Cantor and Thompson, 2012). Western States Minerals drill targeted this type of system at Scraper Springs in 1994-1997, intercepting 140 ft @ 0.017 oz/t Au in SS-1, and 25 ft of 0.020 oz/t Au (Howell, 2007, not verified).

8.5 Porphyry

The majority of porphyry Cu–Au deposits are associated with large volumes of hydrous calc-alkaline magmas (high Sr/Y) derived from melts driven from subducting oceanic plates rising into the overlying continental crust (Hedenquist et al 1998). Metal endowment increases with repeated cycling of magma and hydrothermal activity. Alteration minerals associated with base-metal rich porphyry systems are moderate-high pH, and range through epithermal to mesothermal and higher temperatures. These porphyry systems form over 10's of millions of years, and the thermal profiles of a porphyry system are complex and longer lived resulting from the repeated activity and deeper formation in the earth's crust (Corbett and Leach, 1997).

Due to the cumulative size and clustering of the magmatic sources, alteration zones may extend great distances away from the porphyry centers and will often range from adjacent potassic alteration (k-feldspar, hematite, magnetite, plagioclase, biotite-chlorite) through phyllic alteration (quartz, sericite, plagioclase, chlorite-mica) to distal propylitic (sodic feldspar, chlorite, pyrite, epidote). Advanced argillic alteration also can occur within overlying lithocaps and along late structures cutting copper-porphyry systems.

Porphyry intrusions typically encounter episodic rapid cooling in active structural regimes, characterized by small to large isolated crystals supported within fine-grained chilled groundmass. Disseminated, clotty, and vein-hosted mineralization in porphyry environments can be hosted within the parent sources, the adjacent host rocks, within breccias and cross-cutting structural networks (Sillitoe, 2012, Figure 14).

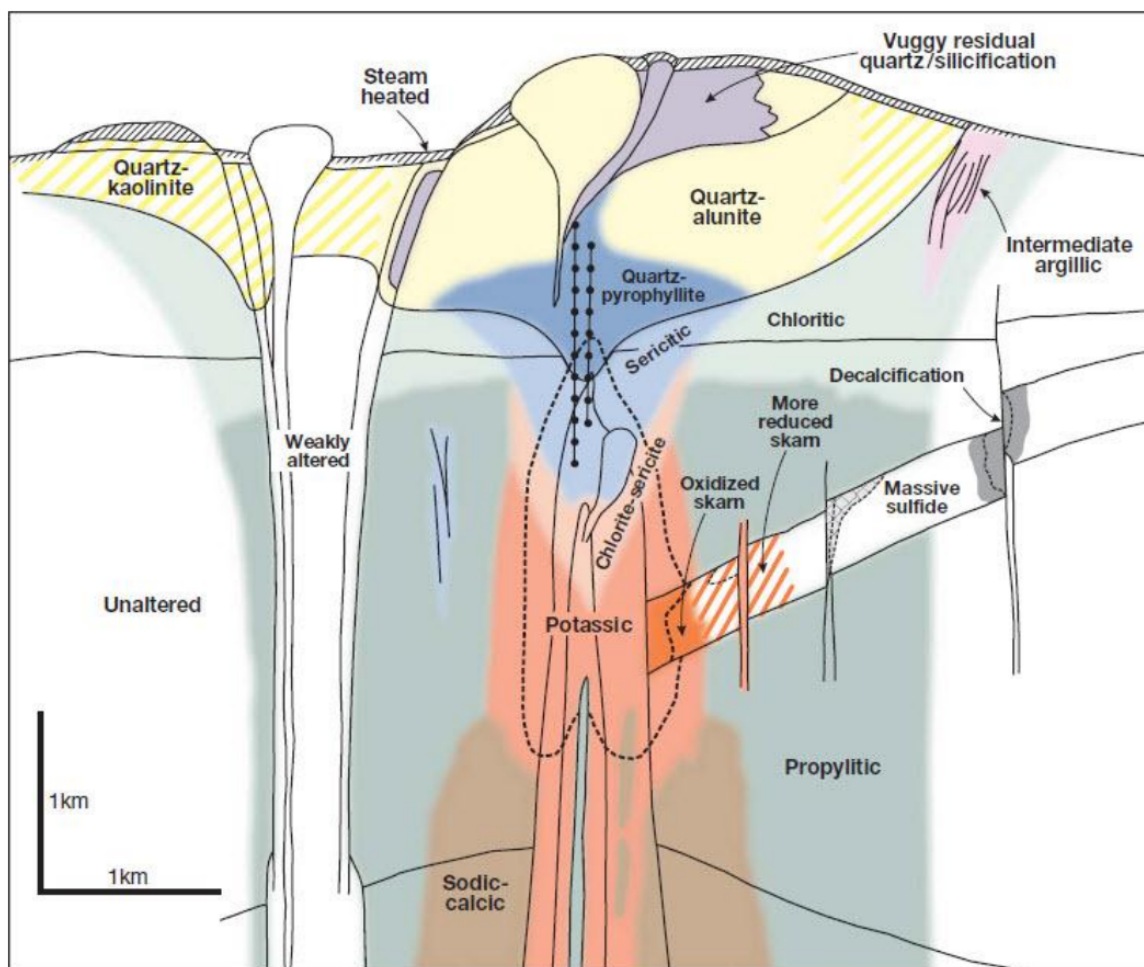


Figure 14. Telescoped porphyry system model (Sillitoe, 2010).

9 EXPLORATION

9.1 Geophysics

9.1.1 Regional Isostatic Gravity

Isostatic gravity maps are useful for examining density contrasts in the earth's crust. For example, intrusion centers and large sulphide bodies are likely to exhibit high density, while fault zones, limestones and unconsolidated sediments may exhibit low densities.

The isostatic residual gravity method subtracts long-wavelength anomalies from the Bouger anomaly map that are assumed to result from isostatic compensation of topographic loads deep within the crust or mantle. Isostatic anomalies therefore reveal density distributions within the upper crust that are of interest in many geologic studies (USGS, 1998). The USGS published an isostatic gravity map for the conterminous United States in 1998, with a surface pixel resolution of approximately 250m.

Figure 15 highlights that Scraper Springs, Goldstrike (Betze), Carlin, and the Jerritt Canyon Mines all share proximal relationships to high isostatic gravity anomalies. The anomaly at Scraper Springs may represent an intrusive center at depth; the anomaly should be evaluated with higher resolution ground-based methods and may yield vectors toward a porphyry magmatic source.

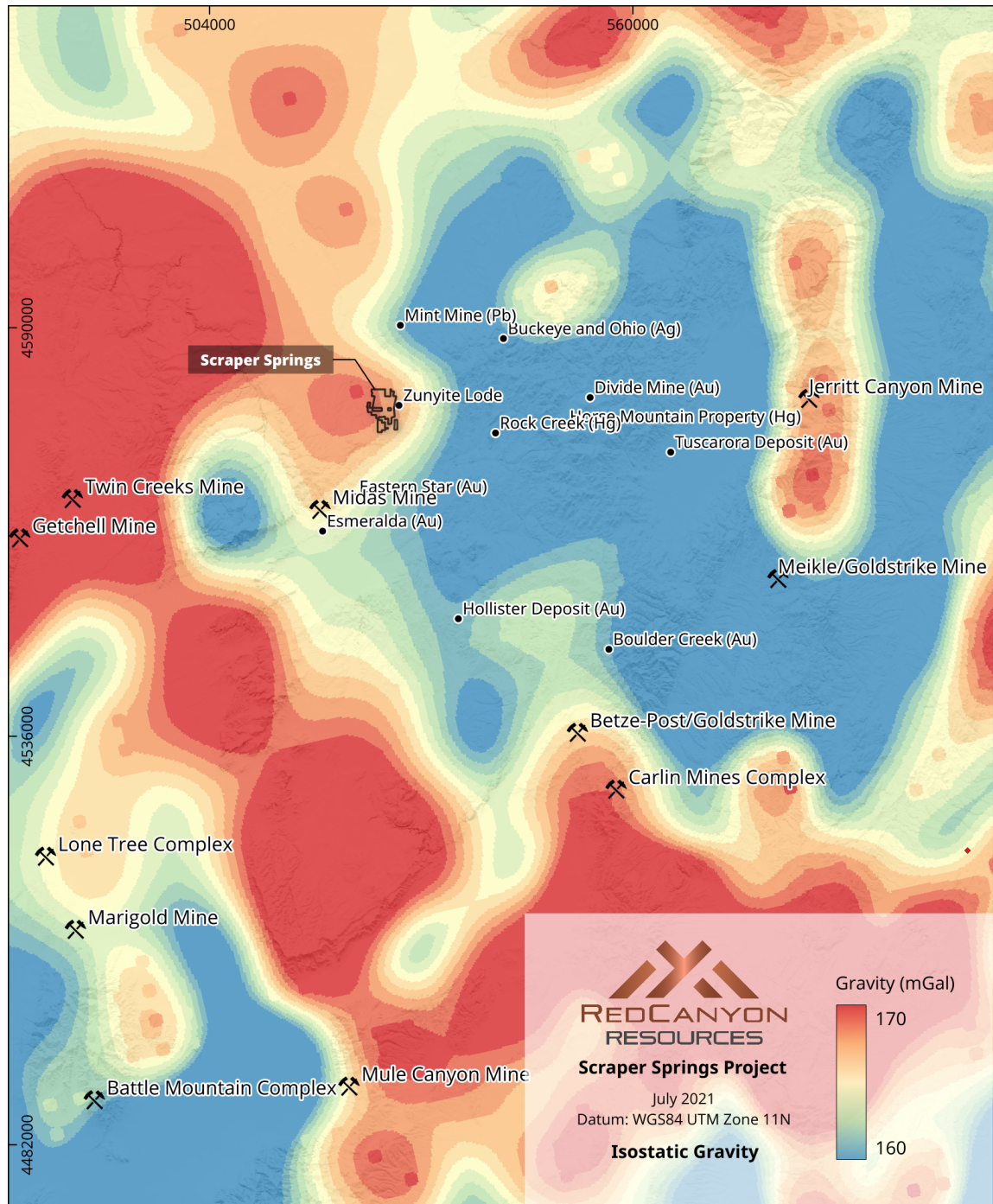


Figure 15. Regional isostatic gravity map of the greater Scrapper Springs region (USGS, 1998).

9.1.2 Ground Magnetic Survey (2004)

Zonge Geosciences, Inc. performed a GPS-based ground magnetic survey on the Scraper Springs Project for Cordex in 2004. The first phase of the survey was conducted during the period of 07 April to 10 April, and was extended to the south from 27 May to 29 May. Magnetic data were acquired on 37 east-west lines spaced 400 feet apart for the general survey, and 200 feet apart in the area of interest. A north-east to south-west diagonal line over the area of interest and one north-south tie line were also collected for a total of approximately 60 line-miles of data acquisition (Figure 16).

The magnetics data express two distinct patterns: broadly anomalous coverage in the northwest, and tight discrete coverage in the southeast.

Anomalies within the northwestern portion spatially coincide with the North and South diorite stocks and indicate these stocks are magnetic relative to the host rocks. These anomalies exhibit tight south-western boundaries and broadly-dipping northeastern zonation, such that they may be interpreted as dipping to the northeast. Alternatively, the two breccia zones coincide with moderate-low magnetism and may represent a mag-destructive event with sharp boundaries.

Tight, discrete linears in the magnetics along the southeastern portion align along a distinct northeast-striking trend, which is also weakly-reflected in the broader anomalous coverage in the northwest of the Project area, and coincident in orientation with the Rebel Fault and related northeast-striking fault system.

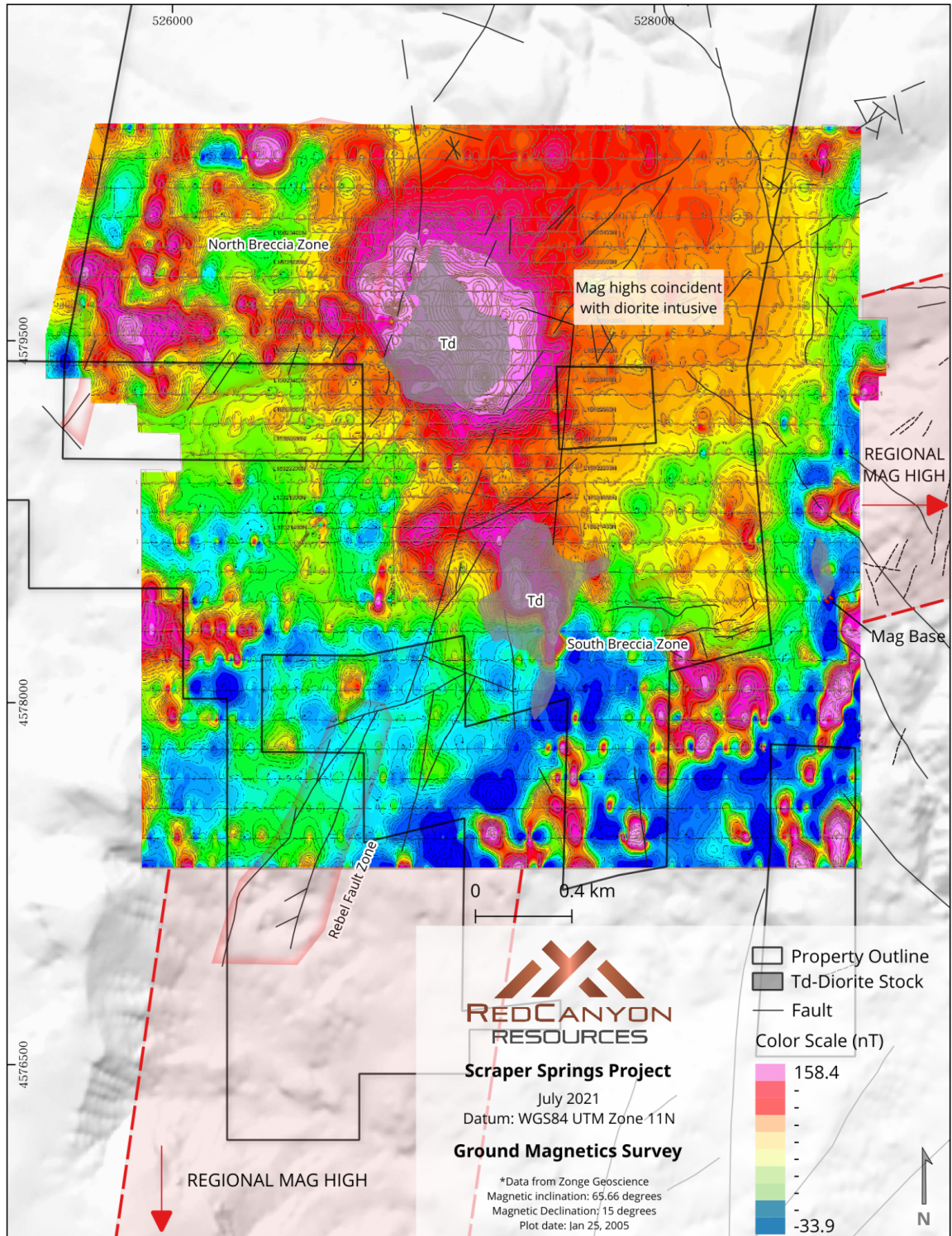


Figure 16. Ground magnetics survey from Zonge Geoscience for Cordex (2004) showing total magnetic field intensity in nT, upward continued to 10 ft and reduced to pole.

9.1.3 Hyperspectral Imaging (2008)

Newmont acquired a hyperspectral survey covering Scraper Springs in 2008. This work was contracted from a joint data acquisition campaign by SpecTIR, using SpecTIR's Eagle and Hawk dual sensor and Aerospace Corporation's SEBASS systems mounted in the same aircraft. SpecTIR sensors captured the visible wavelengths (VNIR, 400-970 nm) and short-wave infrared (SWIR, 970-2450nm); SEABASS sensors captured data in the mid-infrared (MIR, 3-5.5 μ m) and Thermal Infrared (TIR, 7.8-13.5 μ m).

At Scraper Springs, the SpecTIR data confirmed the existence and general extent of the mapped alteration and succeeded in identifying broader high-temperature zones for further investigation.

Broadly, montmorillonite is a common surficial alteration of kaolinite, which are both widespread and likely related to surface weathering. Silica accompanies this assemblage over wide patches in the lower elevations, but it is unclear if this is a result of true silicification or surface sedimentation isolating quartz grains.

Illite and muscovite ("sericite") occupy the general north central area coincident with the exposure of Vinini quartzites, in the central structural block. This assemblage, with further field testing, may represent a quartz-sericite alteration present through the Vinini (as it is at depth).

Alunite predominantly occupies brecciated areas and halos around the stocks, in Tertiary and Vinini altered rocks. Alunite can occur over a wide range of temperatures and with a variety of minerals but its assemblage with dickite and pyrophyllite pins the fluid system as mildly acidic with mesothermal temperatures (Figure 10).

Both dickite and pyrophyllite sit along the northern and southern northeast-trending fault systems and breccia zones.

Zunyite occurs with alunite in the volcanics where they are cut by a northeast-trending system of faults through the North Stock and Breccia Zones; zunyite may implicate an important series of fluid conduit(s) (Zhang, 2020). However, Howel (2007) reports that the hyperspectral imaging did not catch the 'large zunyite vein', the reasons for which should be considered (Figure 17).

Structural controls on both silica and white micas are seen distal to the high-temperature phases but reflect the same ENE trend and an additional NNE trend. In a system with such strong alteration and such clearly defined high temperature zones, if mineralization is not seen in the core of the system, there may be some justification in testing the more distal structures as defined by the silica-muscovite trends (Agar, 2008).

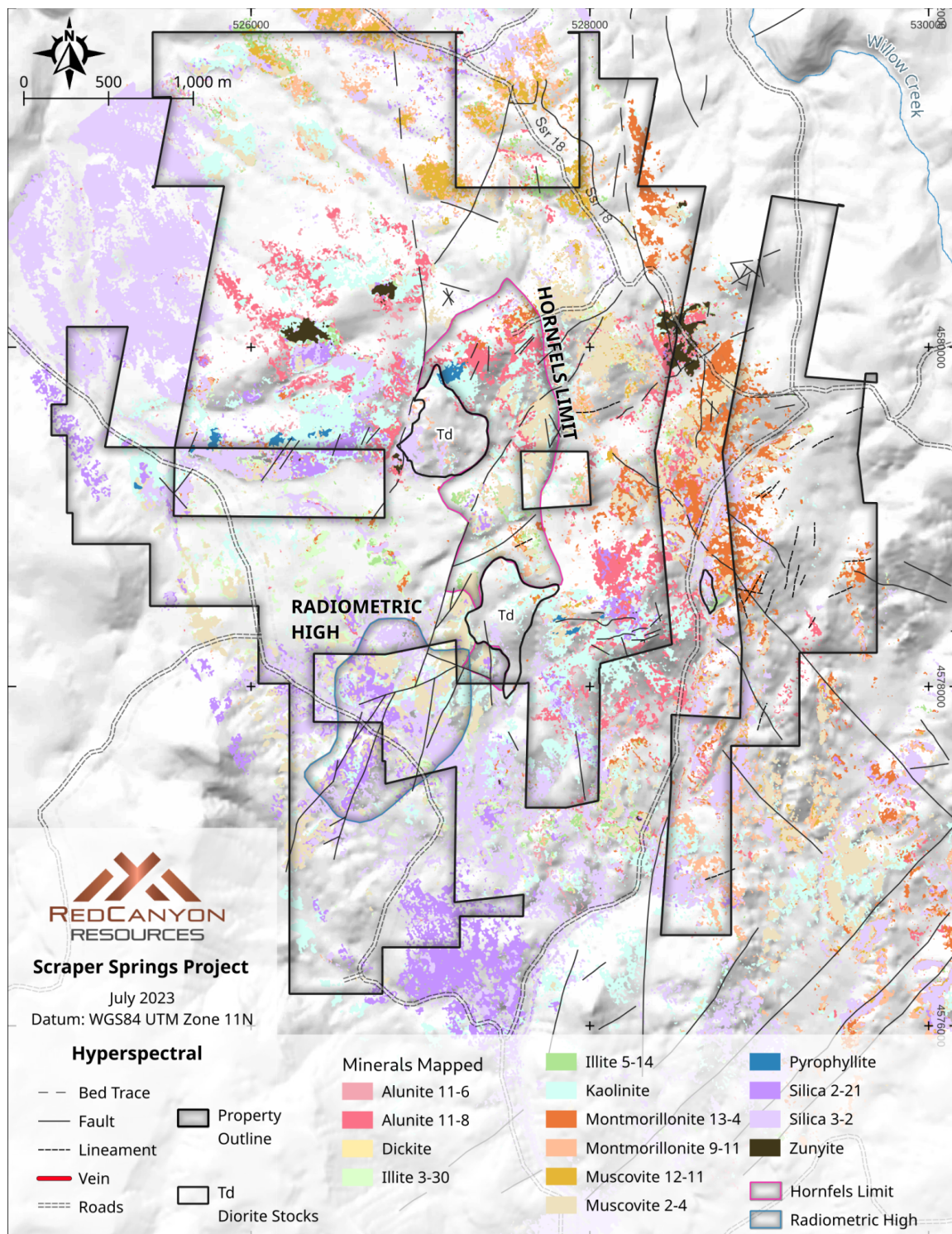


Figure 17. Hyperspectral composite map of alteration minerals (Newmont, 2008).

9.1.4 Induced Polarization (IP) & Resistivity Survey (2008)

In 2008, Zonge Geoscience was contracted to perform an Induced Polarization (IP) and Resistivity survey covering the area on and around the diorite stocks. Two lines trend east-northeast (lines 1 and 2) and eight lines (lines 5000, 5300, 5600, 5900, 6200, 6500, 6800 and 7100) trend northwest (Figure 18). Unfortunately a report covering the IP geophysics was either not produced or is unavailable at this time, but the IP calculated sections are included in Appendix D.

The IP and resistivity surveys distinctly show discrete, relative chargeable and resistivity anomalies associated with the Tertiary diorite stocks. Several additional discrete anomalies coincide with zones of faulting and brecciation.

Line 6065's calculated section extends from the northwest across a fault juxtaposing the Tertiary volcanics with the Vinini, across a two diorite stocks (the former at surface in the Vinini and the southern at surface in the Tertiary volcanics), along the South Breccia Zone (Figures 18, 19).

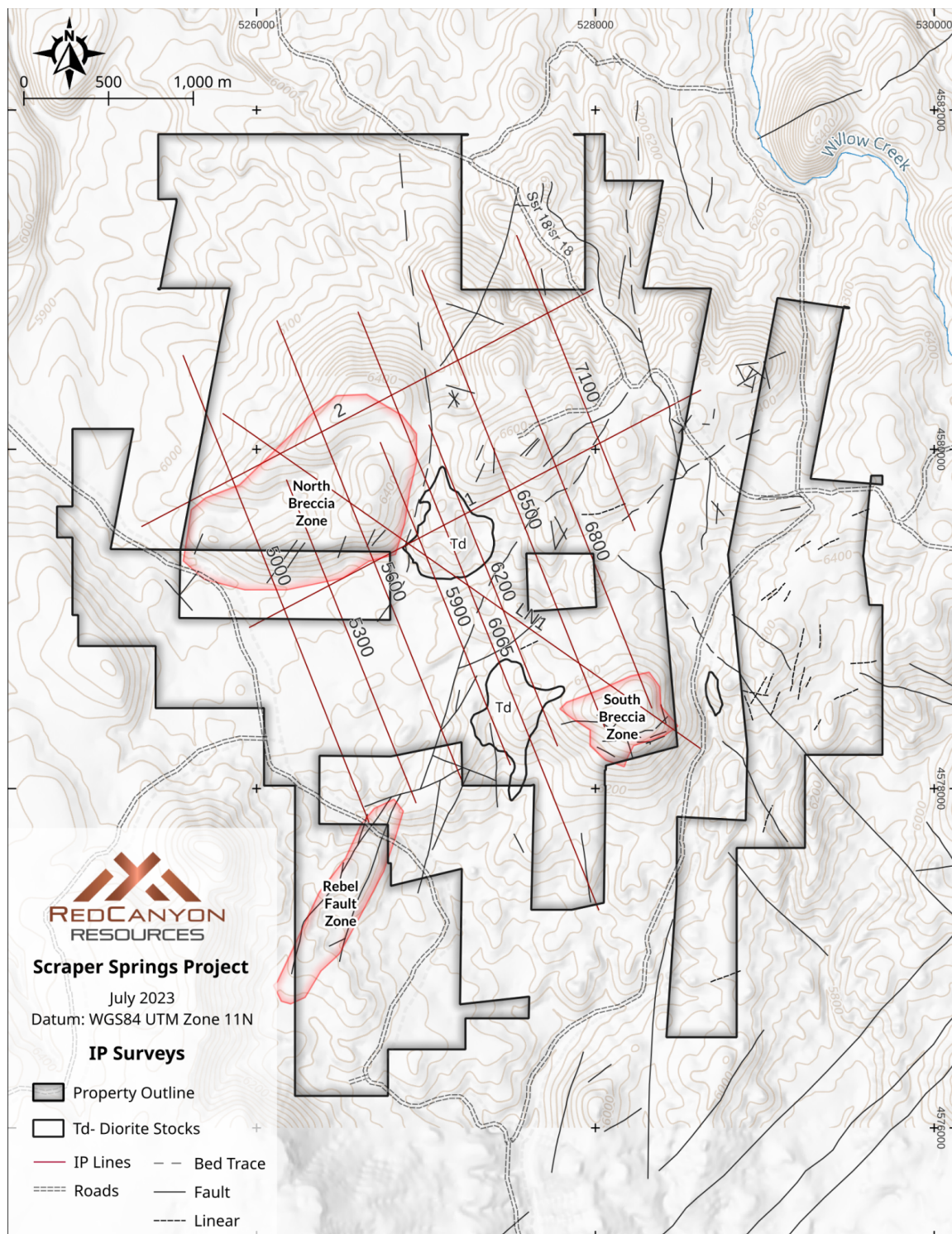


Figure 18. IP line locations from Newmont, Cordex and Red Canyon.

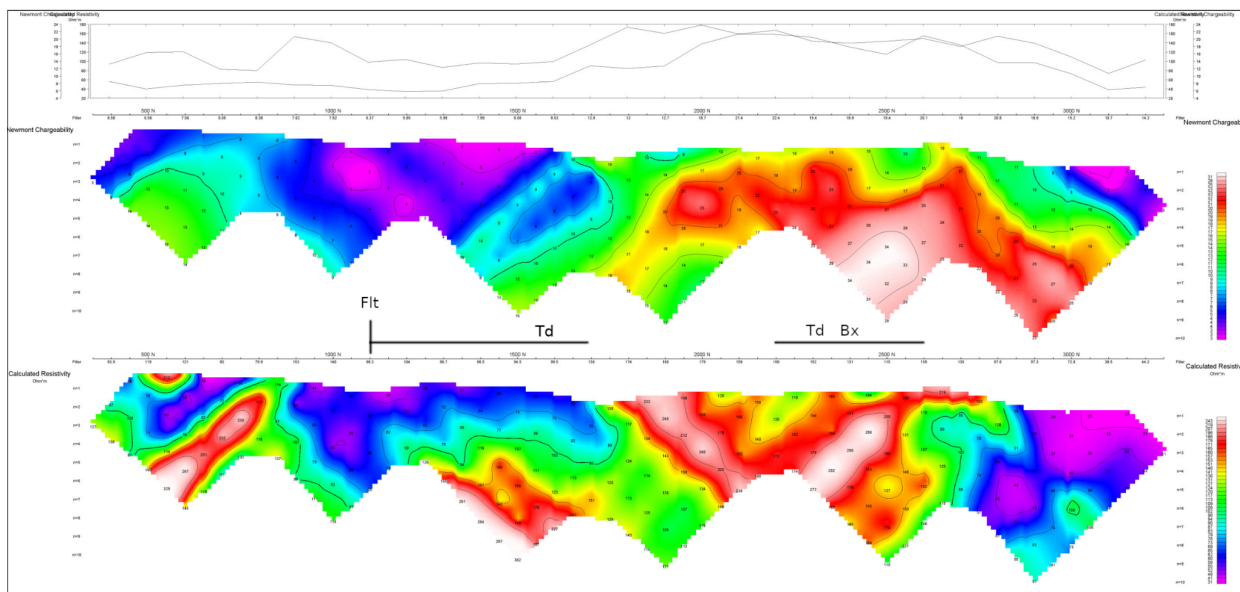


Figure 19. IP survey line 6065 showing interpreted chargeability (upper) and resistivity (lower) across at least one major basement fault (Flt), two diorite stocks (Td) and the South Breccia Zone (Bx).

Resistivities are usually in the range 10–30 Ωm . Resistivity values may decrease to less than 10 Ωm in areas of advanced argillic alteration, often due to the presence of clay minerals, and increase in Ωm in areas of quartz - mica (propylitic) alteration.

The stock's chargeability of 17-30 mV/V implicates the chargeable response could be due to sulphides; the high resistivity of the diorite stocks (140 - 250 Ωm) implies that the host is significantly silicified and thus, if present, the mineralization is disseminated (Dusabemariya et al., 2020). The chargeable and resistivity plots do not express total parity however, and may indicate sulphides or other alteration minerals are not evenly distributed throughout the stocks - sites of higher chargeability (> 15 mV/V) and lower resistivity (< 10 Ωm) within/adjacent to the stocks could be further explored.

The responses across the stocks indicate that they are both chargeable and resistive, they do not exhibit the same explicit signature, and the host Vinini is significantly less chargeable than the Tertiary volcanics (or developed unique alteration characteristics).

Chargeability is governed by sulphides that may be associated with alteration proximal to the stock and dikes. Pyrite concentrations generally increase away from intrusions and into regions of sericitic alteration. Thus, the greatest chargeability is expected to lie somewhat outboard of the mineralizing source.

Newmont additionally created a 3D IP interpretation and two horizontal plan maps (depth slices) at 1750 and 1800 m elevation. These maps illustrate 1) lower resistivities and chargeabilities coinciding with the diorite intrusions (especially coincident with the North stock), 2) generally-higher chargeabilities and resistivities relating to the Tertiary volcanic rocks (Figure 20).

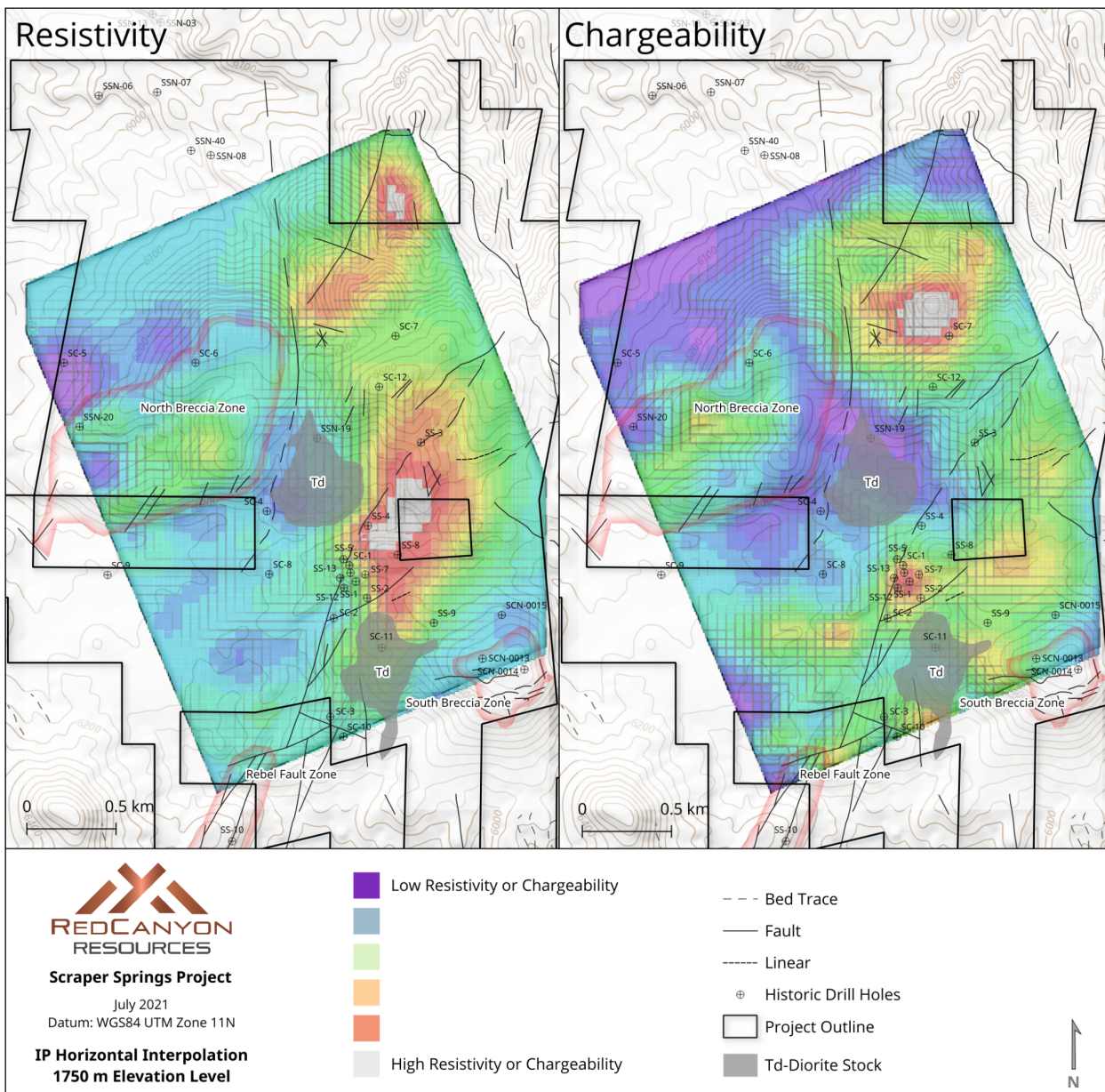


Figure 20. Plan view of IP resistivity and chargeability horizontal interpolation at 1750m elevation above sea level.

9.1.5 Induced Polarization (IP) & Resistivity Survey (2021)

In 2021, Zonge Geoscience was contracted to perform an Induced Polarization (IP) and Resistivity survey comprising 3.3 line-kilometres of coverage. Line 1 transected the property northwest-southeast, with dipole length (a-spacing) of 300m (Figure 21).

Data was acquired using the ZEN distributed array system, developed and manufactured by Zonge. Two-channel receivers were left active during acquisition along the entire length of the line, in both the leading and trailing directions of the active transmitter dipole. This permitted acquisition of n-spacings up to 8.5. The receiver wire was run along the line and two transmitter wires were offset from the receiver wires by 50-metres to minimize coupling.

The data show coincident chargeability and resistivity highs at shallow depths below the prominent knob associated with the South Breccia Zone (Figures 22 and 23). This breccia unit is paired with intense silification and acid leach alteration. The chargeability anomaly forms two coalescing peak highs, where the northernmost peak is directly below a resistivity high of a greater intensity.

A sharp contrast at the top of the chargeability high, close to surface, and a gradational contrast at the bottom of the chargeability high indicate that the mineralization has an apparent southeast dip.

A weaker chargeability high occurs at roughly 750 metres depth in the SW-central portion of the IP line. This chargeability high is moderately coincident with a resistivity high that extends to surface.

The geometry of resistivity highs indicates a shallow dip to the NW, likely expressing the dip of the chert within the stratigraphy. The geometry of the chargeability highs indicates a shallow dip to the SE, likely expressing fluid and alteration conduits formed through faulting and fracturing within the South Fault System.

It is important to note that pervasive clay minerals associated with argillic-propylitic alteration zones cause low-resistivity anomalies comparable in size to the original geothermal system. While resistivity decreases in the presence of interconnected sulfide grains or argillic alteration, some parts of hydrothermal alteration zones may have high resistivity because of increased concentrations of silica, including zones of quartz veins, chalcedony, sinter terraces, and lithocaps (Irvine and Smith, 1990; Hedenquist and others, 2000).

At Scrapper Springs, the apparent lack of resistivity anomalies likely indicate that the silicification is overprinting, or more intense than the argillic alteration. A high chargeability in IP suggests that sulfides are present within the acid leach cap (Wise, 2008). Given this, the most prospective targets identified by the IP survey are where chargeability and resistivity highs coincide, or where resistivity highs are directly above chargeability highs.

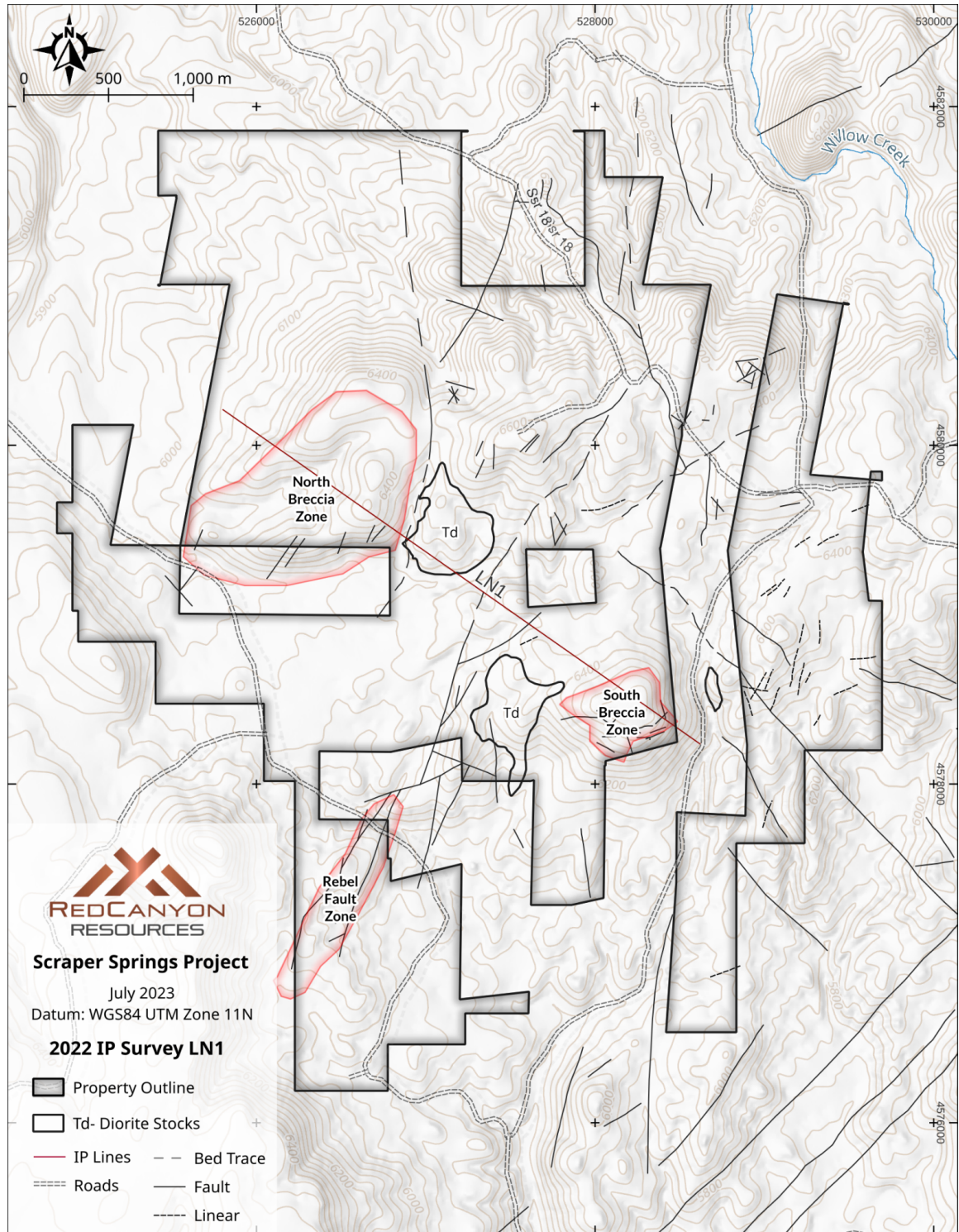


Figure 21. 2022 IP survey Line 1 location.

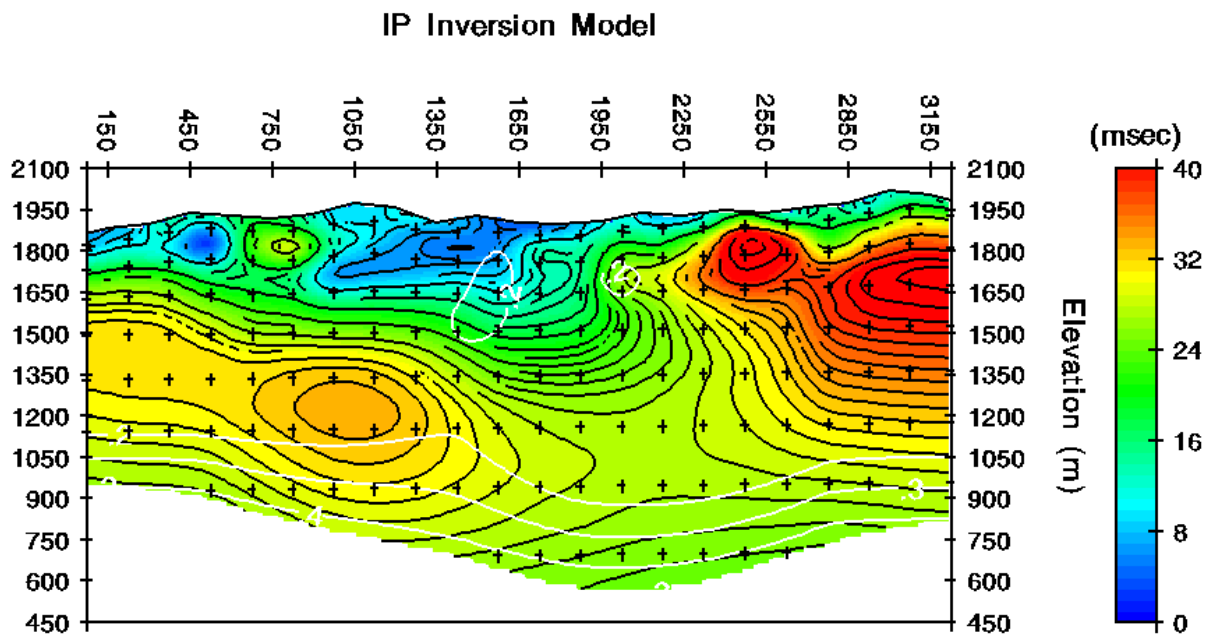


Figure 22. Line 1 2021, chargeability, viewing NE.

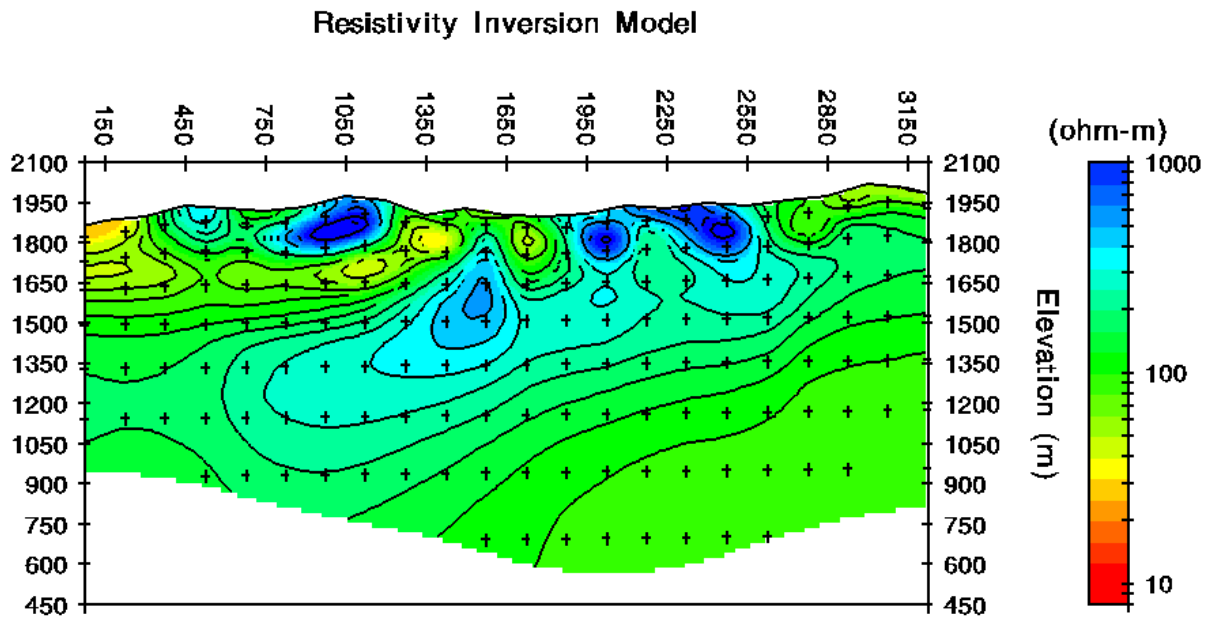


Figure 23. Line 1 2021, resistivity, viewing NE.

9.2 Sampling

From 1989-1991 Cordex Exploration performed extensive mapping, rock and soil sampling, auger grid drilling and CSAMT (Howell, 2007). From 1994-1997 Western States Minerals collected rock and soil samples primarily in the Ruby Hill or Barite Area and, to a lesser extent, in the Rebel area. From 2003, Cordex (funded at the time by Metallic Ventures) re-mapped the Project, and performed more soil sampling. Newmont (with Cordex) performed additional sampling in 2008, and In late 2021, Red Canyon performed resampled soils overlying a portion of the central Project previously covered but lacking multi-element data.

Of the approximately 2700 total soils and 345 rocks, 787 soil samples have usable assay results and 345 rock chip samples can be used for plotting (Figures 24, 25). The best metal values assayed to date from the soils are 0.276 g/t Au, and 9.76 g/t Ag; the best rock chip samples assayed 1.03 g/t Au and 2370 ppm Ag (76 oz/t).

Sampling identified several zones of anomalous gold mineralization at surface; typically along NE trending faults and areas of intense structural deformation. The Rebel Fault Zone, within the tertiary tuffaceous rocks, produced overall elevated gold values in both the soils and rock chip samples.

Rock sampling of The South Breccia Zone produced weakly anomalous gold, and the North breccia Zone produced elevated gold values only in the W-NW portion (Figure 25). This portion of the North Breccia Zone has not been drill tested. Rock chip sampling in these areas have somewhat inconsistent results, perhaps due to selective sampling techniques.

Another notable zone of surface sampling occurs just east of the North diorite stock. Here, a rock chip sample assayed 1.03 g/t Au and 1.8 g/t Ag (Figure 25). This is the highest gold value of all recorded and assayed surface sampling. The surface lithology here is Ordovician Vinini chert (Ovc), and as expected is intensely faulted in this area.

The primary target of historic drilling sits directly between the north and south diorite stocks, on the contact between Tvt1 and Ovc. Sampling overlying this area produced only weakly anomalous gold in soils and few samples with elevated gold in rock chip samples; it is likely that surface mineralization here is confined to structures, with little outward mobility.

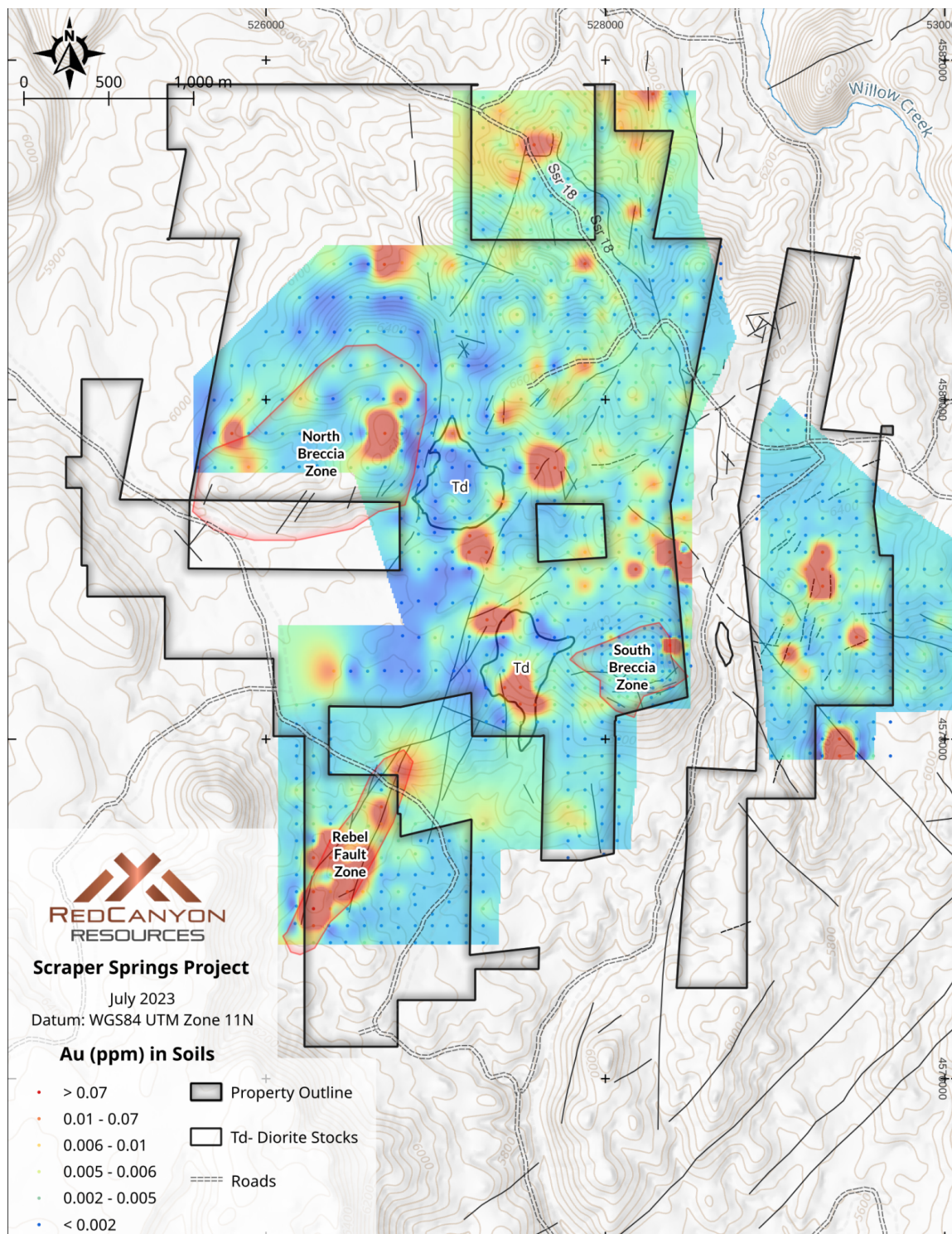


Figure 24. Gold in soils geochemistry map showing both Newmont (2008) and Red Canyon (2022) soil assay results.

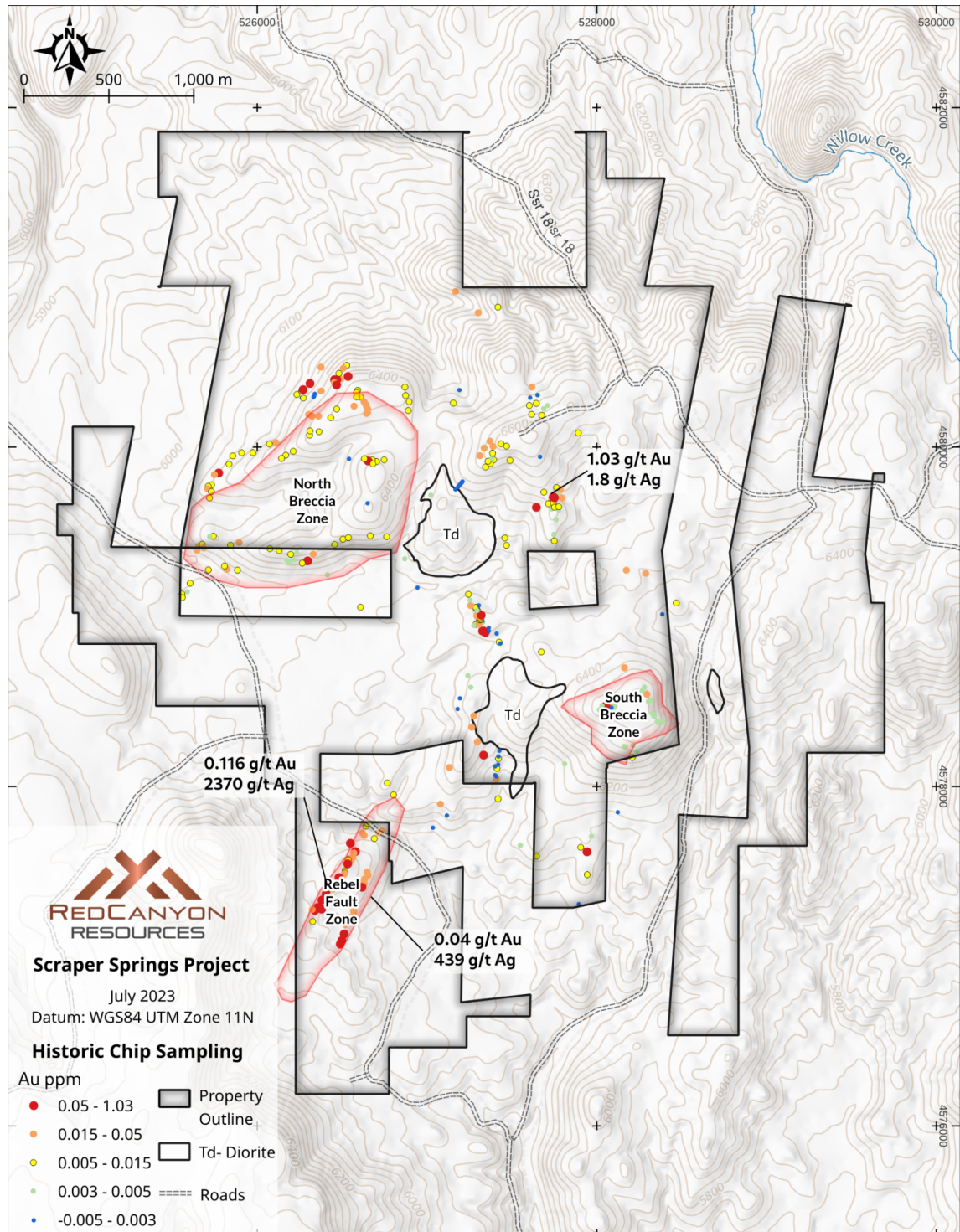


Figure 25. Rock chip sampling geochemistry map showing Au assay results.

9.3 Petrography

Cantor (2012) performed thin section analysis on 116 thin sections cut from samples in the North Stock and Breccia Zone and the South Stock and Breccia Zone. Cantor's work on mineral paragenesis found that the north and south breccia zone differ slightly in abundance and type of minerals, but share similarities in overall alteration assemblages. Additionally, the main difference between both exposures of diorite is that the South Stock contains significant epidote mineralization, whereas the north stock exhibits actinolite in place of epidote (Cantor and Thompson, 2012).

Most notably, Cantor (2012) was able to confirm the presence of potassic alteration in both the north and south stocks. Thin sections show that potassic alteration occurs as orthoclase veins forming stockworks in local areas. Orthoclase veining tends to occur as veinlets, approximately 50 to 100 microns in width. Veining tends to be more obvious in the porphyritic diorite. In more equigranular diorite, orthoclase veining is less obvious, but occurs in grungy selvages several millimeters wide. Cantor was also able to confirm the presence of argillic, propylitic, silicification, and sericite alteration, previously mapped using SpecTIR hyperspectral imaging in 2008.

9.4 Multivariate Exploratory Factor Analysis

Ethos Geological performed in-house exploratory multivariate factor analyses on the available drill core assay data, soil assays, and chip samples at Scrapper Springs. Exploratory multivariate factor assesses the data for clustering, able to establish correlations within a multidimensional matrix.

Factor analysis was performed on the assays with the intention of determining the following:

- 1) Correlated groups of minerals and elements
- 2) Pattern associations, if any, of the above with mineralization, lithology, or alteration zones

How it Works

Exploratory factor analysis considers the clustering of groups of data by first considering two starting variables from a sample, compared with their corresponding relationship within every other sample. The variables may or may not be found to be correlable among the samples. Two new variables are considered, and so on, until every variable has been compared to every other variable among every sample.

The inputs were varinormalized so that the standard deviations within any particular element are independent of their units, and only the first five (5) factors were selected, as any more factors than this have been determined by the Author through experience to be insignificant.

Output

This method of analysis produces factors (groups of correlative variables), and scores (values that rank each sample according to its correlation with a factor).

Ethos' results are factor groupings- aka 'fingerprints' or 'clusters'- of variables that are statistically correlable. For example, a grouping may contain kaolinite and plagioclase, or orthoclase and amphibole for systems containing an andesite.

The correlation of each variable with a given factor is expressed as a new value "factor loading" that ranges from -1 to 1. Variables with high positive loadings are correlated (typically above 0.3), loadings around 0 indicate an indifference or no effect, and high negative values indicate an inverse correlation with those variables scoring high positives.

Factor scores- the values that make for easy plotting and visualization of each sample- are values assigned to each sample that implicate the strength of the correlation of that sample with a factor grouping. Score units are arbitrary.

Warnings and limitations

Factor loadings - the results ranking variables within factor groupings- are values scaled from 1 (positively correlated) to 0 (no correlation, indifferent, neutral), to -1 (strongly inversely correlated). These values are not quantitative and only describe the fit of that variable with those of a group.

Bias toward certain variables may be present when a variable is strongly right-skewed (eg. when a high number of samples have a low quantity of an element, and a low number of samples contain a high quantity, like Au). This bias may potentially produce a high correlation of that variable with a factor, but the high correlation will be misleading in that the correlation is describing a correlation with the absence of the variable, not its existence.

Additionally, certain minerals and elements have a natural tendency to form groups based upon naturally-occurring processes. A factor analysis of geochemistry from granite and gabbro may be unable to determine protolith, as both may contain many similar underlying minerals.

Therefore, care must be taken while interpreting factor analyses, considering 1) factors demonstrate a correlation among variable(s) that are irrespective of quantity, and 2) factor correlations may be influenced by natural grouping.

Finally, factor scores are estimated values normalized against all values internal to the input dataset that describes the relative positioning of a sample, or rank, according to a given factor. Factor scores typically range from -2 to 2. These scores are relative, their scale both arbitrary and unique to the dataset, yet still maintain the relationship of an inverse correlation with negative scores, positive correlation with positive scores.

9.4.1 Soil Geochemistry Factors

The factor analysis was able to identify five factors interpreted to represent grouping of alteration, lithology, and/or mineralization fingerprints (Table 6, Figure 26). Factor analysis on the soils was limited to Newmont's 2008 sample set due to the availability of full elemental assay results and Red Canyon's soils sampled in 2002; Cordex's 2004 soils covering the central portion of the Project only supplied a few elements and are statistically unusable for statistical correlation.

Factor 1: This factor found positive correlation between Al, Li, K, Ga, Ti, Hf, Sc, Rb, Zr, Mg, Nb, Be, Cr, and Ge respectively. This factor strongly aligns with the Vinini Formation, and structures or breccias or volcanics (that may have incorporated similar material). This factor is inversely correlated within the diorite stocks.

Factor 2: This factor found positive correlation between Co, Ce, Mn, Mg, Zn, La, Be, Sc, Y, Cr, Ni, Al, Ga, Cd, P, Cu, V, Ca, and Ge respectively. Factor 2 appears to identify a halo of mafic-affinity chemistry forming broad anomalies over the Tvt2, Tva, and Tvxt volcanic rocks.

Factor 3: This factor found strong positive correlation almost wholly contained within the South Breccia Zone. This factor group includes positive correlations between Bi, Sn, In, Mo, Te, Fe, Se, V, Tl, Sr, and Ge respectively. This group represents a solid fingerprint for breccia formation and hydrothermal source fluids at Scrapper Springs. Directly south of the breccia formation, the positive correlation is likely due to surface erosion and downslope deposition.

Factor 4: This factor found positive correlation between As, Sb, Au, Ag, Pb, S, and Hg respectively. With this group of elements, factor 4 is likely a good fingerprint for high-sulfidation epithermal mineralization at Scrapper Springs. Specifically, Factor 4 highlights the Rebel fault zone and other faults along strike in the central portion of the Project, indicating a key structural component to mobilization of mineralizing fluids where surface samples indicate the highest Au and Ag values. Uniquely, Factor 4 anomalies overly the southern diorite stock and Rebel Fault zones, but display inverse correlation overlying the northern stock and both northern and southern breccia zones; indicating the Rebel Fault Zone and southern stock may be genetically related.

Factor 5: Highlights both the northern and southern stocks and volcanic rocks adjacent to the north breccia zone and, generally, the rocks overlying the Vinini west of the stocks. Volcanic rocks elsewhere only exhibit weak to no correlation with this Factor 5.

Table 6. Soil factors showing positive and inverse correlations and interpretation.

Factor	Positive Correlation	Inverse	Inferred Source
Factor 1	Al, Ba, Cr, Cs, Cu, Ge, Hf, K, Li, Ni, Rb, Sc, Th, Ti, U, Zr	P, Sr, S, Ca, La	Vinini, Breccias
Factor 2	Al, Be, Ca, Ce, Co, Fe, Ga, Mg, Mn, P, Sc, V	Nb, S	Volcanics
Factor 3	Bi, In, Mo, Na, Se, Sn, Sr, Tl	La, Ce, Mn, Zn	South Breccia
Factor 4	As, Ag, Au, Pb, S, Sb	Al, Ca, Ga, K, Mg	Hydrothermal Alt
Factor 5	Al, B, Be, Hf, Na, Zr	Cd, Re, Ta, Zn	Diorite, Volcs

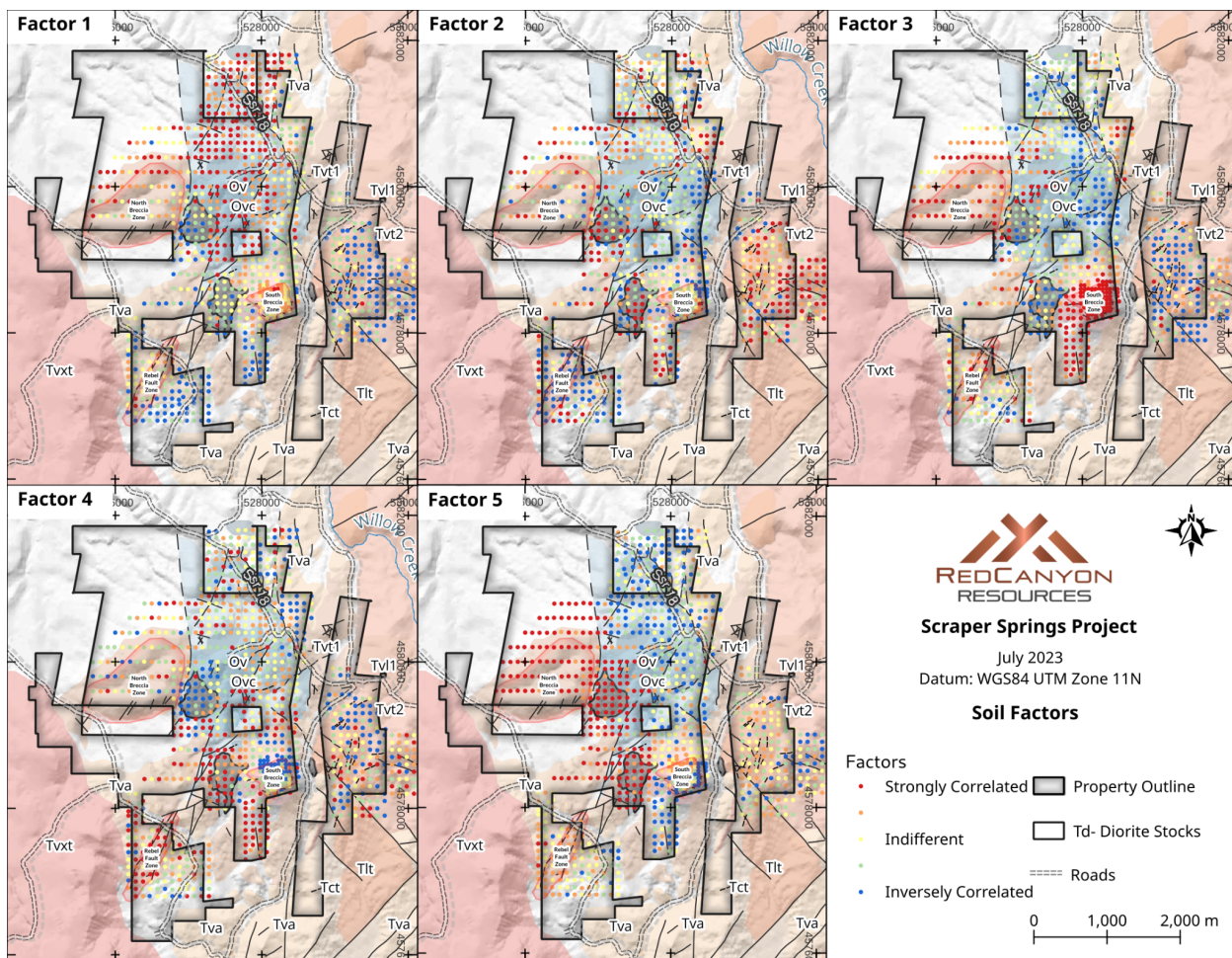


Figure 26. Multi-element factor analysis on soil samples from Newmont's and Red Canyon's soil campaigns. Soils having high positive correlation with a factor are shown in, through a spectrum to blue indicating inverse factor correlation. See geology figure(s) for legend.

9.4.2 Rock Chip Geochemistry Factors

Using the same process as the soils, 204 rock chip samples collected in 2004 and 2008 by Cordex and Newmont underwent factor analysis (Table 7, Figure 27). The results produced five factors that uniquely fingerprint the rock geochemistry.

Factor 1: This factor displays positive correlation between Ni, Cu, U, Co, Fe, Zn, V, Cd, Cr, Ba, and Mo. This grouping is similar to that of the inferred Vinini Formation fingerprint in the above section, and shows strong correlation where the Vinini Formation is at surface. A unique spatial correlation exists with this factor with the North Breccia Zone. This area is mapped as Tertiary volcanics and may indicate that factor 1 represents an alteration zone distal to epithermal mineralization. Factor 1 is also moderately anti-corellable within the Rebel Zault Zone.

Factor 2: This factor displays positive correlation between La, K, Al, Mg, Zn, As, Ba, and Ti respectively, as well as inverse correlation between Cr, and Mo. This factor appears to represent alteration associated with epithermal mineralization represented strongly in the Rebel Fault Zone, and within samples collected along the dominant northeast-striking fault system within the Vinini Formation. This factor is also strongly inversely correlated with the North and South Breccia Zones. This factor grouping is similar to that of Factor 1 in the soils and the Factor 5 of the drill core.

Factor 3: Sb, Ag, Pb, and Mn dominate this fingerprint, highly coincident with the Rebel Fault Zone, and similar with Factor 5 in the soils, Factor 1 in the drill core.

Factor 4: This factor uncovered positive correlation among Ca, P, Ti, V, Mo, Fe, and Mg, and an inverse correlation between Au and K. This factor 4 within the rocks, like Factor 3 in the soils, is strongly coincident with the North and South Breccias and may represent late carbonate / retrograde skarn alteration. Au and K are both strongly inversely-correlated with this factor.

Factor 5: This factor displays a positive correlation among Sr, Na, As, P, and K, and inverse correlation between Ti, Mg, Zn, and Ba. This factor may represent a subset of epithermal activity, expressing a positive correlation in both faulted tuffaceous rocks and faulted Ordovician Vinini rocks; perhaps indicating k-feldspar veining.

Table 7. Rock factors.

Factor	Positive Correlation	Inverse	Inferred Source
Factor 1	Ni, Cu, U, Co, Fe, Zn, V, Cd, Cr, Ba, Mo		Ordovician
Factor 2	La, K, Al, Mg, Zn, As, Ba, Ti	Cr, Mo	Alteration / Epithermal
Factor 3	Sb, Ag, Pb, Mn		Epithermal 1
Factor 4	Ca, P, Ti, V, Mo, Fe, Mg	Au, K	Breccia
Factor 5	Sr, Na, As, P, K	Ti, Mg, Zn, Ba	Epithermal 2

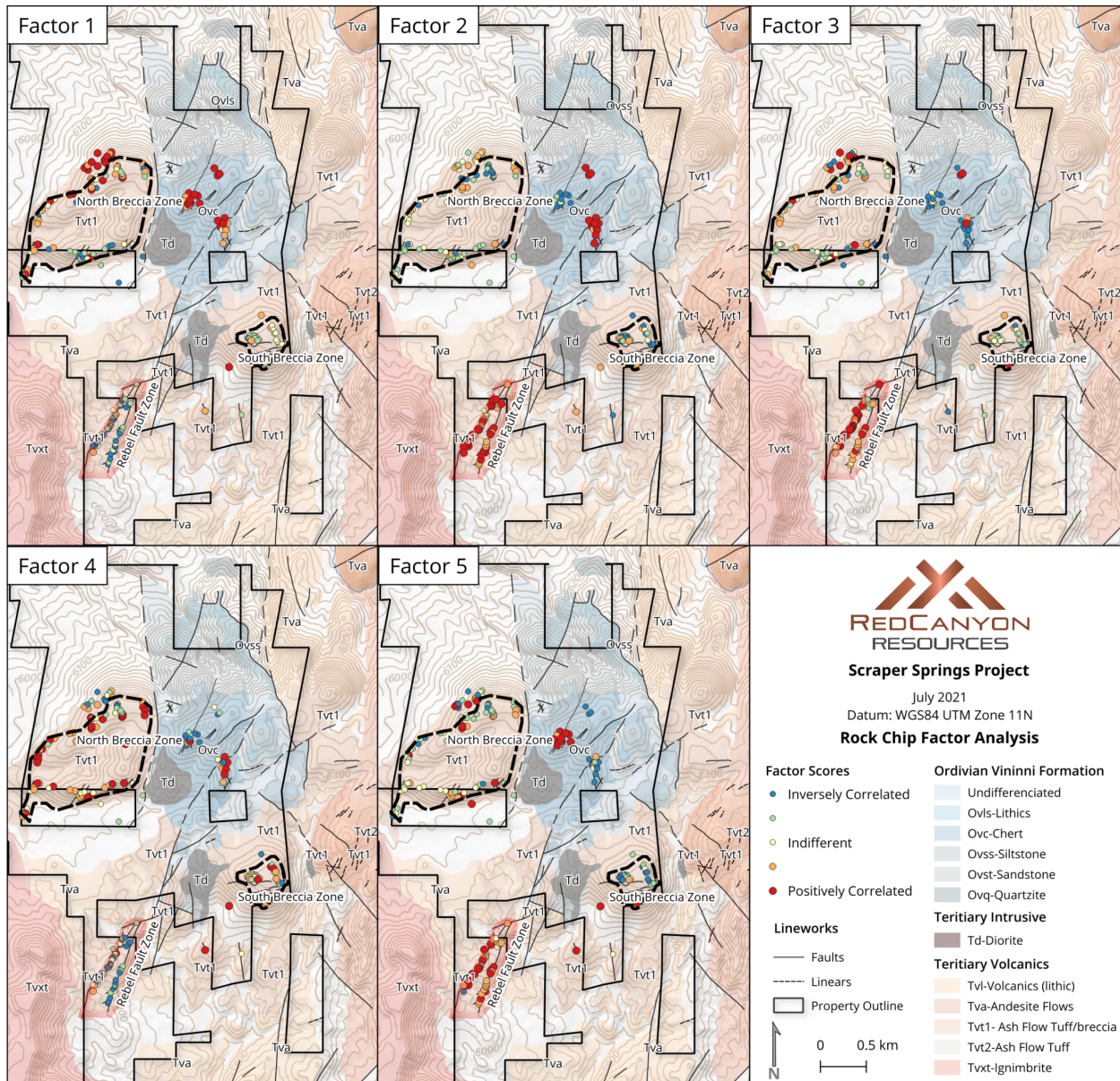


Figure 27. Multi-element factor analysis on rock samples from Newmont and Cordex (2004, 2008) chip sampling. Inversely correlated groups are shown in blue, positively correlated groups are shown in red. Underlying lithology and structural features are included for reference. Note: property outline represents boundary prior to additional claim staking by Red Canyon Resources in late 2021.

9.4.3 Historic Drill Hole Geochemistry Factors

Eleven holes from the Cordex (2004) held sufficient assays to perform multi-element factor analysis. This analysis produced similar groupings (factors) as those from the soils and rocks, implicating that the geochemical patterns are consistent and reliable from surface to depth (Table 8, Figure 28).

Factor 1: As, Sb, Au, Ag, Hg, Cd, W, and U dominate this factor grouping. Factor 1 displays a high similarity with factor 5 in the soils (Rebel Fault Zone) and factor 3 in the rock chips, and represents an assemblage of hot-springs fault-related epithermal activity. This correlable association is also present within holes SC-01 and SC-02, located along the Project's prominent northeast-striking fault system.

Factor 2: This factor shows positive correlation among Na, Sr, Ca, Al, Mg, P, and Ti; Cr and Ni are inversely-correlated. Factor 2 may possibly represent the more mafic andesites (Tertiary) or the breccia and related rocks, resulting from both the fingerprint's spatial coincidence of drill holes within this lithologies and similarities with Factors from other analyses (Factor 4 in rocks, and Factor 3 from the soils), and the inverse spatial correlation with the Vinini.

Factor 3: The elements V, Co, Fe, Mg, Cr, Al, Mn, Ti, Tl, Ni, P, and U dominate this factor, which is highly similar to Factor 4 from the soils and factor 1 from the rock chips, interpreted to represent the Ordovician Vinini Formation.

Factor 4: This factor represents a distinctly base-metal fingerprint: Zn, Pb, Cd, Ag, Cu.

Factor 5: La, K, P, Mn, Ba are strongly correlated in this Factor and unique to the area surrounding and within diorite of the South Stock.

Table 8. Drill hole factors.

Factor	Positive Correlation	Inverse	Inferred Source
Factor 1	As, Sb, Au, Ag, Hg, Cd, W, U		Epithermal 1
Factor 2	Na, Sr, Ca, Al, Mg, P, Ti	Cr, Ni	Tertiary Volc? Breccia?
Factor 3	V, Co, Fe, Mg, Cr, Al, Mn, Ti, Tl, Ni, P, U		Ordovician Vinini Formation
Factor 4	Zn, Pb, Cd, Ag, Cu (weak Au)		Metal
Factor 5	La, K, P, Mn, Ba	U, Bi, Ti	South Stock diorite

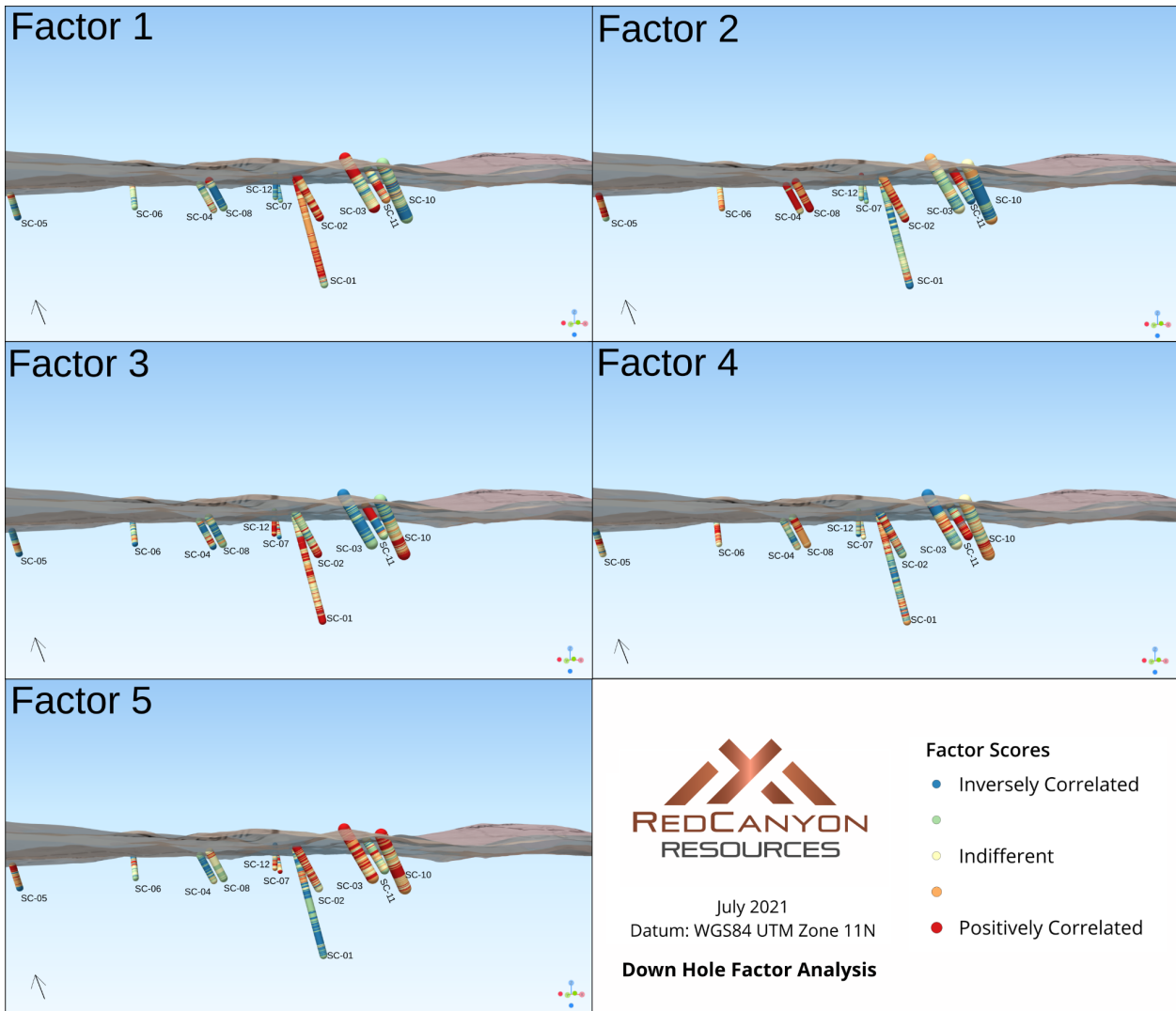


Figure 28. Multi-element factor analysis on drill data from Cordex/Metallic Ventures (2004).

9.5 3D Modeling

In 2022, the Company compiled all new and historic available data to build a 3D model in LeapFrog. The model includes subsurface geology, alteration and structures. The model assisted in planning accurate drill holes and investigating subsurface trends (Figure 29). The model also allows 3D visualization of historic cross sections, geophysical surveys and historic assay data.

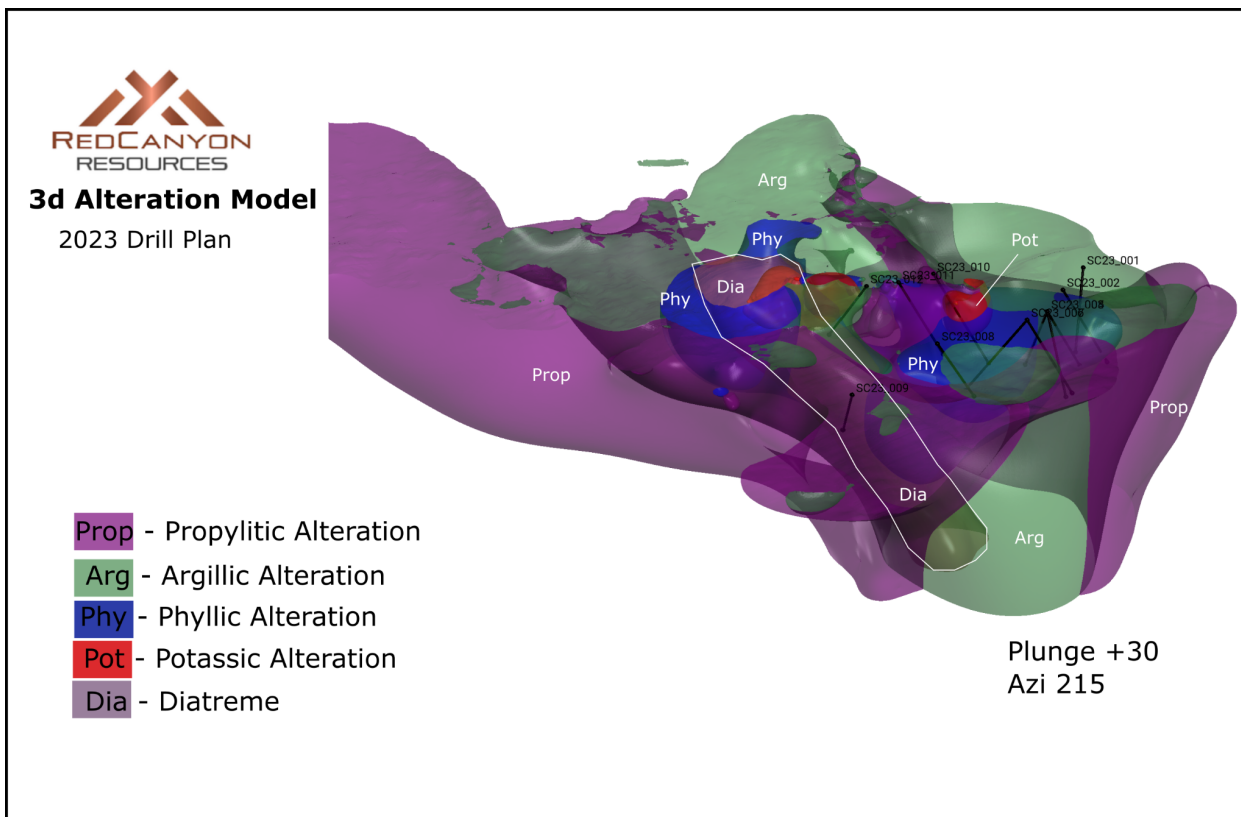


Figure 29. 3D model preview showing alteration zones and proposed drill holes

9.6 Age Dating

In 2022, Red Canyon invited Emily White, Ph.D candidate at Texas A&M, to perform age dating and thermochronometry of the northern and southern stocks from Scrapper Springs as part of this thesis work currently in progress.

U/Pb dating indicates that zircons from the northern stock crystallized at approximately 91.70 ± 0.98 Ma, during the Cretaceous, and the southern stock crystallized at approximately 38.35 ± 0.37 Ma, during the late Eocene. Difference in these ages is further supported by the difference in appearance between the two hand samples, and difference in their bulk and trace element geochemistry (Figure 30, E. White pers. comm. 2023).

Additionally, K-Ar dating from biotite of the northern stock exhibits a date of ~ 38 Ma (Cantor and Thompson, 2012), and apatite (U-Th)/He closure temperature from the northern stock exceeds ($55-80^{\circ}\text{C}$), coincident with the eruption of Miocene volcanics (E. White pers. comm. 2023).

In summary, the northern stock has a complex history; at least one phase of the stock initially crystallized in the Cretaceous, then cooled in the upper crust during the late Eocene at approximately the same time of crystallization and cooling in the southern stock.

The Eocene cooling event coincides with the age of the volcanics that directly overlie the stocks, suggesting de-roofing of the stocks was associated with the volcanic activity. Apatite from the northern stock was then reset in the Miocene during a later stage of regional volcanism.

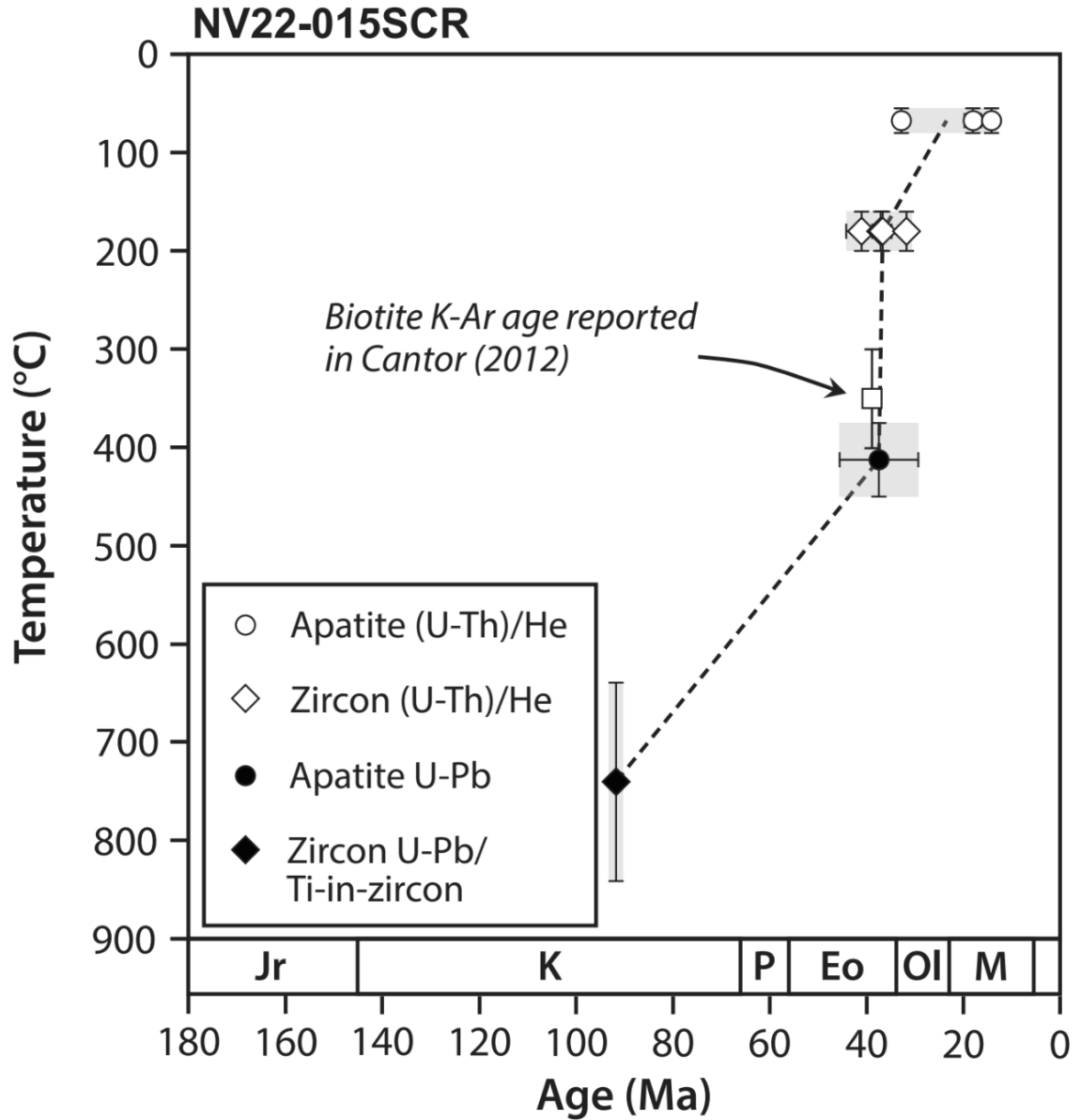


Figure 30. Results of age dating of the northern stock (E. White pers. comm. 2023).

10 DRILLING

There has been no recent drilling on the Project.

11 SAMPLE PREPARATION, ANALYSES, AND SECURITY

Soil samples were collected by Philip Zirbes, on behalf of the Issuer, Red Canyon Resources, at approximately 100 meter spacing on either 100 meter or 200 meter spaced east-west oriented lines. A narrow blade steel spade was used to dig a hole to 1.0-3.0 feet deep (averaging 18 inches, or 40 cm) targeting C-horizon soil as close to the bedrock interface as possible. Soil was not field sieved but any large rocks were removed. Approximately 1 kg of soil was bagged at each site. Sample depth, soil color and dominant float lithology were noted and a handheld GPS point with a geotagged photo was taken at each sample station.

The samples were held in care by Mr. Zirbes until delivered by freight to ALS Minerals, a division of ALS Global, with a lab located in Reno, Nevada.

ALS processing methods utilized are the ME-MS41 assay method with an Au-AA23 finish to specifically test for gold in the soils. ICP and MS methods use acid to digest the sample which is then aerosolized with Argon gas and quantified through count via mass spectrometry for multi-element determination. The Au-AA23 processing is a fire assay method performed on a sample of 30g in size to determine the presence of gold in trace limits greater than 0.005 ppm. The digestion quantitatively dissolves nearly all minerals in the majority of geological materials. However, barite, rare earth oxides, columbite-tantalite, and titanium, tin and tungsten-bearing minerals may not be fully digested.

The analytical results for the soils were received by Red Canyon directly from ALS Minerals and constructed into a database with the sample id, location, and depth information provided by Mr. Zirbes. The sample preparation, security, and analytical procedures are adequate and suitable for use in geochemical targeting and exploration as described in this Report.

12 DATA VERIFICATION

The Issuer's sample soil collection procedures have been reviewed by the Author, have been accurately transcribed from their original source, and are suitable to be used. The data was verified by the Author by reconstructing the Issuer's soils database from the original source location and assay information and found to be accurate.

Other geochemical data, including previous operators' rock and soil assays and historical drill information, were provided as digital databases to the Author as compiled by a third party and

have not been verified, as the original assays from previous operators are not available in the public record, to the Issuer, or the Author. This data is suitable for use as guidance for exploration only, and is not to be relied upon as an indication of future results or guarantee of mineralization until the original assay certificates can be found, compiled, and validated through the use of check assays and further verification.

Zonge Geophysics, a widely-used geophysical investigation company, provided Reports detailing their data collection procedures for the IP geophysics collected at the Project. Spectral data was collected by Spectir, of Reno, Nevada, who also provided documentation on their data collection and analytical procedures. The Author reviewed Zonge's and Spectir's reports, confirmed their collection and analytical methodologies are adequate; and transcribed the data used within this Report from these original sources.

13 MINERAL PROCESSING AND METALLURGICAL TESTING

Not applicable at the current stage of the Project.

14 MINERAL RESOURCES ESTIMATE

Not applicable at the current stage of the Project.

15 MINERAL RESERVE ESTIMATE

Not applicable at the current stage of the Project.

16 MINING METHODS

Not applicable at the current stage of the Project.

17 RECOVERY METHOD

Not applicable at the current stage of the Project.

18 PROJECT INFRASTRUCTURE

Not applicable at the current stage of the Project.

19 MARKET STUDIES AND CONTRACTS

Not applicable at the current stage of the Project.

20 ENVIRONMENTAL STUDIES, PERMITTING & SOCIAL IMPACT

Environmental or social impact studies are applicable at the current stage of the Project.

21 CAPITAL AND OPERATING COSTS

Not applicable at the current stage of the Project.

22 ECONOMIC ANALYSIS

Not applicable at the current stage of the Project.

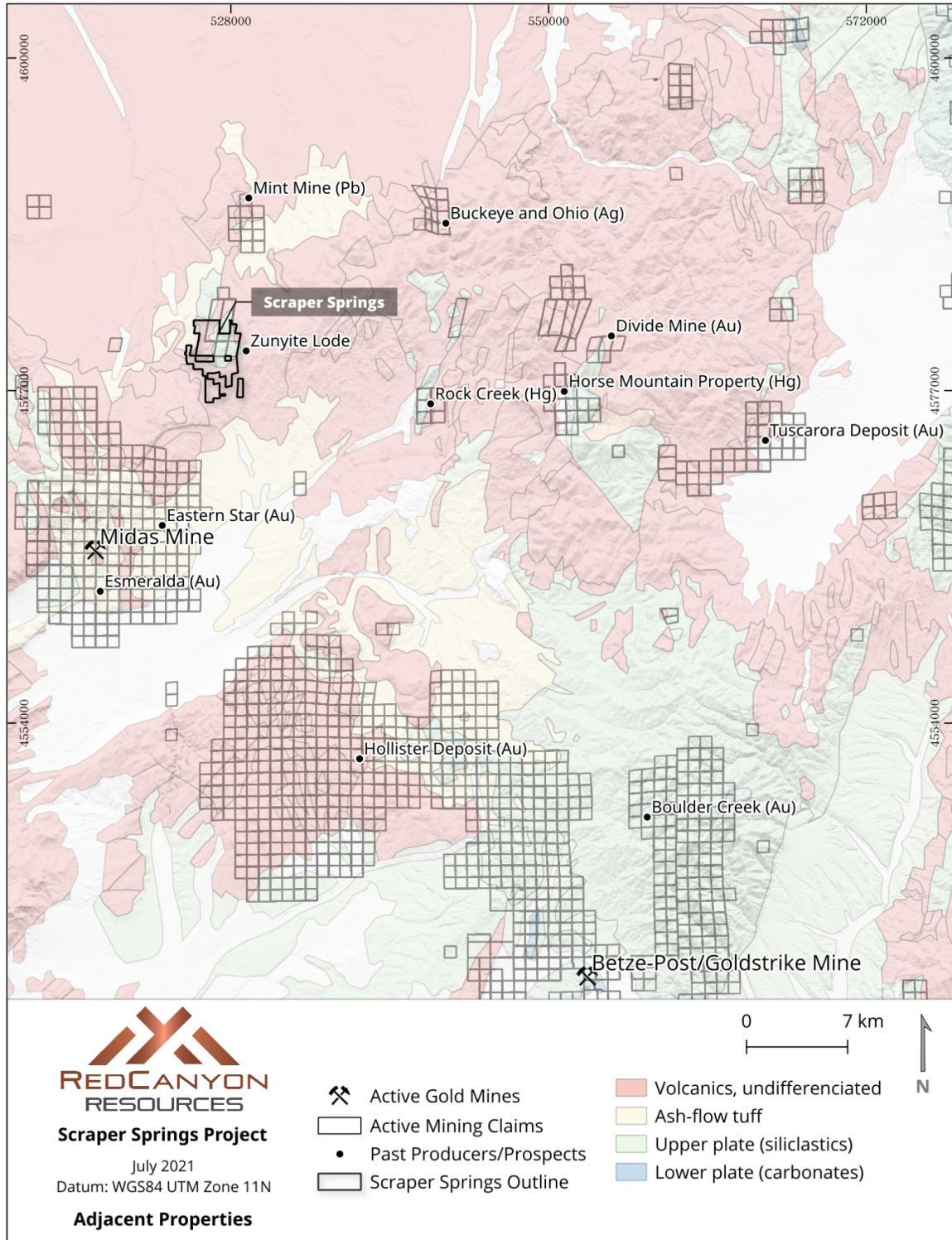


Figure 31. Map showing adjacent properties and generalized active mining claims.

23 ADJACENT PROPERTIES

Scraper Springs sits within a trend of mineral systems associated with the Northern Nevada Rift ('NNR') at the very northern extent of the Carlin Trend (NNR, John et al., 2000); including Midas, eight miles to the southwest; Hollister, 15 miles to the southeast; the Tuscarora district, approximately 20 miles to the east; and Goldstrike, 30 miles to the southeast (Figure 31).

The Author has been unable to verify information on the adjacent properties, is reliant upon other resources for this information, and cautions the reader that this information is not necessarily indicative of mineralization on the Project that is the subject of this technical report.

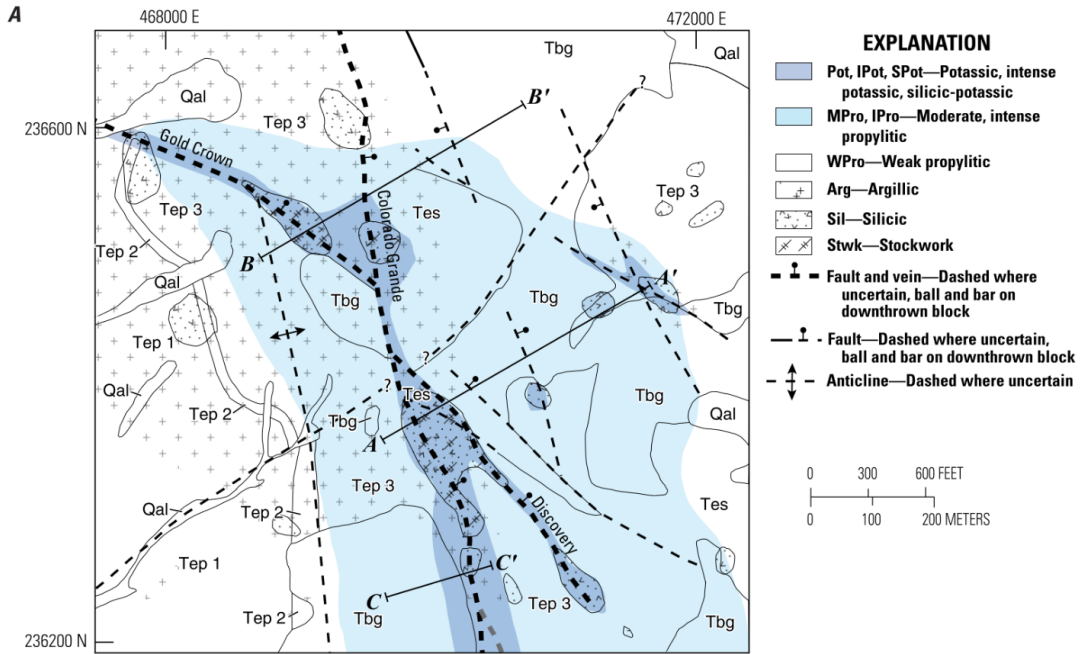
23.1 Midas Mine (Miocene)

Hecla Mining's Midas Mine (Figure 32) is located eight miles to the southwest of the Scraper Springs Project. Gold and silver mineralization at Midas sits within low-sulphidation epithermal veins cutting altered tuff and tuffaceous sediments of the Eocene Tuscarora volcanics (Leavitt et al., 2003). Potassic alteration sits within the system core, flanked by a wider zone of quartz, sericite and pyrite (Figure 32).

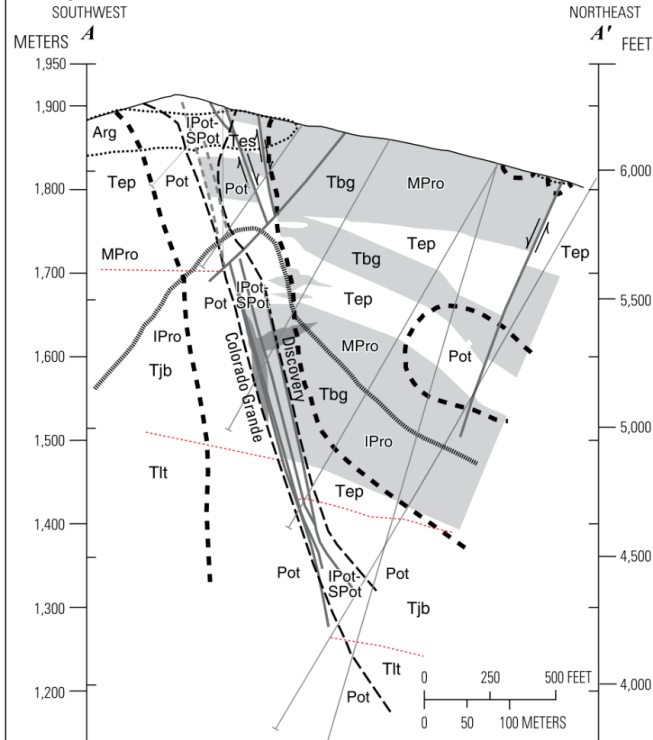
Veins containing greater than 10 ounces per tonne of gold have been discovered at the Midas mine (Howell, 2004), mostly aligned with several north and northwest-striking systems, and the veins are divided into four principal groups based on their location and orientation. The Main Veins dip easterly and are gold dominant, while the East Veins dip to the west and contain higher silver grades than the Main Veins. The Main Veins produced more than 2.2 million ounces of gold and 26.9 million ounces of silver between 1998 and 2013, principally from the Colorado Grande and Gold Crown Veins (Allen et al, 2020).

Mining at Midas began in 1998, with production by Franco-Nevada Mining, Normandy, Newmont, Klondex, and Hecla. Production rates peaked in 2011 and declined in succeeding years along with gold grades. Grades of silver increased in 2013 reflecting the shift in production from the Main Veins to the East Veins where the silver-gold ratio is substantially greater. Mine production was halted in 2019 with some remnant mining during that year (Allen et al, 2020).

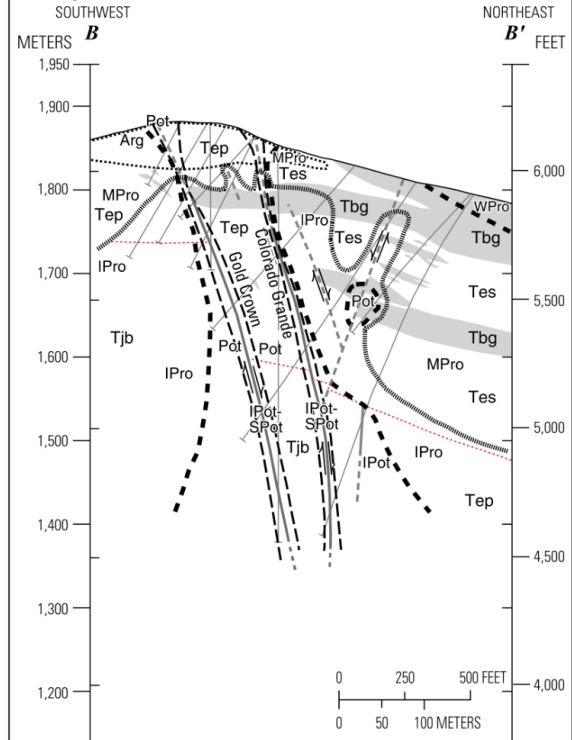
Figure 32. (Following page). Plan map and schematic cross sections of the alteration and geology of the Midas Mine (John et al 2010 after Leavitt and Arehart, 2005). Tes: tufts and volcanoclastics; Tbg: basalt and andesite sills and flows; Tep1: undifferentiated tufts and silt/sandstones; Tep1: lithic tuff; Tep2: carbonaceous sediments; Tep3: lapilli tuff (John et al 2010).



B. Interpretive overlay, 1400 N, Ken Synder mine, Midas



C. Interpretive overlay, 2600 N, Ken Synder mine, Midas



- EXPLANATION**
- Boundary of argillic alteration
 - Boundary of intense potassic and silicic-potassic alteration
 - - - Boundary of potassic alteration
 - Stratigraphic contact
 - Epidote isograd
 - Fault—Dashed where uncertain, arrows show relative motion
 - ⊥ Drill hole

23.2 Hollister Mine (Miocene)

The Hollister Mine (Figure 33), owned and operated by Hecla Mining, is located approximately 15 miles to the southeast of Scraper Springs Project. The age of mineralization is suggested to have occurred within the Miocene (Wallace, 2003).

Drilling at Hollister first intercepted anomalous Au, As, and Sb values at depths of approximately 800 feet within the Ordovician Valmy Formation of the Upper Plate of the Roberts Mountain Allochthon, sitting at upper mine levels below a blanket of Tertiary volcanic cover. A lower zone of anomalous mineralization was intercepted at nearly 7000 ft depth within the Ordovician Hanson Creek Formation (Oelofse et al., 2009).

Low-grade disseminated gold was initially extracted from two open pits at the Hollister Mine targeting the base of the Tertiary cover at its unconformity with the underlying Devonian rocks. Combined, mining activities have produced >450,000 ounces of gold and >2.5 million ounces of silver from ore averaging ~34 g/t Au (1.00 oz/t) and 200 g/t Ag (5.83 oz/t) from cut-and-fill and longhole stoping from 2007 to present (Allen et al, 2020).

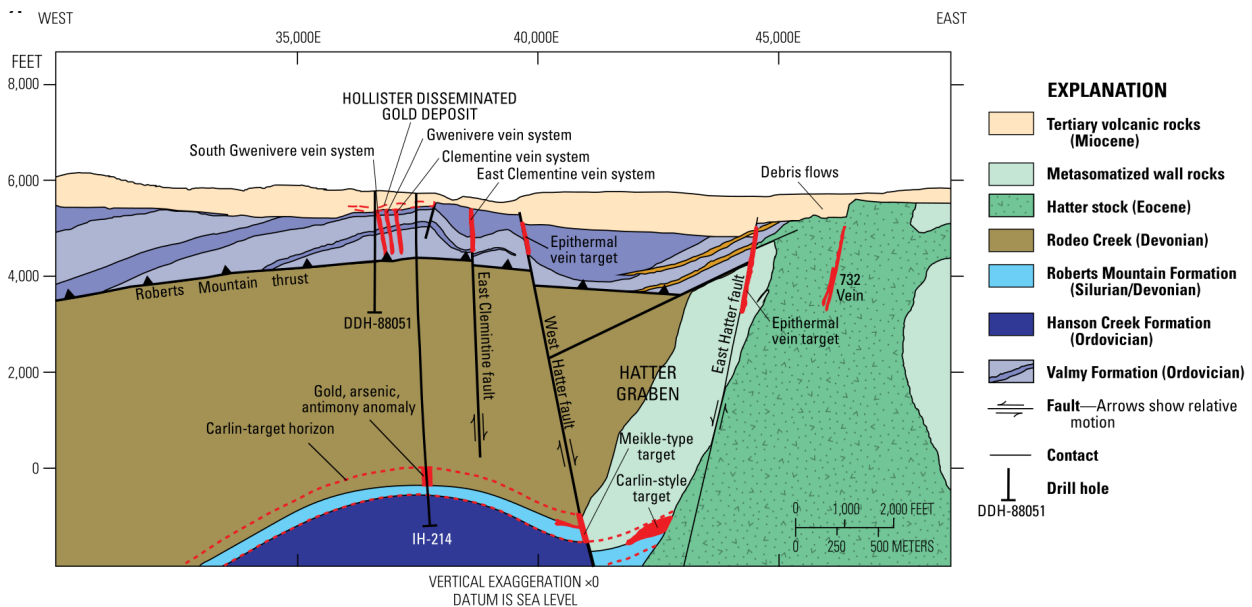


Figure 33. Schematic cross section showing geology, structure and mineralization at the Hollister Mine (John et al., 2010).

23.3 Tuscarora Deposit (Eocene)

The Tuscarora Deposit is currently owned by American Pacific Mining Corp. Since 1982, the Tuscarora District has had a sustained exploration effort, with each subsequent operator building

on the previous work. Historic drilling intersected over 368 g/t gold in quartz-adularia veins at relatively shallow depths at Tuscarora. Over 500,000 ounces of gold and 7,632,000 ounces of silver were produced from quartz veins and stockworks from 1867 to 1990 (American Pacific Mining Corp, 2020).

The Tuscarora district (Figure 31) contains Eocene ash-flow tuffs and hosts an Eocene-aged granodiorite intrusive (Henry and Boden, 1998, 1999; Henry et al., 1999). Henry and Boden (1998, 1999) and Henry et al. (1999) determined that multiple caldera complexes located at Tuscarora are the likely source of tuffaceous units in the greater region, extending as far as Scrapper Springs.

The Mount Neva granodiorite exposed within the Tuscarora volcanic complex produced an $39 \text{ Ar}/40 \text{ Ar}$ age date of $39.37 \pm 0.28 \text{ Ma}$ (Henry and Boden, 1999).

23.4 Goldstrike Mine (Eocene)

The Goldstrike Mine is a gold-bearing mesothermal shear zone located approximately 30 miles southeast of Scrapper Springs within limestones of the Devonian Popovich Formation, in the Lower Plate of the Roberts Mountain Allochthon (Figures 31, 34).

Debris flows, rip up beds and other sedimentary brecciation within the Popovich limestone and along its transition with the siltstones and shales of the Rodeo Creek Formation were decalcified and structurally deformed by the Jurassic-aged Goldstrike diorite. This deformation is thought to represent zones of weakness and structural inhomogeneity that created natural conduits for later hydrothermal fluid flow; north-northwest trending zones of phyllite, cataclasite, and tectonic brecciation often exploit these conduits and host the majority of the mineralized lodes (Peters et al, 1998).

Alteration associated with mineralized rocks in the Betze ore body, the principal ore zone, are similar to other Carlin-type systems, including carbonation, de-carbonization (decalcification), argillization (illite-clay), and silicification.

The character of ore shoots in the Goldstrike hydrothermal system developed from rutile-silica, illite-clay-pyrite, realgar and orpiment, stibnite, to polymetallic (Hg, Cu, Zn, Ag and native Au). Peters et al, 1998, concludes that the entire system occurred during post-Jurassic, brittle-ductile deformation, based on the incorporation of mineralized pods of the Jurassic diorite and large-scale hydrothermal flow.

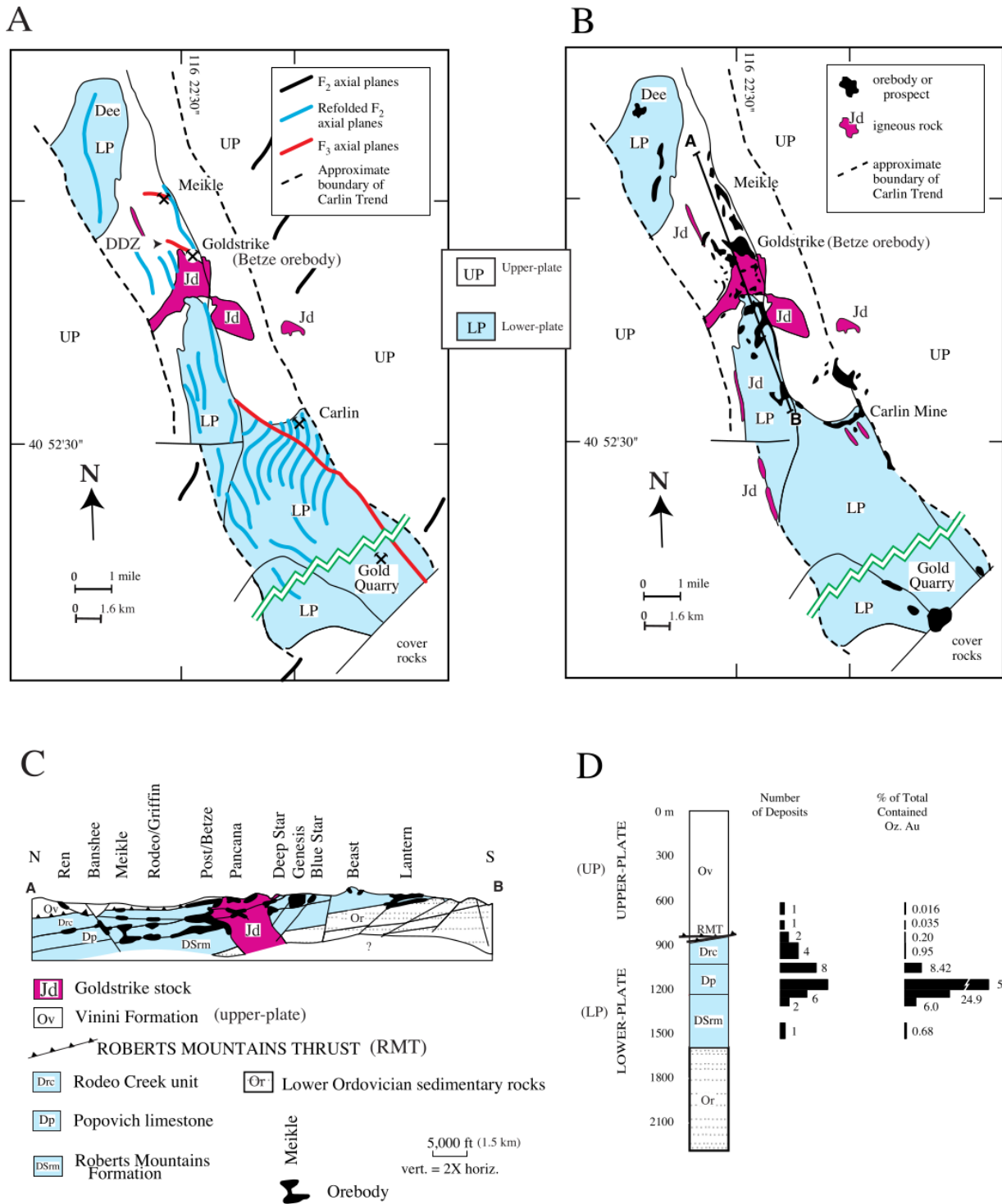


Figure 34. Goldstrike mine maps. A) Plan view map of deformation. B) Ore shoots projected to the surface. C) Cross section showing geology, structure and mineralization. D) Count of deposits with geology (Peters et al. 1998).

24 OTHER RELEVANT DATA AND INFORMATION

Not applicable at this stage of the Project.

25 INTERPRETATIONS AND CONCLUSIONS

Scraper Springs has been tested for mineralization through several programs and exploration concepts, targeting several different geologic, mineral and alteration zones. A fault-hosted hot-springs style epithermal system sits in the south in the Rebel Fault Zone, diorite stocks and breccia mineralization sit in the central and northwest, and elevated copper exists at depth within the central area; all of these are encouraging expressions of hydrothermal activity that support further exploration efforts on the Project.

Newmont (2008) recognized that the geology at Scraper Springs is unique and tested the breccias associated with the diorite stocks. Cordex (2004) drilled 500m into the center of the Project (SC-01) and encountered increasingly anomalous copper associated with carbonaceous rocks; confirming quartz-sericite-pyrite underlies argillic and advanced argillic alteration at surface. Historic reverse-circulation (RC) drilling (SS-1) at Scraper Springs reportedly intercepted similar mineralization to that at the Hollister Mine- 140 ft assaying 0.528 g/t Au (0.017 oz/t Au, Howell, 2007)- but the assay details for this drill hole are unavailable and serve merely as a reference guide to future exploration efforts. Cantor (2012) observed K-feldspar alteration along the margins of the North stock. Together, these efforts support the observation of increasing temperature and elevated hydrothermal activity at depth and along the northeast trending fault systems.

Unfortunately, Scraper Springs lacks consistent, property-wide exploration methodologies and is missing data from several critical locations. For example, the majority of the drilling records hold no assays or rock descriptions; and, historic drilling was shallow and did not test lithologic or structural contacts. Previous operators did not test for targets in the Devonian aged rocks, specifically those predicted to underlie the Vinini; nor did they test for epithermal-type targets at depth along the prominent structural conduits, such as those encountered at the nearby Midas and Hollister mines.

Fortunately, a wide array of surface data exists at Scraper Springs. Hyperspectral imaging, IP/RES, magnetics, surface mapping, sampling and drilling create a diverse suite of information to support a new interpretation and guide future exploration at depth, which is further bolstered by the style of mineralization and geology encountered by other workers at adjacent properties.

25.1 Alteration

The primary alteration minerals exposed at surface throughout Scrapper Springs suggest the surface expression of a quartz-alunite bearing, high sulphidation, acidic epithermal system. The presence of vuggy silica and surface assemblage of alunite, opal, dickite, pyrophyllite, zunyite, topaz, illite, kaolinite and quartz are common in high sulphidation (high acid) environments.

At Scrapper Springs, potassic and skarn-like alteration concentrate around the North Stock, argillic and advanced argillic alteration is abundant at surface in the core area and extends into Tertiary volcanics of the western and eastern structural blocks; and acid-sulphate geochemistry (enriched with Ag, Au, Hg, As, Sb and vuggy silica) is concentrated along the Rebel Fault Zone and South Breccia Zone.

Alunite-zunyite-pyrophyllite (+/- dickite, illite, sericite) are common within high sulphidation systems, and the proximity of zunyite to a heat source within the advanced argillic assemblage and likely coincident with the upper levels of feeder zones have been well documented (Zhang et al, 2017).

K-feldspar has been recognized within the diorites and adjacent volcanic rocks (Cantor and Thompson, 2012), implicating the existence of pH and temperature conditions capable of mobilizing potassium, and the potential for potassic alteration (K-feldspar, biotite) along structures and at depth.

Quartz-sericite-pyrite was observed in many of the drill holes within the central area of the Project, this phyllic assemblage forms at moderately high temperatures (mesothermal and greater) and a range of pH. QSP is common at depth in low-sulphidation epithermal and high-sulphidation epithermal systems closer to a magmatic source, and overlying and/or distal to porphyry intrusions (Figure 35).

25.2 Genesis

Hydrothermal systems driven by porphyry intrusions may express high sulphidation epithermal systems at surface overlying phyllic, quartz-sericite-pyrite alteration and potassic alteration cores at depth, flanked by deep peripheral sodic-calcic alteration (Blakely et al 2010). This is consistent with observations at Scrapper Springs, where Hg, As, Au and Ag appear with quartz late in the formation of these systems along faults cutting the Paleozoic and Tertiary country rock, indicating a general vector of the mineralizing fluids to trend more acidic at higher levels and decreasing temperature.

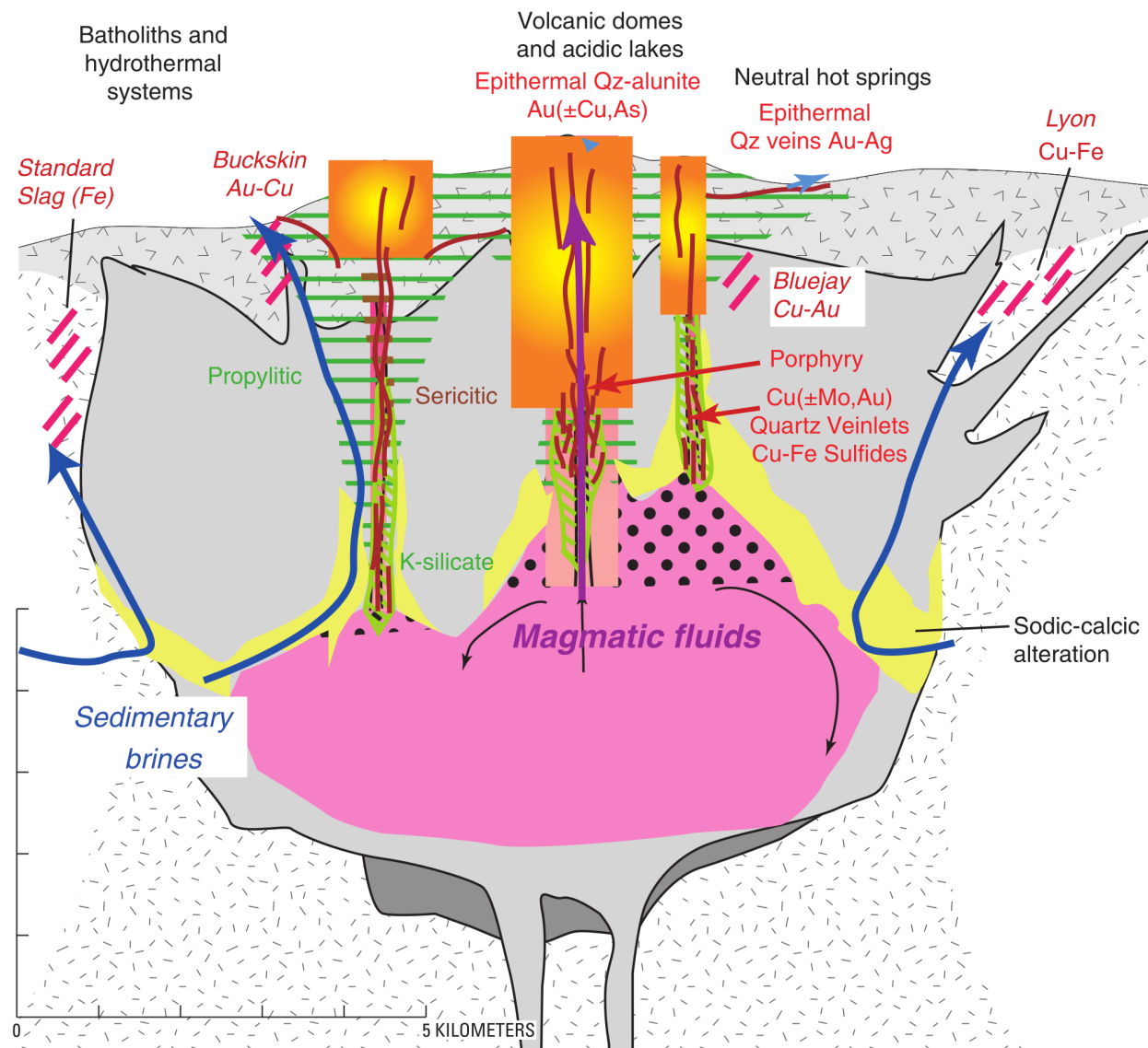


Figure 35. Schematic cross section through a porphyry system based on surface exposures, drill hole data, and interpretation from Yerington, Nevada (Blakely et al 2010).

25.3 Conclusions

Scraper Springs exposes an epithermal quartz-alunite epithermal system centralized along faults, cored by Eocene-age breccias and diorite intrusions, that likely overlie a larger intrusive porphyry system that may be mineralized at depth. Stocks, and breccias exploited the intersections of the

east-northeast and northwest-striking basement faults, contact-metamorphosed the host rock, and drove acidic fluids along structural conduits to create broad and zoned alteration.

Gold and silver mineralization at the surface are concentrated within high acid vuggy silicic and advanced argillic altered fault zones consistent with steam-heated and acid-leach horizons in upper levels of high sulphidation systems (John et al, 2010). Cross cutting relationships and age dates suggest at least one pulse of hydrothermal alteration and mineralization is as young as the late Eocene ~38 Ma (Wise 2008).

Additionally, pyrophyllite and several anomalous concentrations of vein zunyite in the Project trend east-northeast in perhaps two unique fault systems or dilation zones, suggesting structural preparation ideal for hydrothermal fluid flow, and that pyrophyllite and zunyite can be used as a vector toward the heat source (Zhang et al 2017). These conduits should be targets of future drilling (Figures 7 and 11).

Approximately 200m below the surface, advanced argillic alteration at Scrapper Springs transitions to quartz-sericite-pyrite alteration (high pH phyllic, high mesothermal temperature), and drilling between the North and South Stocks report numerous intervals of breccias, diorite-syenite dykes, and intrusive stockwork cutting the Vinini quartzites. The quantity of carbonate material increases with depth; and at approximately 400+ m depth coincides with elevated base metals and a wide zone of anomalous copper > 0.15%. Reactive horizons, structural preparation, and increasing temperature and pH at depth support exploration for a structural or deep sediment-hosted trap.

Whether Scrapper Springs is categorized as epithermal or porphyry is academic; examples of high sulphidation systems overlying porphyritic intrusions are not uncommon (Yerington; Blakely et al 2010) and they sit along natural temporal and spatial evolution pathways (Hedenquist et al 1998) (Figures 14, 35). Of greater importance is whether- and where- gold is concentrated within the high sulphidation portion of the system (if not eroded); if the underlying porphyry(s) evolved from a magmatic system voluminous and hydrous enough to strip, concentrate, and trap precious and base metals; and if the system is close enough to the surface to be tested and/or economic.

Structural extension of the overlying ignimbrite host, and general lack of dome or dome-like geology in the central Project area, implicate that a bulk of the high-sulphidation, epithermal component of Scrapper Springs has been offset by faulting or eroded, thus exposing the fluid conduits and magmatic roots leading to the parent source below.

Exploration, therefore, should focus on two potential mineralization styles: structurally-controlled permeable traps and veins where vuggy silica hosts disseminated to massive sulphide and gold mineralization in the high-sulphidation, lower temperature portions of the system, using the zunyite-alunite-pyrophyllite as a vector for feeder horizons, and at much greater depths along structural traps or permeable horizons near an intrusive core (Figure 9, 11).

26 RECOMMENDATIONS

The Vinini quartzites are likely to form a significant barrier through which structures restrict and focus fluids to deposit within dilation zones or along permeable horizons. Deep targets include traps created by interbedded carbonate-rich shales and siltstones within the Vinini quartzites, underlying Rodeo Creek or similar carbonaceous members of the Lower Plate, or the host intrusion itself.

Three targets should be investigated at Scrapper Springs:

1. Epithermal gold-silver (+ vuggy silica-alunite) along
 - a. faults,
 - b. Ordovician/Tertiary unconformity,
 - c. clastic or permeable zones intersecting structures;
2. Concentrated sulphide zones within/adjacent to breccias and diorite intrusions; and
3. Cu +/- Au and base metal mineralization in reactive horizons near the base of, or below, the Vinini quartzites, especially where reactive zones may interact with intrusions or northwest-striking basement faults at depth.

By volume, base metal +/- gold mineralization deep in the system is likely to constitute the largest drill intercepts, and concentrated high-grade gold lodes higher in the system are likely to aid the economy of accessing it.

Targeting these zones will require multi-element soil sampling to infill the geologic gaps of mineralization and alteration at surface; a structural study and gravity map to determine the character of the basement; descriptive fieldwork to refine the timing of intrusion, brecciation, alteration and fluid evolution; CSAMT to isolate the depths of the conductive targets; and deep drilling.

26.1 Structural Analysis

The mineral showings and mines along the Carlin and NNR trends are highly influenced by structure. The orientations of structures, association with mineralization and alteration, character, and senses of motion are poorly represented in the current data available at Scrapper Springs. Performing detailed mapping of the east-northeast fault systems controlling the alunite/zunyite/pyrophyllite distribution, and of the structures cutting or cut by the breccias and stocks will provide a great foundation for unraveling the timing of alteration and mineralization.

26.2 Gravity Survey

Scrapper Springs and Goldstrike both sit on the margins of regional isogravimetric highs. Furthermore, several of these highs are slightly elongated in a northwest trend, consistent with

regional structures created during the Eocene. Hollister and Midas mines similarly sit along a northwest trend in regional isogravity, but coincide with gravimetric lows, not highs.

Ground gravity is a cost effective method to investigate subsurface density contrasts. Intrusions and sulphides both should express higher density than the neighboring quartzites and younger rocks. Tight gravity grids, or even closely-spaced measurements along lines crossing basement fractures and/or extending from west to east across the project area should identify the locations of a buried suite of intrusions and/or related sulphides.

26.3 Descriptive Field Mapping

The problem to solve is: if this system overlies a Cu-Au porphyry, where does the mineralization reach closest to the surface? Finding the youngest entity on a project and working backward is often very revealing of genesis, but it requires careful observation of structures, clasts and contacts, which are often overlooked during early exploration phases. Several points of investigation may include:

- Do the east-northeast striking fault systems exist, and do they have other sinistral motion indicators? Are the secondary faults dilational, eg. reidel shears, mode 1 tension veins, voids, or void-filled?
- Do the diorites cut, or are they included as clasts within phases of the breccia? Do clasts of syenite or cumulate phases of the diorite exist in the breccia?
- Do the diorites cut, or are they cut by the fault systems (be careful to omit minor reactivation fracturing)? If cut by the fault systems, and the structural motion resolved, where are the deepest level diorites?
- The North and South Diorites do not exhibit the same alteration; are there other differences between them, and what impact does this have on the understanding of the related intrusion and fault systems?
- The character of the breccias: do the breccias contain mineralized or diorite clasts, does alteration cut across breccia boundaries, do they exhibit episodic activity, and/or what is the activity of brecciation?
- Timing of the diorite intrusions, brecciation, alteration, and formation of the Tertiary volcanics: what is the extent of alteration within the Tertiary volcanics? Is the alteration restricted to the aureoles of the faults or the Vinini formation or other specific units? What is the age of the Tertiary volcanics, and what does this imply about the timing of hydrothermal activity?

26.4 CSAMT

The controlled-source audio frequency magnetotelluric (CSAMT) electromagnetic method is often used to explore for deep-seated porphyry style mineralization. The magnetotelluric (MT) EM method uses natural EM to observe electrical resistivities of the subsurface. The AMT method may use natural signals, such as lightning, as the transmitter to create tensor variations.

Controlled-source AMT (CSAMT) methods rely on an artificial signal source and often result in high precision and economical measurements.

AMT has been used to map major base metal deposits from 50m to several kilometres (Zonge and Hughes, 1991). The depth of investigation depends on the frequencies used and the resistivity of the subsurface; zones of high conductivity may obscure deeper features.

Very low resistivities should correlate with fracture zones and interstitial clay or water, and sericitic zones with and without pyrite. Potassic zones should have higher resistivities reflecting silicification, disseminated sulfides and overall less abundant sulfide and clay. The diorite stocks should express high resistivity as compared with low resistivity of surrounding volcanic rocks due to propylitic alteration (Blakely et al, 2010).

An approximate cost of several 2-km long CSAMT lines transecting the deeper targets is \$40,000 (Figure 36).

26.5 Drilling

The central structural block exposes the Vinini quartzite at surface and may also represent the thinnest section of Vinini with which to test for a porphyry complex ranging from 500m to over 1000m depth. However, because the subsurface structural information is poorly researched at Scraper Springs, the geometry of the Vinini underlying other areas of the Project should be tested by drilling (Figure 36).

Drill targets sit along the favorable fluid conduits and at depth below the potential Vinini quartzite trap where the gravity survey indicates the host rock is the most dense, and IP indicates a correlable zone of low resistivity. Table 9 illustrates several drill holes designed in 2023 to intercept these horizons.

Table 9. Proposed drill holes, contingent on CSAMT geophysics.

Drillhole	Pad	Easting	Northing	Elevation	Azi	Dip	Depth ft	Depth m	Comment
SC23-01	SC-A	1725766	15024883	6128	45	55	2000	610	DCIP & 2021 IP charg highs
SC23-02	SC-B	1726976	15025666	6244	330	55	2000	610	IP anomaly
SC23-03	SC-C	1728053	15026464	6362	200	55	2700	823	2021 IP charge on existing road
SC23-04	SC-C	1728053	15026464	6362	270	60	2000	610	Zunyite anomaly
SC23-05	SC-C	1728053	15026464	6362	10	60	2000	610	Zunyite anomaly
SC23-06	SC-D	1728719	15026576	6397	330	55	2000	610	Zunyite Anomaly
SC23-07	SC-D	1728719	15026576	6397	140	55	2500	762	Pyrophyllite Anomaly
SC23-08	SC-E	1731287	15026611	6606	320	55	1500	457	IP anomaly
SC23-09	SC-F	1734120	15027281	6507	200	60	1500	457	Zunyite anomaly
SC23-10	SC-G	1728862	15023173	6169	330	55	2500	762	2021-IP charge anomaly
SC23-11	SC-H	1729885	15023196	6270	330	55	2000	610	Tgd
SC23-12	SC-I	1730666	15023011	6323	120	55	1500	457	Diatreme & break in 2021 IP
Total							24,200	7,378	

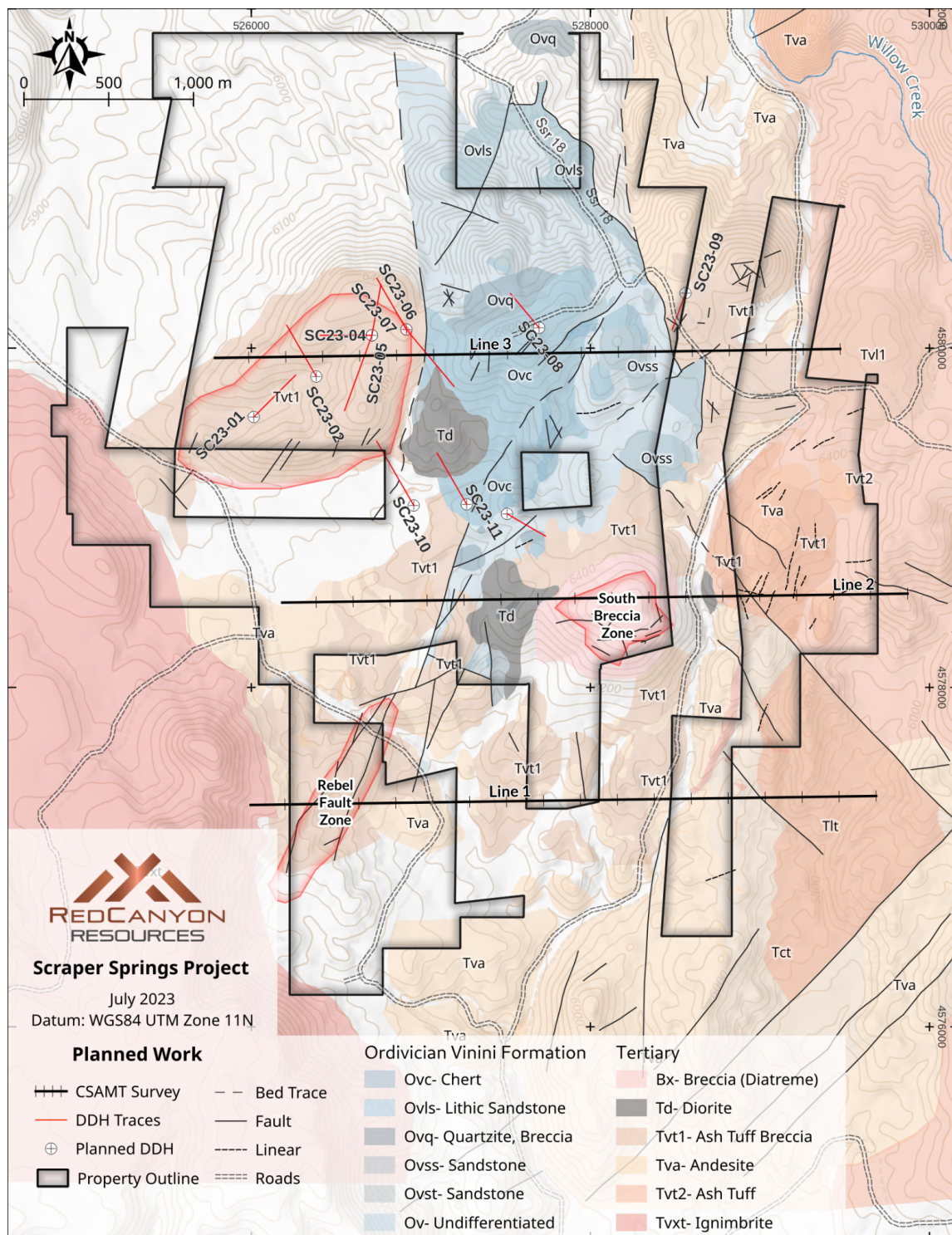


Figure 36. Drill plan map showing possible drill pads, drill holes, drill hole traces, and CSAMT lines, developed as part of the 2023 Report. Geologic base map for reference.

The phase 2 drill plan accounts for approximately 7,500 metres to target mineralization among several areas. Drill targets should be defined based on positive results from phase 1 work. At this time, a primary target is the North Breccia Zone, having associated zunyite anomalies and related IP chargeability highs along fault splays (North Fault System) from the fault bounded block between the NE trending Rebel Fault Zone and the Diatreme Fault. These splays include the North Breccia Fault zone and the NE Fault. Additional targets include drilling an inferred diatreme and the diorite intrusion for deep seated porphyry mineralization.

Ethos Geological (the Authors) did not select nor verify the geologic perspective of planned drill holes, these drill targets were developed by the internal team at Red Canyon Resources using the data described within this Report (Figure 37, Table 9).

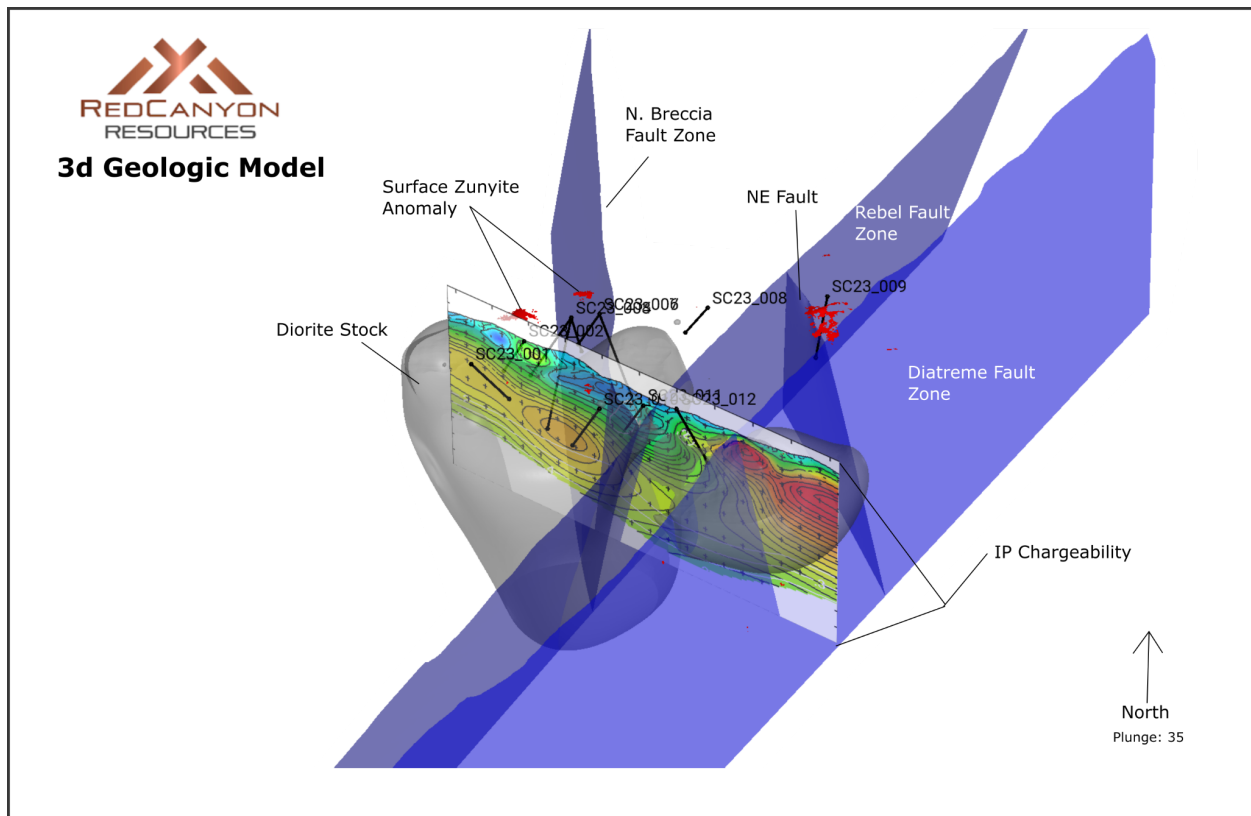


Figure 37. Proposed drill plan in 3D showing drill traces, major structures, IP chargeability highs, and the diorite stock.

26.6 Budget

This Report considers two phases of exploration: Phase 1 includes surface geophysics with the intention to outline prospective horizons below the Vinini formation for potential traps for mineralization, including a porphyry-style hydrothermal system (Table 10). Phase 2, contingent upon the success of Phase 1, comprises a deep exploration drill campaign to test these targets (Table 11), and additional down-hole IP geophysics and additional surface CSAMT to help target the drill program. Calculations and assumptions included within the following tables are derived from experience by the Author.

Table 10. Proposed Phase 1 exploration budget and itemized estimates. Values are rounded up to the nearest 1000 or 10000 interval.

Main activity	Sub-activities		
Geophysics	CSAMT	40,000	50%
	Gravity	40,000	50%
	Subtotal Geophysics	80,000	55%
Field Surveys	Soil Sampling	30,000	67%
	Geologic/ Structural Mapping	15,000	33%
	Subtotal Field Surveys	45,000	31%
Geochemistry	Core Assay	0	0%
	Rock/Soil/QAQC Assay	10,000	100%
	Other	0	0%
	Subtotal Geochemistry	10,000	7%
Reports & Permitting	Technical Reporting	10,000	100%
	Drill Permitting (PoO)	0	0%
	Subtotal Report/Permitting	10,000	7%
Total with contingency		\$ 145,000	

Table 11. Proposed Phase 2 exploration budget and itemized estimates, contingent upon the success of Phase 1. Values are rounded up to the nearest 1000 or 10000 interval.

Main activity	Sub-activities		
Drilling <i>7500m Core Single Drill Rig ~180 Day Program Length</i>	Diamond Drilling	2,780,000	97%
	Pad / Road Building	25,000	1%
	Mobilization	15,000	1%
	Reclamation	10,000	0%
	Bonds	40,000	1%
	Subtotal Drilling	2,870,000	64%
Drill Personnel	Professional Staff	240,000	25%
	Field Staff	670,000	71%
	Consultants & Advisors	20,000	2%
	Travel	20,000	2%
	Subtotal Drill Personnel	950,000	21%
Drill Support	Food/Consumables	26,000	14%
	Field Supplies	18,000	10%
	Lodging	83,000	46%
	Freight	18,000	10%
	Fuel	10,000	6%
	Automobile	23,000	13%
	Subtotal Drill Support	180,000	4%
Geophysics	CSAMT	40,000	50%
	Downhole IP	40,000	50%
	Subtotal Geophysics	80,000	2%
Field Surveys	Soil Sampling	30,000	67%
	Geologic/ Structural Mapping	15,000	33%
	Subtotal Field Surveys	45,000	1%
Geochemistry	Core Assay	270,000	84%
	Rock/Soil/QAQC Assay	40,000	13%
	Other	10,000	3%
	Subtotal Geochemistry	320,000	7%
Reports & Permitting	Technical Reporting	30,000	75%
	Drill Permitting (PoO)	10,000	25%
	Subtotal Report/Permitting	40,000	1%
Total with contingency		\$ 5,000,000	

27 REFERENCES

- Agar, B., 2008, Alteration Mineral Mapping At the Scraper Project, Nevada, Using Both SpectIR and SEBASS, Hyperspectral Image Data Consultant, Spectral Geology & Remote Sensing, Newmont Mining, Global Exploration Solutions.
- Allen, D.K., Blair, K., 2020, 2020 Annual Report: Hecla Mining Company.
- Bahadori, A., and Holt, W., 2019, Geodynamic evolution of southwestern North America since the Late Eocene, *Nature Communications* 10, n. 5231, 18 p.
- Bakken, B., 1990, Gold Mineralization, Wall-Rock Alteration, and the Geochemical Evolution of the Hydrothermal System in the Main Orebody, Carlin Mine, Nevada, unpublished Ph.D. dissertation, Stanford University.
- Blakely, R., McPhee, D., and Mars, J., 2010, Geophysical Characteristics in Porphyry Copper Deposit Model Chapter B of Mineral Deposit Models for Resource Assessment, John. D. eds, 2010-5070-B, 179 p.
- Bon, R.L.; Krahulec, K.A., 2007, 2006 Summary of Mineral Activity in Utah, Utah Geological Survey Mining Engineering. 22p.
- Cantor, B., and Thompson, T.B., 2012, Petrography and Field Mapping of Eocene Intrusions and Adjacent Breccia Zones at the Scraper Springs Prospect, Elko County, Nevada: University of Nevada Reno M.Sc Thesis, 109p.
- Castor, S.B., Boden, D.R., Henry, C.D., Cline, J.S., Hofstra, A.H., McIntosh, W.C., Tosdal, R.M., and Wooden, J.P., 2003, The Tuscarora Au-Ag district: Eocene volcanic-hosted epithermal deposits in the Carlin gold region, Nevada: *Economic Geology*, v. 98, pp. 339-366.
- Christiansen, R.L., and Yeats, R.S., 1992, Post-Laramide geology of the U.S. Cordillera region in Burchfiel, B.C., Lipman, P.W., and Zoback, M.L., eds., *The Cordilleran orogen: Conterminous U.S.: Geological Society of America, The Geology of North America*, v. G-3, p. 261-406.
- Cox, D.P., and Singer, D.A., 1986, Mineral deposit models: U.S. Geological Survey Bulletin 1693, 379 p.
- Dusabemariya, C., Qian, W. , Bagaragaza, R. , Faruwa, A. and Ali, M., 2020, Some Experiences of Resistivity and Induced Polarization Methods on the Exploration of Sulfide: A Review. *Journal of Geoscience and Environment Protection*, 8, pp 68-92.

- Hedenquist, J.W., Arribas, A., Jr., and Reynolds, T.J., 1998, Evolution of an intrusion-centered hydrothermal system: Far Southeast-Lepanto porphyry-epithermal Cu-Au deposits, Philippines: *Economic Geology*: v. 93, p. 373-404.
- Henry, C.D., 2008, Ash-flow tuffs and Paleovalleys in northeastern Nevada: Implications for Eocene paleogeography and extension in the Sevier hinterland, northern Great Basin: *Geosphere*, v. 4, pp. 1-35.
- Henry, C.D., and Boden, D.R., 1998, Geology of the Mount Blitzen Quadrangle, Elko County, Nevada: Nevada Bureau of Mines and Geology Map 110, 20p.
- Henry, C.D., and Boden, D.R., 1999, Geology of the southern part of the Toe Jam Mountain Quadrangle: Nevada Bureau of Mines and Geology Map 117, 12p.
- Henry, C.D., Castor, S.B., and Boden, D.R., 1999, Geology of the Tuscarora Quadrangle, Elko County, Nevada: Nevada Bureau of Mines and Geology Map 116, 20p.
- Hemley, J.J., Montoya, W., Marinenko, J.W., and Luce, R.W., 1980, Equilibria in the system Al₂O₃-SiO₂-H₂O and some general implications for alteration/mineralization processes: *Economic Geology*, v. 75, pp. 210-228.
- Howell, F.S., 2004, Geology and Alteration/Mineralization of the Scraper Springs Project: Unpublished Report, Cordilleran Exploration Co., 1p.
- Howell, F.S., 2007, Scraper Springs Project Summary, Unpublished Report, Cordex, 6p.
- John, D. A., Vikre, P., du Bray, E., Blakely, R., Fey, D., Rockwell, B., Mauk, J., Anderson, E., and Graybeal, F., 2010, Descriptive Model for Epithermal Gold-Silver Deposits, Chapter Q of Mineral Deposit Models for Resource Assessment, USGS Scientific Investigations Report 2010-5070, 264 p.
- Leavitt, E.D., and Arehart, G.B., 2005, Alteration, geochemistry, and paragenesis of the Midas epithermal gold-silver deposit, Elko County, Nevada: Proceedings of the Window to the World Symposium 2005, Reno, May 2005: Geological Society of Nevada, p. 563–627.
- Leavitt, E. D., Spell, T. L., Goldstrand, P. M., & Arehart, G. B., 2004, Geochronology of the Midas Low-Sulfidation Epithermal Gold-Silver Deposit, Elko County, Nevada. *Economic Geology*, 99(8), 1665-1686.
- Parry, W.T., Wilson, P.N., Moser, D., and Heizler, M.T., 2001, U-Pb dating of zircon and ⁴⁰Ar/³⁹Ar dating of biotite at Bingham, Utah: *Economic Geology*, v. 96, p. 1671–1683.
- Peters, S., Ferdock, G., Woitsekhowskaya, M., Leonardson, R., and Rahn, J., 1998, Oreshoot Zoning in Carlin-type Betze Orebody, Goldstrike Mine, Eureka County, Nevada. USGS Open File Report 98-620, 59 p.
- Radke, A.S., 1985, Geology of the Carlin Ore Deposit, Nevada, USGS Professional Paper n. 1267.

- Sillitoe, R.H., 1985, Ore-Related Breccias in Volcano Plutonic Arcs: Economic Geology, v. 80, pp. 1467-1514.
- Sillitoe, R.H., 2010, Porphyry Copper Systems: Economic Geology: v. 105, pp. 3-41.
- Wallace, A. R., & John, D. A. (1998). New Studies of Tertiary Volcanic Rocks and Mineral Deposits, Northern Nevada Rift. Contributions to Gold Metallogeny of Northern Nevada.
- Watt, J. T., Glen, J. M., John, D. A., & Ponce, D. A. (2007, December). Three-dimensional Geologic Model of the Northern Nevada Rift and the Beowawe Geothermal System, North-Central Nevada. Geosphere, 3(6), 667-682.
- Wise, J.M., 2008a, Geologic Map of the Scraper Springs Project: unpublished report, Newmont Mining Corp., 1p.
- Wise, J.M., 2008b, Annual Technical Report, Scraper Springs Joint Venture: unpublished report, Newmont Mining Corp., 1p.
- Zhang, L., Chin, J., Jimenez, C., White, N, Cooke, D., and Orovan, E., 2017, Characteristics of Zunyite in the Advanced Argillic Alteration Zones of High-Sulphidation Epithermal Deposits Implications for Exploration in Lithocaps, Society of Economic Geologists Conference Abstract, 2017, 1 p.
- Zoback, M. L., McKee, E. H., Blakely, R. J., and Thompson, G. A., 1994, The Northern Nevada Rift: Regional Tectono_Magnetic Relations and Middle Miocene Stress Direction. Geologic Society of America Bulletin n. 106, pp 371-382.

APPENDIX A: LODE CLAIMS

Claim ID	Claimant	Lead #	Serial #	County #	Located
SC-2	RC Metals Inc.	NV105278427	NV105278427	798014	2021/09/03
SC-4	RC Metals Inc.	NV105278427	NV105278428	798015	2021/09/03
SC-6	RC Metals Inc.	NV105278427	NV105278429	798016	2021/09/03
SC-7	RC Metals Inc.	NV105278427	NV105278430	798017	2021/09/02
SC-8	RC Metals Inc.	NMC1217521	NMC1217521	779455	2020/11/24
SC-9	RC Metals Inc.	NV105278427	NV105278431	798018	2021/09/02
SC-10	RC Metals Inc.	NMC1217521	NMC1217522	779456	2020/11/24
SC-11	RC Metals Inc.	NV105278427	NV105278432	798019	2021/09/02
SC-12	RC Metals Inc.	NMC1217521	NMC1217523	779457	2020/11/24
SC-13	RC Metals Inc.	NV105278427	NV105278433	798020	2021/09/02
SC-14	RC Metals Inc.	NMC1217521	NMC1217524	779458	2020/11/24
SC-15	RC Metals Inc.	NV105278427	NV105278434	798021	2021/09/02
SC-16	RC Metals Inc.	NMC1217521	NMC1217525	779459	2020/11/24
SC-17	RC Metals Inc.	NMC1217521	NMC1217526	779460	2020/11/23
SC-18	RC Metals Inc.	NMC1217521	NMC1217527	779461	2020/10/13
SC-19	RC Metals Inc.	NMC1217521	NMC1217528	779462	2020/11/23
SC-20	RC Metals Inc.	NMC1217521	NMC1217529	779463	2020/10/13
SC-21	RC Metals Inc.	NMC1217521	NMC1217530	779464	2020/11/23
SC-22	RC Metals Inc.	NMC1217521	NMC1217531	779465	2020/10/13
SC-23	RC Metals Inc.	NMC1217521	NMC1217532	779466	2020/11/23
SC-24	RC Metals Inc.	NMC1217521	NMC1217533	779467	2020/10/13
SC-25	RC Metals Inc.	NMC1217521	NMC1217534	779468	2020/11/23
SC-26	RC Metals Inc.	NMC1217521	NMC1217535	779469	2020/10/13
SC-27	RC Metals Inc.	NMC1217521	NMC1217536	779470	2020/11/23
SC-28	RC Metals Inc.	NMC1217521	NMC1217537	779471	2020/10/13
SC-29	RC Metals Inc.	NMC1217521	NMC1217538	779472	2020/11/23
SC-30	RC Metals Inc.	NMC1217521	NMC1217539	779473	2020/10/13
SC-31	RC Metals Inc.	NMC1217521	NMC1217540	779474	2020/11/23
SC-32	RC Metals Inc.	NMC1217521	NMC1217541	779475	2020/11/23
SC-34	RC Metals Inc.	NMC1217521	NMC1217542	779476	2020/11/23
SC-36	RC Metals Inc.	NMC1217521	NMC1217543	779477	2020/11/23
SC-47	RC Metals Inc.	NV105278427	NV105278435	798022	2021/09/03
SC-49	RC Metals Inc.	NV105278427	NV105278436	798023	2021/09/03
SC-51	RC Metals Inc.	NMC1217521	NMC1217544	779478	2020/11/24
SC-52	RC Metals Inc.	NV105278427	NV105278437	798024	2021/09/03
SC-53	RC Metals Inc.	NMC1217521	NMC1217545	779479	2020/11/24
SC-54	RC Metals Inc.	NV105278427	NV105278438	798025	2021/09/03
SC-55	RC Metals Inc.	NMC1217521	NMC1217546	779480	2020/11/24
SC-56	RC Metals Inc.	NV105278427	NV105278439	798026	2021/09/03

SCRAPER SPRINGS PROJECT, ELKO COUNTY, NV
2023 NI 43-101 TECHNICAL REPORT



SC-57	RC Metals Inc.	NMC1217521	NMC1217547	779481	2020/11/24
SC-58	RC Metals Inc.	NV105278427	NV105278440	798027	2021/09/03
SC-59	RC Metals Inc.	NMC1217521	NMC1217548	779482	2020/11/24
SC-60	RC Metals Inc.	NMC1217521	NMC1217549	779483	2020/11/24
SC-61	RC Metals Inc.	NMC1217521	NMC1217550	779484	2020/10/13
SC-62	RC Metals Inc.	NMC1217521	NMC1217551	779485	2020/10/13
SC-63	RC Metals Inc.	NMC1217521	NMC1217552	779486	2020/10/13
SC-64	RC Metals Inc.	NMC1217521	NMC1217553	779487	2020/10/13
SC-65	RC Metals Inc.	NMC1217521	NMC1217554	779488	2020/10/13
SC-66	RC Metals Inc.	NMC1217521	NMC1217555	779489	2020/10/13
SC-67	RC Metals Inc.	NMC1217521	NMC1217556	779490	2020/10/13
SC-68	RC Metals Inc.	NMC1217521	NMC1217557	779491	2020/10/13
SC-69	RC Metals Inc.	NMC1217521	NMC1217558	779492	2020/10/13
SC-70	RC Metals Inc.	NMC1217521	NMC1217559	779493	2020/10/13
SC-71	RC Metals Inc.	NMC1217521	NMC1217560	779494	2020/10/13
SC-72	RC Metals Inc.	NMC1217521	NMC1217561	779495	2020/10/13
SC-73	RC Metals Inc.	NMC1217521	NMC1217562	779496	2020/10/13
SC-74	RC Metals Inc.	NMC1217521	NMC1217563	779497	2020/10/13
SC-75	RC Metals Inc.	NMC1217521	NMC1217564	779498	2020/11/23
SC-76	RC Metals Inc.	NMC1217521	NMC1217565	779499	2020/11/23
SC-77	RC Metals Inc.	NMC1217521	NMC1217566	779500	2020/11/23
SC-78	RC Metals Inc.	NMC1217521	NMC1217567	779501	2020/11/23
SC-79	RC Metals Inc.	NMC1217521	NMC1217568	779502	2020/11/23
SC-80	RC Metals Inc.	NMC1217521	NMC1217569	779503	2020/11/23
SC-81	RC Metals Inc.	NV105278427	NV105278441	798028	2021/09/03
SC-82	RC Metals Inc.	NV105278427	NV105278442	798029	2021/09/03
SC-83	RC Metals Inc.	NV105278427	NV105278443	798030	2021/09/03
SC-84	RC Metals Inc.	NV105278427	NV105278444	798031	2021/09/03
SC-85	RC Metals Inc.	NV105278427	NV105278445	798032	2021/09/03
SC-99	RC Metals Inc.	NMC1217521	NMC1217570	779504	2020/11/24
SC-100	RC Metals Inc.	NV105278427	NV105278446	798033	2021/09/03
SC-101	RC Metals Inc.	NMC1217521	NMC1217571	779505	2020/10/13
SC-102	RC Metals Inc.	NMC1217521	NMC1217572	779506	2020/10/13
SC-103	RC Metals Inc.	NMC1217521	NMC1217573	779507	2020/10/13
SC-104	RC Metals Inc.	NMC1217521	NMC1217574	779508	2020/10/13
SC-105	RC Metals Inc.	NMC1217521	NMC1217575	779509	2020/10/13
SC-106	RC Metals Inc.	NMC1217521	NMC1217576	779510	2020/10/13
SC-107	RC Metals Inc.	NMC1217521	NMC1217577	779511	2020/10/13
SC-108	RC Metals Inc.	NMC1217521	NMC1217578	779512	2020/10/13
SC-109	RC Metals Inc.	NMC1217521	NMC1217579	779513	2020/10/13
SC-110	RC Metals Inc.	NMC1217521	NMC1217580	779514	2020/10/13
SC-111	RC Metals Inc.	NMC1217521	NMC1217581	779515	2020/10/13
SC-112	RC Metals Inc.	NMC1217521	NMC1217582	779516	2020/10/13
SC-113	RC Metals Inc.	NMC1217521	NMC1217583	779517	2020/10/13
SC-114	RC Metals Inc.	NMC1217521	NMC1217584	779518	2020/10/13

SCRAPER SPRINGS PROJECT, ELKO COUNTY, NV
2023 NI 43-101 TECHNICAL REPORT



SC-115	RC Metals Inc.	NMC1217521	NMC1217585	779519	2020/10/13
SC-116	RC Metals Inc.	NMC1217521	NMC1217586	779520	2020/10/13
SC-117	RC Metals Inc.	NMC1217521	NMC1217587	779521	2020/10/13
SC-118	RC Metals Inc.	NMC1217521	NMC1217588	779522	2020/10/13
SC-119	RC Metals Inc.	NMC1217521	NMC1217589	779523	2020/11/23
SC-120	RC Metals Inc.	NMC1217521	NMC1217590	779524	2020/11/23
SC-121	RC Metals Inc.	NMC1217521	NMC1217591	779525	2020/11/23
SC-122	RC Metals Inc.	NMC1217521	NMC1217592	779526	2020/11/23
SC-123	RC Metals Inc.	NMC1217521	NMC1217593	779527	2020/11/23
SC-124	RC Metals Inc.	NMC1217521	NMC1217594	779528	2020/11/23
SC-145	RC Metals Inc.	NMC1217521	NMC1217595	779529	2020/10/14
SC-146	RC Metals Inc.	NMC1217521	NMC1217596	779530	2020/10/14
SC-147	RC Metals Inc.	NMC1217521	NMC1217597	779531	2020/10/14
SC-148	RC Metals Inc.	NMC1217521	NMC1217598	779532	2020/10/14
SC-149	RC Metals Inc.	NMC1217521	NMC1217599	779533	2020/10/14
SC-150	RC Metals Inc.	NMC1217521	NMC1217600	779534	2020/10/14
SC-152	RC Metals Inc.	NMC1217521	NMC1217601	779535	2020/10/14
SC-154	RC Metals Inc.	NMC1217521	NMC1217602	779536	2020/11/24
SC-156	RC Metals Inc.	NV105278427	NV105278447	798034	2021/09/03
SC-159	RC Metals Inc.	NMC1217521	NMC1217603	779537	2020/11/23
SC-161	RC Metals Inc.	NMC1217521	NMC1217604	779538	2020/11/23
SC-163	RC Metals Inc.	NMC1217521	NMC1217605	779539	2020/11/23
SC-165	RC Metals Inc.	NMC1217521	NMC1217606	779540	2020/11/23
SC-189	RC Metals Inc.	NMC1217521	NMC1217607	779541	2020/10/14
SC-190	RC Metals Inc.	NMC1217521	NMC1217608	779542	2020/10/14
SC-191	RC Metals Inc.	NMC1217521	NMC1217609	779543	2020/10/14
SC-192	RC Metals Inc.	NMC1217521	NMC1217610	779544	2020/10/14
SC-193	RC Metals Inc.	NMC1217521	NMC1217611	779545	2020/10/14
SC-194	RC Metals Inc.	NMC1217521	NMC1217612	779546	2020/10/14
SC-195	RC Metals Inc.	NMC1217521	NMC1217613	779547	2020/10/14
SC-196	RC Metals Inc.	NV105278427	NV105278448	798035	2021/09/03
SC-197	RC Metals Inc.	NV105278427	NV105278449	798036	2021/09/03
SC-199	RC Metals Inc.	NV105278427	NV105278450	798037	2021/09/03
SC-200	RC Metals Inc.	NV105278427	NV105278451	798038	2021/09/03
SC-201	RC Metals Inc.	NV105278427	NV105278452	798039	2021/09/02
SC-202	RC Metals Inc.	NV105278427	NV105278453	798040	2021/09/02
SC-203	RC Metals Inc.	NV105278427	NV105278454	798041	2021/09/02
SC-204	RC Metals Inc.	NV105278427	NV105278455	798042	2021/09/02
SC-205	RC Metals Inc.	NV105278427	NV105278456	798043	2021/09/02
SC-206	RC Metals Inc.	NV105278427	NV105278457	798044	2021/09/02
SC-207	RC Metals Inc.	NV105278427	NV105278458	798045	2021/09/02
SC-208	RC Metals Inc.	NV105278427	NV105278459	798046	2021/09/02
SC-209	RC Metals Inc.	NV105278427	NV105278460	798047	2021/09/02
SC-210	RC Metals Inc.	NV105278427	NV105278461	798048	2021/09/02
SC-211	RC Metals Inc.	NV105278427	NV105278462	798049	2021/09/02

SCRAPER SPRINGS PROJECT, ELKO COUNTY, NV
2023 NI 43-101 TECHNICAL REPORT



SC-212	RC Metals Inc.	NV105278427	NV105278463	798050	2021/09/02
SC-213	RC Metals Inc.	NV105278427	NV105278464	798051	2021/09/02
SC-214	RC Metals Inc.	NV105278427	NV105278465	798052	2021/09/02
SC-215	RC Metals Inc.	NV105278427	NV105278466	798053	2021/09/02
SC-216	RC Metals Inc.	NV105278427	NV105278467	798054	2021/09/02
SC-217	RC Metals Inc.	NV105278427	NV105278468	798055	2021/09/02
SC-218	RC Metals Inc.	NV105278427	NV105278469	798056	2021/09/02
SC-219	RC Metals Inc.	NV105278427	NV105278470	798057	2021/09/02
SC-220	RC Metals Inc.	NV105278427	NV105278471	798058	2021/09/02
SC-221	RC Metals Inc.	NV105278427	NV105278472	798059	2021/09/02
SC-222	RC Metals Inc.	NV105278427	NV105278473	798060	2021/09/02
SC-223	RC Metals Inc.	NV105278427	NV105278474	798061	2021/09/02
SC-224	RC Metals Inc.	NV105278427	NV105278475	798062	2021/09/02
SC-225	RC Metals Inc.	NV105278427	NV105278476	798063	2021/09/02
SC-226	RC Metals Inc.	NV105278427	NV105278477	798064	2021/09/02
SC-227	RC Metals Inc.	NV105278427	NV105278478	798065	2021/09/02
SC-228	RC Metals Inc.	NV105278427	NV105278479	798066	2021/09/02
SC-229	RC Metals Inc.	NV105278427	NV105278480	798067	2021/09/02
SC-230	RC Metals Inc.	NV105278427	NV105278481	798068	2021/09/02
SC-231	RC Metals Inc.	NV105278427	NV105278482	798069	2021/09/02
SC-232	RC Metals Inc.	NV105278427	NV105278483	798070	2021/09/02
SC-233	RC Metals Inc.	NV105278427	NV105278484	798071	2021/09/02
SC-235	RC Metals Inc.	NV105278427	NV105278485	798072	2021/09/02
SC-236	RC Metals Inc.	NV105278427	NV105278486	798073	2021/09/02
SC-237	RC Metals Inc.	NV105278427	NV105278487	798074	2021/09/02
SC-238	RC Metals Inc.	NV105278427	NV105278488	798075	2021/09/02
SC-239	RC Metals Inc.	NV105278427	NV105278489	798076	2021/09/02
SC-240	RC Metals Inc.	NV105278427	NV105278490	798077	2021/09/02
SC-242	RC Metals Inc.	NV105278427	NV105278491	798078	2021/09/02
SC-262	RC Metals Inc.	NV105278427	NV105278492	798079	2021/09/02
SC-264	RC Metals Inc.	NV105278427	NV105278493	798080	2021/09/02
SC-266	RC Metals Inc.	NMC1217521	NMC1217614	779548	2020/11/23
SC-266	RC Metals Inc.	NV101901066	NV101901066	799743	2021/10/05
SC-268	RC Metals Inc.	NMC1217521	NMC1217615	779549	2020/11/23
SC-268	RC Metals Inc.	NV101901067	NV101901067	799744	2021/10/05
SC-270	RC Metals Inc.	NMC1217521	NMC1217616	779550	2020/11/23
SC-270	RC Metals Inc.	NV101901068	NV101901068	799745	2021/10/05
SC-272	RC Metals Inc.	NV105288684	NV105288687	799746	2021/10/05
SC-274	RC Metals Inc.	NV105288684	NV105288688	799747	2021/10/05
SC-276	RC Metals Inc.	NV105288684	NV105288689	799748	2021/10/05
SC-278	RC Metals Inc.	NV105288684	NV105288690	799749	2021/10/05
SC-279	RC Metals Inc.	NV105288684	NV105288691	799750	2021/10/05
SC-280	RC Metals Inc.	NV105288684	NV105288692	799751	2021/10/05
SC-281	RC Metals Inc.	NV105288684	NV105288693	799752	2021/10/05
SC-282	RC Metals Inc.	NV105288684	NV105288694	799753	2021/10/05

SCRAPER SPRINGS PROJECT, ELKO COUNTY, NV
2023 NI 43-101 TECHNICAL REPORT



SC-283	RC Metals Inc.	NV105288684	NV105288695	799754	2021/10/05
SC-284	RC Metals Inc.	NV105288684	NV105288696	799755	2021/10/05
SC-285	RC Metals Inc.	NV105288684	NV105288697	799756	2021/10/05
SC-286	RC Metals Inc.	NV105288684	NV105288698	799757	2021/10/05
SC-287	RC Metals Inc.	NV105288684	NV105288699	799758	2021/10/05
SC-288	RC Metals Inc.	NV105288684	NV105288700	799759	2021/10/05
SC-289	RC Metals Inc.	NV105288684	NV105288701	799760	2021/10/05
SC-290	RC Metals Inc.	NV105288684	NV105288702	799761	2021/10/05
SC-291	RC Metals Inc.	NV105288684	NV105288703	799762	2021/10/05
SC-292	RC Metals Inc.	NV105288684	NV105288704	799763	2021/10/05
SC-293	RC Metals Inc.	NV105288684	NV105288705	799764	2021/10/05
SC-294	RC Metals Inc.	NV105288684	NV105288706	799765	2021/10/05
SC-295	RC Metals Inc.	NV105288684	NV105288707	799766	2021/10/05
SC-296	RC Metals Inc.	NV105288684	NV105288708	799767	2021/10/05
SC-298	RC Metals Inc.	NV105288684	NV105288709	799768	2021/10/05
SC-300	RC Metals Inc.	NV105288684	NV105288710	799769	2021/10/05